

Accepted Manuscript

Title: Paleomagnetic and geochronological studies of the mafic dyke swarms of Bundelkhand craton, central India: implications for the tectonic evolution and paleogeographic reconstructions

Authors: Vimal R. Pradhan, Joseph G. Meert, Manoj K. Pandit, George Kamenov, Md. Erfan Ali Mondal

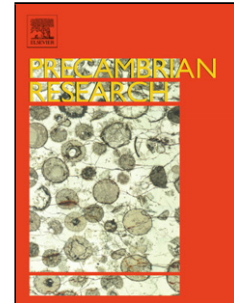
PII: S0301-9268(11)00251-8
DOI: doi:10.1016/j.precamres.2011.11.011
Reference: PRECAM 3476

To appear in: *Precambrian Research*

Received date: 12-7-2011
Revised date: 6-11-2011
Accepted date: 18-11-2011

Please cite this article as: Pradhan, V.R., Meert, J.G., Pandit, M.K., Kamenov, G., Mondal, Md.E.A., Paleomagnetic and geochronological studies of the mafic dyke swarms of Bundelkhand craton, central India: implications for the tectonic evolution and paleogeographic reconstructions, *Precambrian Research* (2010), doi:10.1016/j.precamres.2011.11.011

This is a PDF file of an unedited manuscript that has been accepted for publication. As a service to our customers we are providing this early version of the manuscript. The manuscript will undergo copyediting, typesetting, and review of the resulting proof before it is published in its final form. Please note that during the production process errors may be discovered which could affect the content, and all legal disclaimers that apply to the journal pertain.



- (1). Robust age control on the Bundelkhand dykes;
- (2). Revised insights on the Columbia reconstruction;
- (3). Provides further age control on the Vindhyan basin, Central India.

Accepted Manuscript

1
2 Paleomagnetic and geochronological studies of the
3 mafic dyke swarms of Bundelkhand craton, central
4 India: implications for the tectonic evolution and
5 paleogeographic reconstructions
6

7 Vimal R. Pradhan^{1*}, Joseph G. Meert¹, Manoj K. Pandit², George
8 Kamenov¹, Md. Erfan Ali Mondal³

9 ¹Department of Geological Sciences, University of Florida, 241 Williamson Hall, Gainesville,
10 FL 32611 USA

11 ²Department of Geology, University of Rajasthan, Jaipur 302004, Rajasthan, India

12 ³Department of Geology, Aligarh Muslim University, Aligarh 202002, India
13
14

15 *Corresponding author Fax: +1-352- 392- 9294

16 E-mail address: vimalroy@ufl.edu
17

18 November - 2011
19
20
21

22 Abstract

23 The paleogeographic position of India within the Paleoproterozoic
24 Columbia and Mesoproterozoic Rodinia supercontinents is shrouded in
25 uncertainty due to the paucity of high quality paleomagnetic data with strong
26 age control. New paleomagnetic and geochronological data from the
27 Precambrian mafic dykes intruding granitoids and supracrustals of the
28 Archean Bundelkhand craton (BC) in northern Peninsular India is significant
29 in constraining the position of India at 2.0 and 1.1 Ga. The dykes are
30 ubiquitous within the craton and have variable orientations (NW-SE, NE-SW,
31 ENE- WSW and E-W). Three distinct episodes of dyke intrusion are inferred
32 from the paleomagnetic analysis of these dykes. The older NW-SE trending
33 dykes yield a mean paleomagnetic direction with a declination = 155.3° and an
34 inclination = -7.8° ($k = 21$; $\alpha_{95} = 9.6^\circ$). The overall paleomagnetic pole
35 calculated from these twelve dykes falls at 58.5°N and 312.5°E
36 ($dp/dm=6.6^\circ/7.9^\circ$). The overall mean direction calculated from four ENE-WSW
37 Mahoba dykes has a declination = 24.7° and inclination = -37.9° ($k = 36$; $\alpha_{95} =$
38 15.5°). The virtual geomagnetic pole (VGP) for these four dykes falls at 38.7°S
39 and 49.5°E ($dp/dm = 9.5^\circ/16.3^\circ$). A third, and distinctly steeper,
40 paleomagnetic direction was obtained from two of the NE-SW trending dykes
41 with a declination = 189.3° and inclination = 64.5° . U-Pb geochronology
42 generated in this study yields a U-Pb Concordia age of 1979 ± 8 Ma for the NW-
43 SE trending dykes and a mean $^{207}\text{Pb}/^{206}\text{Pb}$ age of 1113 ± 7 Ma for the Mahoba
44 suite of ENE – WSW trending dykes, confirming at least two dyke emplacement
45 events within the BC. We present global paleogeographic maps for India at 1.1
46 Ga and 2.0 Ga using these paleomagnetic poles. These new paleomagnetic
47 results from the ~ 2.0 Ga NW-SE trending Bundelkhand dykes and the
48 paleomagnetic data from the Bastar/Cuddapah suggest that the North and
49 South Indian blocks of the Peninsular India were in close proximity by at least
50 2.5 Ga.

51 The paleomagnetic and geochronological data from the Mahoba dyke is
52 significant in that it helps constrain the age of the Upper Vindhyan strata. The
53 pole coincides in time and space with the Majhgawan kimberlite (1073 Ma) and
54 the Bhandar-Rewa poles from the Upper Vindhyan strata. The most
55 parsimonious explanation for this coincidence is that the age of the Upper
56 Vindhyan sedimentary sequence is >1000 Ma.

57

58

59

60

61

62

63

64

65

66

67

68

69

70 Keywords: Bundelkhand craton, mafic dykes, central India, paleomagnetism,
71 geochronology, paleogeography.

72 **Introduction**

73 The Indian subcontinent holds a key position when attempting to unravel
74 the intricacies of Precambrian paleogeography, such as the Paleoproterozoic
75 Columbia supercontinent (Rogers, 1996; Rogers and Santosh, 2002; Meert,
76 2002; Santosh et al., 2003; Zhao et al., 2004a; b), the Meso-Neoproterozoic
77 Rodinia supercontinent (McMenamin and McMenamin, 1990; Meert and
78 Torsvik, 2003; Meert and Powell, 2001; Li et al., 2008), and the Ediacaran-
79 Cambrian Gondwana supercontinent (Meert, 2003; Meert and Van der Voo,
80 1996; Burke and Dewey, 1972; Pisarevsky et al., 2008). India offers target
81 rocks that are both accessible and of appropriate age for conducting
82 paleomagnetic and geochronological investigations (Meert, 2003; Powell and
83 Pisarevsky, 2002; Meert and Powell, 2001; Pesonen et al., 2003). These target
84 rocks include Precambrian mafic dykes and dyke swarms that intrude the
85 Archean-Paleoproterozoic cratonic nuclei, as well as volcanic and sedimentary
86 successions exposed in the Dharwar and Aravalli protocontinents of the Indian
87 peninsular shield (figure 1).

88 The correlation of mafic dyke swarms in terms of their distribution,
89 isotopic age, geochemistry and paleomagnetism is critical in order to fully
90 evaluate Precambrian plate reconstructions and possible configuration of
91 supercontinents (Halls, 1987; Van der Voo and Meert, 1991; Halls, 1995;
92 Mertanen et al., 1996; Park et al., 1995; Bleeker and Ernst, 2006; Ernst and
93 Srivastava, 2008; Piispa et al., 2011). The Indian peninsular shield is

94 traversed by numerous Precambrian mafic dyke swarms (Drury, 1984; Murthy,
95 1987, 1995; Ramachandra et al., 1995; French et al., 2008, 2010; Meert et al.,
96 2010; Pati et al., 1999; 2008; Pradhan et al., 2008; Ernst et al., 2008;
97 Srivastava and Gautam, 2008; Srivastava et al., 2008). These dykes intrude
98 the granite-greenstone terranes of the major Indian cratonic nuclei, namely
99 Dharwar in the south, Bastar in the east central, Singhbhum in the east and
100 the Aravalli and Bundelkhand in the north-west and the north (Halls, 1982;
101 figure 1). The dykes are the focus of considerable scientific attention aimed at
102 defining their geochemical and geophysical characteristics, geochronology,
103 paleomagnetism and tectonic controls on their emplacement (Devaraju, 1995,
104 Radhakrishna and Piper, 1999, Srivastava et al., 2008; Halls et al., 2007;
105 French et al., 2008, 2010; Pradhan et al., 2008, 2010; Pati et al., 1999; 2008;
106 Piispa et al., 2011; Ratre et al., 2010; Ernst et al., 2008; Ernst and Bleeker,
107 2010; Meert et al., 2011). Paleomagnetic and geochronological studies on these
108 Precambrian mafic dyke swarms as well as the volcanic and sedimentary
109 successions of the Gwalior, Cuddapah and Vindhyan basins, provide insight
110 into India's changing paleogeographic position during the critical Paleo- to
111 Mesoproterozoic interval and may, in some circumstances, allow for further age
112 constraints to be placed on the poorly dated sedimentary basins of India
113 (Pradhan et al., 2008, 2011; Gregory et al., 2006; Malone et al., 2008; Meert et
114 al., 2010, 2011; French et al., 2008; French, 2007; Halls et al., 2007; Ratre et
115 al., 2010; French and Heaman, 2010; Piispa et al., 2011).

116 This study focuses on the Precambrian mafic dyke swarms intruding the
117 Bundelkhand craton in north-central India (Pati et al., 1999). The most
118 prominent of the Paleo-Mesoproterozoic (2.5-1.0 Ga) magmatic events are
119 represented by three mafic dyke swarms that intrude the Archean granitic-
120 gneissic basement of the Bundelkhand craton. The dykes follow two major
121 trends, suggesting at least two major pulses of magmatic emplacement within
122 the craton. Based on field cross-cutting relationships, the ENE-WSW trending
123 dykes are the youngest in the craton, and are represented by the “Great Dyke
124 of Mahoba” (figures 3c-d). Previous paleomagnetic studies on these dykes were
125 hindered by poor age constraints (Poitou et al., 2008). Existing isotopic ages
126 allow an age bracket between 2150 Ma and 1500 Ma for the older suite of mafic
127 dykes (Rao, 2004; Rao et al., 2005; Basu, 1986; Sarkar et al., 1997; Sharma
128 and Rahman, 1996).

129 We report new paleomagnetic and geochronological data on the
130 Bundelkhand mafic dykes from the Mahoba, Banda, Khajurao and nearby
131 areas of the Bundelkhand province in the central India (figure 2). This study
132 offers the first robust age constraints on the paleomagnetic poles calculated
133 from these mafic dykes. These data will ultimately aid in improving our models
134 for the Precambrian tectonic evolution of the Indian cratons, clarify the role of
135 India in the Columbia and Rodinia supercontinents, and generate data for
136 developing an apparent polar wander path (APWP) for India in this poorly
137 resolved period of Earth history.

138 **Geological setting and previous work**

139 The Archaean-early Proterozoic Bundelkhand craton (BC), commonly
140 known as Bundelkhand Granite Massif (BGM) is a semi-circular to triangular
141 province that forms the northernmost part of the Indian peninsula (figure 2). It
142 covers an area of ~29,000 km² and lies between latitudes 24°30' and 26°00'N
143 and longitudes 77°30' E and 81°00' E (Sharma, 1998). The BC is delimited to
144 the west by the Great Boundary Fault, to the northeast by the Indo-Gangetic
145 alluvial plains and to the south and southeast by the Narmada-Son lineament
146 (figure 2). The southwestern margin is marked by relatively small outcrops of
147 Deccan Basalt; additionally, Paleoproterozoic rocks of the Bijawar and Gwalior
148 Groups are exposed in the SW and NE parts of the BC. The arcuate Vindhyan
149 basin overlies the BC in the south and southeastern sections (Goodwin, 1991;
150 Naqvi and Rogers, 1987; Pati et al., 2008; Meert et al., 2010). Sharma and
151 Rahman, (2000) divide the Bundelkhand craton into three litho-tectonic units:
152 (a) the ~3.5 Ga highly deformed granite-greenstone basement; (b) ~2.5 old
153 multiphase granitoid plutons and associated quartz reefs; and (c) the mafic
154 dykes and dyke swarms. The BGM represents a significant phase of felsic
155 magmatism associated with a complex of pre-granite sedimentary rocks (Basu,
156 1986). The basement is represented by a highly deformed granite-greenstone
157 terrane that consists of various enclaves of Archean gneisses, amphibolites,
158 ultramafics, BIF's, Tonalite-Trondhjemite-Gneiss, marble, calc-silicate rocks,
159 fuchsite quartzites and other metasediments (Roy et al., 1988; Basu, 1986;
160 Sharma, 1998; Sinha-Roy et al., 1998; Mondal and Zainuddin, 1996; Mondal

161 et al., 2002). Three different phases of granitoid emplacement are identified in
162 the BGM. In order of decreasing $^{207}\text{Pb}/^{206}\text{Pb}$ age, these granites include $2521 \pm$
163 7 Ma hornblende granite, 2515 ± 5 Ma biotite granite, and 2492 ± 10
164 leucogranites and constitute 80-90% of its exposed area (Gopalan et al., 1990;
165 Wiedenbeck and Goswami, 1994; Wiedenbeck et al., 1996; Mondal et al., 1997,
166 1998, 2002; Malviya et al., 2004, 2006). Granitoid emplacement in the BC was
167 followed by a number of minor intrusions including widespread pegmatitic
168 veins, porphyry dykes and dyke swarms, and felsic units (rhyolites, dykes of
169 rhyolitic breccias with angular enclaves of porphyries). Numerous quartz veins
170 of varied size with mainly NNE-SSW and NE-SW trends are observed in parts of
171 the BC representing episodic tectonically controlled hydrothermal activity (Pati
172 et al., 1997, 2007).

173 The youngest phase of magmatism in the BGM is represented by mafic
174 dykes and dyke swarms that traverse all the above lithologies. More than 700
175 mafic dykes are known to intrude the granitoid rocks of the BC (Pati et al.,
176 2008). The majority of these dykes trend in a NW-SE direction, with
177 subordinate ENE-WSW and NE-SW trending dykes including the ENE-WSW
178 Great dyke of Mahoba (Basu, 1986; Mondal and Zainuddin, 1996; Mondal et
179 al., 2002; figure 2). These mafic dykes are subalkaline to tholeiitic in
180 composition and display continental affinity (Pati et al., 2008). The dykes are
181 commonly exposed as a series of discontinuous and bouldery outcrops
182 extending in length from few tens of meters to more than 17 km. The 'Great
183 Dyke' of Mahoba has maximum strike length of ≥ 50 km (figure 2 & figures 3c,

184 d). The dykes are generally non-foliated, relatively unaltered and exhibit sharp
185 chilled contacts with the host granitoids (figure 3b). Basu (1986) distinguished
186 at least three generations of dykes based on their cross-cutting relationships.
187 The oldest, coarse grained NW-SE trending suite is cut by ENE-WSW and NE-
188 SW trending medium-grained dykes that include small bodies and lenticles of
189 an aphanitic dolerite. Numerous intermediate to felsic dykes are exposed in the
190 west-central part of the massif between Jhansi and Jamalpur, including diorite
191 porphyry, syenite porphyry and fine-grained syenite porphyry (Basu, 1986).

192 The ages for the Archaean rocks in the BGM are poorly constrained due
193 to limited isotopic studies. The oldest rocks in the massif are associated with
194 the TTG magmatism intruding the basement rocks and are assigned an age of
195 3503 ± 99 Ma (Rb-Sr isochron; Sarkar et al., 1996). Zircons from the basement
196 gneiss yield an ion microprobe $^{207}\text{Pb}/^{206}\text{Pb}$ age of 3270 ± 3 Ma (Mondal et al.
197 2002). The Bastar, Dharwar and Aravalli cratons (Sarkar et al., 1993;
198 Wiedenbeck et al., 1996) in peninsular India also contain coeval Archean
199 basement rocks suggesting that these protocontinents played an important role
200 in the earliest stages of nucleation of the Indian shield. The overall
201 stabilization age for the massif has been interpreted to be ~ 2.5 Ga based on the
202 $^{207}\text{Pb}/^{206}\text{Pb}$ ages of the granitoids (Meert et al., 2010; Crawford, 1970; Mondal
203 et al., 1997, 1998, 2002; Roy and Kröner, 1996). The large scale granitic
204 magmatism in the BC overlaps with similar events of granite magmatism and
205 mineralization in adjacent Bastar (2490 ± 10 Ma; Stein et al., 2004) and
206 Dharwar cratons (2510 Ma; Jayananda et al., 2000) indicating widespread

207 granitic plutonism throughout much of the Indian shield at the Archean –
208 Proterozoic boundary. Age control on the Bundelkhand mafic dykes is
209 problematic and is loosely constrained to between ca. 2.1 and 1.5 Ga
210 (Crawford, 1975; Crawford and Compston, 1970; Sarkar et al., 1997). More
211 recent *in-situ* $^{40}\text{Ar}/^{39}\text{Ar}$ laser ablation data yielded 2150 Ma and 2000 Ma ages
212 for mafic dykes (Rao, 2004; Rao et al., 2005) indicating two pulses of dyke
213 emplacement, however, no details on the locations of the samples were
214 provided in those publications. The majority of the laser spots for the *in situ*
215 ^{40}Ar - ^{39}Ar analysis were in the 2000 Ma range, suggesting that some of the older
216 spot ages may suffer from excess argon within the samples.

217

218 **Sampling and Methodology**

219 **Paleomagnetic methods**

220 We sampled 27 sites (dykes) and collected a total of ~380 core samples
221 from the mafic dykes intruding the Bundelkhand craton for paleomagnetic
222 analysis (figure 2). Out of these, only 18 sites (dykes) yielded consistent results
223 and are discussed in this paper (table 1). All samples were drilled in the field
224 using a water cooled portable drill. The samples were oriented using both sun
225 and magnetic compass and readings were corrected for local magnetic
226 declination and errors. Samples were returned to the University of Florida
227 where they were cut into standard sized cylindrical specimens. These
228 specimens were stepwise demagnetized by using both thermal and alternating
229 field (AF) methods in order to identify the best treatment for isolating vector

230 components within the samples. Alternating field demagnetization was
231 conducted using a home-built AF demagnetizer and with fields up to 100 mT.
232 Thermal demagnetization was conducted up to temperatures of 600° C with an
233 ASC-Scientific TD-48 thermal demagnetizer. Based upon the magnetic strength
234 of the samples and instrument sensitivity the measurements were made on
235 either a Molspin® spinner magnetometer or a 2G 77R Cryogenic magnetometer
236 at the University of Florida. In samples that showed a very high initial NRM,
237 samples were treated in liquid Nitrogen baths prior to thermal or AF treatment
238 to remove any viscous multi-domain magnetism. Linear segments of the
239 demagnetization trajectories were analyzed via principal component analysis
240 using the IAPD software (Torsvik et al., 2000).

241 *Rock magnetic tests*

242 Curie temperature experiments were run on representative sample
243 fragments from each site on a KLY-3S susceptibility Bridge with a CS-3 heating
244 unit. Isothermal Remanence Acquisition (IRM) studies were performed on
245 samples using an ASC-IM30 impulse magnetizer to further characterize the
246 magnetic behavior.

247

248 **Geochronological methods**

249 Two samples from the NE-SW trending “Great Dyke of Mahoba” and five
250 samples from the NW-SE trending older suite of mafic dykes from the
251 Bundelkhand craton were processed for geochronology (figure.2). To ascertain
252 the presence of uranium bearing phases, selected samples were thin sectioned

253 and then imaged via scanning electron microscopy (SEM) for
254 zircon/baddeleyite using the back scattered diffraction (BSD) method. Out of
255 the dozen samples imaged, only two from the NE-SW trending younger suite
256 (GDM and GDM-1) and four (including analyzed sample I9GS-13) from the NW-
257 SE trending older suite displayed bright spots representative of zircon or
258 baddeleyite, ranging in size between 2 and 100 μm (figure 4a and 4b). We
259 pulverized sample I9GS_13 from the older suite and Mahoba dyke samples
260 (GDM and GDM-1) for conventional methods of mineral extraction. Using
261 standard gravity and magnetic separation techniques, the zircon grains were
262 concentrated from pulverized samples at University of Florida. The samples
263 were crushed, then disk milled and sieved to < 80 - mesh grain size fraction.
264 The fractions were then rinsed using Calgon (an anionic surfactant), followed
265 by water table treatment with slow sample feed rates. This was followed by
266 heavy liquid mineral separation with multiple agitation periods to reduce the
267 number of entrapped grains in the lower density fraction. Finally, the samples
268 were repeatedly passed through a Frantz Isodynamic magnetic separator up to
269 a current of 1.0 Amps ($2-4^\circ$ tilt). Approximately 15-20 clear, euhedral to nearly
270 anhedral zircon grains and zircon fragments were handpicked from the two
271 samples of the NE-SW trending younger Mahoba suite (GDM and GDM-1) and
272 25-35 subhedral to euhedral zircon grains from the NW-SE trending older suite
273 (I9GS_13) under an optical microscope to ensure the selection of only the
274 clearest grains and fragments of grains. Further hand-picking of the grains
275 reduced the number to only 7-8 good grains from the Mahoba dolerites and 10-

276 15 grains from the I9GS-13 dyke sample. The grains were then mounted in
277 resin and then polished to expose medial sections. Further sonication and
278 cleaning of the plugs in 5% nitric acid (HNO_3) helped to remove any common-
279 Pb surface contamination.

280 U/Pb isotopic analyses were conducted at the Department of Geological
281 Sciences (University of Florida) on a Nu Plasma multi-collector plasma source
282 mass spectrometer equipped with three ion counters and 12 Faraday detectors.
283 The LA-ICPMC-MS is equipped with a specially designed collector block for
284 simultaneous acquisition of ^{204}Pb (^{204}Hg), ^{206}Pb and ^{207}Pb signals on the ion-
285 counting detectors and ^{235}U and ^{238}U on the Faraday detectors (Mueller et al.,
286 2008). Mounted zircon grains were laser ablated using a New - Wave 213nm
287 ultraviolet laser beam. During U/Pb analyses, the sample was decrepitated in
288 a He stream and then mixed with Ar-gas for induction into the mass
289 spectrometer. Background measurements were performed before each analysis
290 for blank correction and contributions from ^{204}Hg . Each sample was ablated
291 for ~30 seconds in an effort to minimize pit depth and fractionation. Data
292 calibration and drift corrections were conducted using the FC-1 Duluth Gabbro
293 zircon standard, long term reproducibility were 2% for $^{206}\text{Pb}/^{238}\text{U}$ (2σ) and 1%
294 for $^{207}\text{Pb}/^{206}\text{Pb}$ (2σ) ages (Mueller et al., 2008). There was no significant ^{204}Pb
295 detected in the samples and therefore, no common Pb correction was applied to
296 the U-Pb data. Data reduction and correction were conducted using a
297 combination of in-house software and Isoplot (Ludwig, 1999). Additional
298 details can be found in Mueller et al. (2008).

299

300 **Results**301 **Geochronological results**

302 The U/Pb ages from the zircon/zircon fragments were determined for the
303 older NW-SE trending dyke sample I9GS_13 and the Great dyke of Mahoba
304 samples GDM and GDM1. The dyke sample I9GS_13 yielded a number of well
305 faceted zircons and zircon fragments suitable for U/Pb isotopic analysis.
306 Eleven laser analyses on five different euhedral zircons yielded a concordia age
307 of 1979 ± 8 Ma (2σ ; MSWD (Conc.+Equival.)=0.63; Probability
308 (Conc.+Equival.)=0.90; figure 5a; table 2a). This age is in rough agreement
309 with reported *in-situ* $^{40}\text{Ar}/^{39}\text{Ar}$ laser ablation data cited above (Rao, 2004; Rao
310 et al., 2005). In addition, no crustal ages of 2.0 Ga are known from the
311 Bundelkhand craton and no detrital component of this age has been identified
312 in the adjacent Vindhyan and Marwar basins (Malone et al., 2008; Meert et al.,
313 2010). Therefore, it is our interpretation that the 1978 Ma age reflects
314 the crystallization age of the dyke. Ten analyses on four other fragmentary
315 zircons from sample I9GS_13 yielded moderately discordant $^{207}\text{Pb}/^{206}\text{Pb}$ dates
316 between 2777 and 2686 Ma (figure 5b; table 2a). These results are broadly
317 consistent with the ages of the basement rocks in the region (Mondal et al.,
318 2002). Three analyses of a single zircon are slightly to moderately discordant,
319 and the two least-discordant analyses agree to within uncertainty and yield a
320 weighted mean $^{207}\text{Pb}/^{206}\text{Pb}$ date of 3254 ± 3 Ma (MSWD = 0.88) that is also a

321 common age for basement rocks in the Bundelkhand craton (see Meert et al.,
322 2010).

323 The two Mahoba dyke samples yielded only two well faceted grains and
324 several fragments/tips of zircons (figure 4a). The regression derived from
325 $^{207}\text{Pb}/^{206}\text{Pb}$ ratios from five laser analyses on three different zircon grains and
326 zircon fragments/tips yielded a minimum concordant age of 1096 ± 19 Ma (2σ ;
327 MSWD=0.3; figure 5c; table 2b). The weighted mean $^{207}\text{Pb}^*/^{206}\text{Pb}^*$ age for these
328 five analysis yielded an age of 1113 ± 7 (2σ ; MSWD=0.75; probability of
329 fit=0.56; figure 5d; table 2b).

330

331 **Paleomagnetic results**

332 The paleomagnetic directions/statistics for the individual NW-SE, ENE-
333 WSW and NE-SW trending Bundelkhand mafic dykes are listed in Table 1.
334 Three distinct paleomagnetic directions were recorded for the doleritic dykes
335 suggesting three episodes of dyke emplacement within the BC varying in space
336 and time. A stable uni-vectorial demagnetization trend was observed for a
337 majority of these samples during thermal/AF treatments. The samples show
338 discrete unblocking temperatures between 550 °C and 570°C. The 'B' samples
339 treated with AF demagnetization show gradual decrease in their magnetic
340 intensity and behave consistently over a wide range of coercivity spectrum
341 (figure 6b & 6d).

342 The NRM intensities for the ENE-WSW trending Mahoba dyke samples
343 range between 0.4 A/m and 0.1 A/m (figure 6a & 6b). The intensity plots

344 yielded unblocking temperatures between 550 °C and 560 °C during thermal
345 demagnetization while AF demagnetization yielded wide coercivity spectrum,
346 consistent with low-Ti magnetite as the main carrier of magnetization (figure 6a
347 & 6b). The overall mean direction calculated from four ENE-WSW Mahoba
348 dykes has a declination = 24.7° and inclination = -37.9° ($k = 36$; $\alpha_{95} = 15.5^\circ$)
349 and a resultant virtual geomagnetic pole (VGP) at 38.7°S and 49.5°E ($dp/dm =$
350 $9.5^\circ/16.3^\circ$; (figure 9a).

351 Fifteen dykes were sampled from the older NW-SE trending suite and
352 twelve yielded consistent stable paleomagnetic directions (table 1). The NRM
353 intensities for these samples vary from 0.44 A/m to 0.11 A/m. Figures 6c and
354 6d show the demagnetization behavior of two pilot dyke specimens to the
355 thermal and AF treatments. The mean paleomagnetic direction obtained from
356 these 12 dykes has a declination = 155.3° and inclination = -7.8° ($k = 21$; $\alpha_{95} =$
357 9.6) after inverting one reverse polarity dyke I443 C; (figure 9b; table 1). The
358 overall paleomagnetic pole calculated from these twelve dykes falls at 58.5°N
359 and 312.5°E ($dp/dm=6.6^\circ/7.9^\circ$).

360 In addition to these two directions from the NW-SE and ESE-WNW
361 dykes, a third distinct steep paleomagnetic direction was obtained from two of
362 the NE-SW trending dykes. The overall mean direction calculated for these two
363 dykes has a declination = 189.3° and inclination = +64.5° (figure 9c). This is
364 suggestive, though not conclusive, evidence for a third episode of dyke
365 emplacement within the BC.

366 The Bundelkhand granitic host rock samples were also collected at sites
367 I925 and I927 with the intent to perform a baked contact test. Unfortunately,
368 the vast majority of the granites were dominated by multi-domain magnetite
369 and no consistent directions were obtained with one exception. At site I925
370 numerous mafic dykelets were observed trellising the granitic host rock (figure
371 3b). These granitic samples in contact with the mafic dykelets were taken
372 about 1.5 feet away from the main dyke (figure 3a) and stable paleomagnetic
373 directions were obtained for the host granites that were similar to the main
374 dyke I925 (figure 7a & 7b). In addition, one of the dykes (site I443 C) is of
375 opposite polarity to the characteristic magnetization observed in the majority of
376 dykes (declination = 339° and inclination = -21° ; $k=70$; $\alpha_{95} = 11.1$). While not
377 conclusive, the partial baked contact test, the dual polarity signal and the fact
378 that the three suites of dykes (NE-SW, ENE-WSW and NW-SE) yield distinct
379 paleomagnetic directions support a primary magnetization in the NW-SE
380 trending older suite of dykes and negates arguments for a younger
381 remagnetization in the region.

382

383 *Rock magnetic results*

384 Representative results of thermomagnetic analysis (susceptibility vs.
385 temperature) of ENE-WSW and NW-SE trending dyke samples are shown in
386 figure 8 (a-d). The heating and cooling curves of magnetic susceptibility for the
387 ENE-WSW trending Mahoba dykes as shown in figures 8a, c display two
388 magnetic phases. The heating curves show a prominent peak centered close to

389 250 °C - 300 °C and susceptibility drop above 300° C, indicating the likely
390 existence of pyrrhotite. A rapid decrease in the magnetic susceptibility around
391 550 °C - 575 °C indicates the existence of magnetite (figures 8a & 8c). The
392 cooling curve shows higher susceptibility which is probably caused by the ex-
393 solution and conversion of Ti-magnetite to pure magnetite.

394 The rock magnetic studies on the dominantly occurring NW-SE trending
395 older suite of dykes show nearly reversible Curie temperature runs
396 characteristic of magnetite (figures 8b & 8d). The heating Curie temperature
397 T_{cH} of dyke sample I927-12 is 572.8 °C, and the cooling Curie temperature T_{cC}
398 is 567.5 °C (figure. 8d). Isothermal remanence acquisition (IRM) curves along
399 with back field coercivity of remanence from both these ENE-WSW and NW-SE
400 trending mafic dykes also indicate magnetite as the principal magnetic carrier
401 in the samples. A rapid rise in intensity near saturation at ~0.25-0.3 Tesla was
402 observed for majority of the dyke samples and their magnetization remains
403 constant at higher fields, up to the highest applied field of 1.2 Tesla. The
404 values for the back field coercivity of remanence ranges between 0.07 and 0.1
405 mT (figures 8e-f).

406

407 **Discussion**

408 **1.1 Ga Paleomagnetism**

409 The VGP calculated for the ENE-WSW trending Mahoba dykes of the
410 Bundelkhand craton is significant in terms of its age and the direction. The U-
411 Pb zircon age of 1113 ± 7 Ma for Mahoba dykes falls in the same time bracket

412 as the Majhgawan kimberlite that intrudes both the Lower Vindhyan sequence
413 (~1.6 Ga) and the Baghain sandstone of the Kaimur Group (Upper Vindhyan).
414 Gregory et al. (2006) dated Majhgawan kimberlite at 1073 ± 13.7 Ma via ^{40}Ar -
415 ^{39}Ar analysis of phlogopite phenocrysts and obtained a virtual geomagnetic pole
416 at 36.8°S , 32.5°E ($dp = 9^\circ$; $dm = 16.6^\circ$; also see Miller and Hargraves, 1994)
417 that is statistically indistinguishable from the virtual geomagnetic pole
418 calculated for the Mahoba dyke swarm in this study (figure 10). Malone et al.
419 (2008) conducted a paleomagnetic study on the Bhandar-Rewa Groups (Upper
420 Vindhyan) and obtained a mean paleomagnetic pole at 44°S , 34.0°E ($A95 =$
421 4.3). We note that the VGP's of the Mahoba dykes generated in this study and
422 the penecontemporaneous Majhgawan kimberlite are nearly identical to the
423 paleomagnetic poles obtained from the Bhandar-Rewa Groups in the Upper
424 Vindhyan sequence (figure 10).

425 Azmi et al. (2008) argue that the paleomagnetic data from the
426 Majhgawan kimberlite and the Bhandar-Rewa sequence are indeed age-
427 equivalent and late Neoproterozoic in age, but that the Majhgawan phlogopites
428 crystallized at depth some 400 million years earlier. We acknowledge that the
429 presence of similar magnetizations in three different units in close proximity
430 may also raise concern about the possibility of remagnetization. However, we
431 note that there is no reported ~1.1 Ga remagnetization event within or in the
432 vicinity of the Bundelkhand craton.

433 Additional support for the primary nature of magnetization is found in
434 both Upper Vindhyan sequence and the NW-SE trending older suite of

435 Bundelkhand dykes. Upper Vindhyan sedimentary units show at least eleven
436 geomagnetic reversals supporting a primary magnetization in these rocks.
437 Similarly, the presence of partial baked contact test yielded by the granitic host
438 rock samples traversed by the mafic dykelets at site I925 (figure.7e & 7f) and
439 the dual polarity magnetization shown by one of the dykes (site I443 C) support
440 a primary magnetization in the NW-SE trending older suite of Bundelkhand
441 dykes.

442 *Age implications for the Bhandar-Rewa sequence of the Upper Vindhyan:*

443 The age of deposition in Vindhyan basin located to the south of the
444 Bundelkhand Craton (figure 1) in the northern Indian peninsular shield, has
445 been debated for over 100 years (Oldham, 1893; Auden, 1933; Crawford and
446 Compston, 1970; Venkatachala et al., 1996; Malone et al., 2008; Azmi et al.,
447 2008). The onset of sedimentation in the lower Vindhyan Supergroup is
448 generally well constrained at around 1.6-1.8 Ga by radiometric data
449 (Rasmussen et al., 2002a, b; Ray et al., 2002, 2003 Sarangi et al., 2004;
450 Kumar, 2001); however the age of the Upper Vindhyan is still enigmatic and
451 highly contentious due to lack of targets suitable for geochronology,
452 controversial fossil finds and poorly constrained global stable isotopic
453 correlations (Vinogradov et al., 1964; Crawford and Compston, 1970; Paul et
454 al., 1975; Srivastava and Rajagopalan, 1988; Chakrabarti, 1990; Smith, 1992;
455 Kumar and Srivastava, 1997; Kumar et al., 2002; De, 2003, 2006; Ray et al.,
456 2002, 2003; Rai et al., 1997; Gregory et al., 2006; Malone et al., 2008, Azmi et
457 al., 2008).

458 The Upper Vindhyan sedimentary rocks were typically correlated with the
459 Marwar Supergroup (Rajasthan); sequences in the Salt Range of Pakistan and
460 with the Krol-Tal Group of the Lesser Himalayas (McElhinny et al., 1978;
461 Klootwijk et al., 1986; Mazumdar and Banerjee, 2001). These correlations,
462 however, are based on somewhat similar lithologies and the proximity of the
463 undeformed Marwar and Upper Vindhyan strata.

464 The lithologic comparisons between these units are rather problematic.
465 For example, the evaporite deposits are prevalent within the Marwar and Salt
466 Ranges, but absent in the Upper Vindhyan sequence. Malone et al. (2008)
467 examined detrital zircon suites from both the Upper Vindhyan sedimentary
468 rocks in Rajasthan and the nearby Marwar Supergroup. The $^{207}\text{Pb}/^{206}\text{Pb}$ age
469 distribution observed in the detrital zircon analysis of the Upper Bhandar
470 sandstone yielded several noteworthy peaks between 1850 – 1050 Ma (Malone
471 et al., 2008). In contrast, detrital zircons analyzed from the Sonia and
472 Girbarkhar sandstone of the Marwar Supergroup yielded age peaks in the 840-
473 920 Ma range, a component completely absent in the Upper Bhandar
474 sandstone of the Vindhyan Supergroup. Hence, the results from the detrital
475 zircon geochronology suggest that previous correlations between the two
476 depositional sequences are incorrect. Malone et al. (2008) hypothesized that
477 the closure age of the Upper Vindhyan sedimentation was no younger than 1.0
478 Ga based on their paleomagnetic study on the Bhandar-Rewa Groups of the
479 Upper Vindhyan and the detrital zircon work on Bhandar-Rewa units and the
480 Marwar Supergroup. Additional support for a late Mesoproterozoic closure age

481 came from a paleomagnetic/geochronological study of the Majhgawan
482 kimberlite (Gregory et al., 2006).

483 The paleomagnetic and geochronological data from the Mahoba dykes
484 generated in this study is germane to the discussion of the sedimentation ages
485 in the Upper Vindhyan basin. The VGP obtained for the ~1113 Ma Mahoba
486 dykes (37.8°S, 49.5°E) is nearly identical to the mean paleomagnetic pole from
487 the Bhandar – Rewa Groups and the Majhgawan kimberlite (figure 10; see
488 discussion above). Our interpretation of the Mahoba paleomagnetic and
489 geochronological results therefore lends additional support to the proposal of
490 Malone et al. (2008) and Gregory et al. (2006) that the closure of sedimentation
491 in the Upper Vindhyan sequence is older than ~1.0 Ga.

492 *India in Rodinia supercontinent at 1100 Ma*

493 The late Mesoproterozoic (ca. 1100 Ma) has been postulated as the time
494 interval for the formation of the supercontinent Rodinia (McMenamin and
495 McMenamin, 1990; Dalziel, 1991; Moores, 1991; Hoffman, 1991). The
496 existence of Rodinia is supported by the presence of a number of 1300-900 Ma
497 old orogenic/mobile belts (Dewey and Burke, 1973) and associated geologic
498 links between the various cratonic nuclei (Young, 1995; Dalziel, 1997; Rainbird
499 et al., 1998; Karlstrom et al., 1999; Sears and Price, 2000; Dalziel, 2000).
500 However, the geometry/paleogeography and duration of the Rodinia
501 supercontinent remains extremely fluid and controversial due to a paucity of
502 well dated, high quality paleomagnetic poles from various continental blocks

503 forming the supercontinent (Weil et al., 1998; Meert and Powell, 2001; Meert,
504 2001; Meert and Torsvik, 2003; Li et al., 2008).

505 One of the outcomes of this study is our ability to constrain the
506 paleoposition of Indian sub-continent in Rodinia configuration at ~1.1 Ga. The
507 recent paleomagnetic and geochronological studies from the Majhgawan
508 kimberlite (Gregory et al., 2006) and Bhandar-Rewa Groups of Upper Vindhyan
509 (Malone et al., 2008) provided high quality poles to constrain the
510 paleogeographic position of India at 1.1 Ga.

511 There are a number of paleomagnetic poles available from other elements
512 of the Rodinia supercontinent that are more or less coeval with those from
513 India. Considering the East Gondwana elements, the key pole for this interval
514 in Australia is the ~1070 Ma doleritic rocks of Bangemall sills (Wingate et al.,
515 2002). The Bangemall pole achieves a score of $Q = 7$ in the reliability scheme
516 of Van der Voo (1990).

517 The paleogeographic position for Laurentia is based on the combined
518 mean paleomagnetic data from the Portage Lake volcanics and Keweenawan
519 dykes (Pesonen et al., 2003; Swanson-Hysell et al., 2009). Based on the
520 extensive field and laboratory tests these poles are inferred to be primary and
521 have precise zircon/baddeleyite U-Pb dates of 1095 Ma (Portage Lake
522 Volcanics) and ~1109 Ma (Keweenawan volcanics), respectively (Halls and
523 Pesonen, 1982; Davis and Sutcliffe, 1985; Goodge et al., 2008). More recently,
524 Swanson-Hysell et al. (2009) provided high resolution paleomagnetic data from
525 a series of well-dated basalt flows at Mamainse Point, Ontario, in the

526 Keweenawan Rift and suggested that the previously documented reversal
527 asymmetry for these volcanic rocks is an artefact of the fast motion of the
528 Laurentian plate towards the equator at this interval (also see Meert, 2009).
529 The combined mean of the Portage Lake volcanics and the Keweenawan
530 dolerites pole places Laurentia at intermediate paleolatitudes in our ~1.1 Ga
531 reconstruction.

532 There are two paleomagnetic poles available from the Baltica between ~
533 1100 Ma and 1123 Ma. Most of the Rodinia reconstructions at ~1100 Ma
534 utilize the paleomagnetic data from the Bamble intrusions in southern Norway
535 to constrain the position of Baltica (Brown and McEnroe, 2004; Stearn and
536 Piper, 1984). A Sm/Nd metamorphic age of 1095 Ma has been reported for the
537 Bamble intrusive rocks intruding the high grade granulite facies. Recently,
538 Salminen et al. (2009) reported a virtual geomagnetic pole for the Baltica from
539 their paleomagnetic and rock magnetic studies on the well dated 1122 ± 7 Ma
540 (U-Pb age; Lauerma, 1995) Salla diabase dykes in northeastern Finland. The
541 palaeolatitudinal position of Baltica constrained by the Bamble intrusive poles
542 and the Salla dykes VGP indicate a latitudinal difference of almost 90° . This
543 would require an unusually rapid southward drift of the Baltica plate for the
544 short time interval of ~28 Ma. However, the Salla diabase dyke pole is highly
545 tentative and requires additional verification due to the inadequate averaging of
546 secular variation (Salminen et al., 2009). Given the tentative nature of the
547 Salla diabase pole, we select the previously reported mean paleomagnetic pole

548 from the Bamble intrusions to place Baltica in our reconstruction (Brown and
549 McEnroe, 2004; Stearn and Piper, 1984).

550 A key, well-dated paleomagnetic pole, from the Kalahari craton at ~1.1
551 Ga is based on the Umkondo dolerites and the Kalkpunt poles (Hanson et al.,
552 2004a; Gose et al., 2004; 2006; Jacobs et al., 2008). The precisely dated
553 Umkondo dolerite paleomagnetic data from the Kalahari craton are often
554 correlated with Keweenawan igneous suite of Laurentia (Hanson et al., 2004a;
555 Gose et al., 2006; Jacobs et al., 2008). These two coeval paleomagnetic poles
556 are predominantly of one polarity and thus constrain the relative paleolatitudes
557 of the two cratons within the Rodinia configuration. The paleomagnetic data in
558 our reconstruction at ~1.1 Ga are derived from the mean pole based on the
559 results from Timbavati gabbros, the Umkondo-Borg large igneous province and
560 the Grunehogna province of Antarctica after restoring East Antarctica to its
561 position next to South Africa at ~1.1 Ga (Jones and McElhinny, 1966; Renne et
562 al., 1990; Hargraves et al., 1994; Jones and Powell, 2001; Powell et al., 2001;
563 Pesonen et al., 2003; Hanson et al., 2004a; Gose et al., 2006; Jacobs et al.,
564 2008).

565 The reconstruction discussed herein also utilizes the mean
566 paleomagnetic pole from the granophyres and rhyolite nunataks of Coats Land,
567 Antarctica to evaluate the paleogeographic position of Coats Land in Rodinia
568 and their connection to the Kalahari craton at ~1.1 Ga (Gose et al., 1997). The
569 granophyres and rhyolite nunataks provide indistinguishable mean
570 paleomagnetic directions with precise U-Pb zircon ages of 1112 ± 4 Ma

571 (rhyolites) and 1106 ± 3 Ma (granophyres) respectively. These volcanic rocks
572 are interpreted to represent part of the Umkondo-Borg-Keweenawan magmatic
573 province (Jacobs et al., 2008).

574 The position of North China Block in Late Mesoproterozoic times (~ 1100
575 Ma) is constrained by paleomagnetic data from the Tieling formation of the
576 Jixian Province (Zhang et al., 2006). The paleomagnetic pole appears to be
577 primary having passed both fold and reversal tests; however, the age of the
578 magnetization remains tentative. Nevertheless, we use these results to position
579 the North China block in our reconstruction.

580 The position of the Siberian block is contentious during Rodinia
581 assembly (Sears and Price, 2000; Pisarevsky and Natapov, 2003; Meert and
582 Torsvik, 2003; Li et al., 2008; Pisarevsky et al., 2008). In a majority of Rodinia
583 configurations, Siberia is placed with its (present-day) southern margin in the
584 vicinity of northern Laurentia (Gallet, 2000; Pisarevsky and Natapov, 2003; Li
585 et al., 2008). Others argue for either non – inclusion of the Siberian craton
586 within the Rodinia assembly (Meert and Torsvik, 2003; Pisarevsky et al., 2008)
587 or place Siberia adjacent to the present-day Cordilleran margin of Laurentia
588 (Sears and Price, 2003). We use paleomagnetic data from the Late
589 Mesoproterozoic Malgina and Linok formations of southeastern Uchur-Maya
590 region and northeastern Turukhansk region of the Siberia craton (Gallet, 2000)
591 in our reconstruction. Chemostratigraphic, biostratigraphic and isotopic data
592 constrain the age of these two formations between 1100 and 1050 Ma and the

593 presence of positive fold and reversal tests; together with a conglomerate test
594 suggest a primary magnetization in these rocks.

595 Figure 11 shows the paleogeographic reconstruction of Rodinia at ~1.1
596 Ma utilizing the paleomagnetic poles from the above mentioned cratonic blocks.
597 This time period of 1100 Ma is known to record the first phase of Rodinia
598 assembly (Pesonen et al., 2003). Our reconstruction is based on the “closest
599 approach” technique as described in Meert and Stuckey (2002); Buchan et al.
600 (2000, 2001) and Pesonen et al. (2003), using individual poles to reconstruct
601 the continents to their correct palaeolatitudinal position since paleomagnetism
602 cannot provide longitudinal control.

603 In our reconstruction, the combined mean of Portage Lake volcanics and
604 Keweenawan poles (normal + reversed) (Pesonen et al., 2003; Goodge et al.,
605 2008; Swanson-Hysell et al., 2009) places Laurentia at an intermediate
606 latitudinal position with the North China block at its present day north and
607 Australia located further south. Zhang et al. (2006) suggested a common APW
608 path for the North China Block (NCB) and Laurentia from ca. 1200 Ma to ca.
609 700 Ma in support of an NCB-Laurentia connection during this interval.
610 Siberia is placed at a distance from Laurentia to accommodate the North China
611 block, with its southern margin facing the northern margin of Laurentia
612 (Rainbird et al., 1998; Pisarevsky et al., 2008). While the position of Laurentia
613 is well constrained at this interval, the placement and orientation of Siberia
614 and NCB remains poorly understood and requires additional support. Pesonen

615 et al. (2003) suggested a southerly drift for Baltica away from Laurentia
616 between 1.25 Ga and 1.1 Ga based on the paleomagnetic data from the
617 Sveconorwegian Province (Poorter, 1975; Patchett and Buylund, 1977; Pesonen
618 and Neuvonen, 1981). In our reconstruction, Baltica occupies an independent
619 southerly latitudinal position derived from the combined paleomagnetic pole
620 from the 1095 Ma Bamble intrusives. A tighter fit can be obtained between the
621 Baltica and Laurentia by inverting the polarity of the Bamble dykes pole;
622 however, this position would require southern Baltica to face the northern
623 margin of Laurentia for which there is little support from the geology. Thus, we
624 follow the southern palaeolatitudinal option of Pesonen et al. (2003) to
625 constrain Baltica in our reconstruction (also see Salminen et al., 2009).

626 Based on the available paleomagnetic data from Kalahari and Laurentia,
627 Kalahari is located too far south of Laurentia to support any linkage between
628 the two blocks (Hanson et al., 2004a; Gose et al., 2006). The ~1070 Ma
629 Bangemall Sill pole from Western Australia (Wingate et al., 2002) constrains
630 the Australia-Mawson landmass at low to intermediate palaeolatitudes along
631 the southern margin of Laurentia. In their reconstruction, Powell and
632 Pisarevsky (2002) suggested that the Kalahari craton is separated from
633 Laurentia by the Australia – Mawson cratons. They noted that ~1080 Ma
634 deformation in the Darling belt along the western margin of Australian margin
635 might link with the coeval deformation in the Natal and Maud belts along the
636 southern margin of Kalahari. Such an interpretation is possible within the
637 framework of Figure 11. This separation of the Kalahari and Laurentia at 1.1

638 Ga – 1.0 Ga is such that it allows the placement of parts of East Gondwana to
639 the southwest or south of Laurentia (Meert and Torsvik, 2003; Pesonen et al.,
640 2003). Among the elements of the East Gondwana, the link between India and
641 East Antarctica remains paleomagnetically untested for this interval due to the
642 absence of any paleomagnetic data from East Antarctica at ~ 1100 Ma.
643 However, the proposed geological coherence of the Mawson block with Australia
644 in post-1200 Ma Rodinia reconstructions (Cawood and Korsch, 2008; Payne et
645 al., 2009; Wang et al., 2008; Kelly et al., 2002; Torsvik et al., 2001) and the
646 disposition of India at low latitudes (this study) do favor a loose association of
647 these cratonic elements, with India positioned at the southern margin of the
648 Mawson block. Meert et al. (1995) and Meert (2003) argue that East
649 Gondwanaland was not a coherent entity until late Neoproterozoic or Early
650 Cambrian (see also Fitzsimons, 2000a; b; Boger et al., 2001, 2000; Powell and
651 Pisarevsky et al., 2002). We have reliable paleomagnetic data from India and
652 Australia, but to make any robust conclusion our interpretation relies upon
653 additional paleomagnetic data from the East Antarctica craton at this interval.

654 The time period of ~1.1 Ga represents the initial phase of the Rodinia
655 amalgamation. Our paleomagnetic reconstruction at ~1.1 Ga is based on the
656 existing database with smaller number of continental blocks well constrained
657 in space and time. The palaeoconfiguration of these blocks suggest a loose
658 association within Rodinia with no paleomagnetic poles from majority of the
659 West Gondwana elements.

660 ~ **2.0 Ga Paleomagnetism**661 *Tectonic evolution of the Aravalli and Dharwar protocontinents*

662 A series of collisional events took place during the Paleoproterozoic
663 interval (~2.1 – 1.8 Ga) on a near global scale (Zhao et al., 2002; French et al.,
664 2008). The 2.0 - 1.8 Ga orogenic belts are thought to be the result of accretion
665 of Archaean cratonic nuclei to form numerous supercratons or possibly, a
666 supercontinent (Hoffman, 1988; Gower et al., 1990; 1992; Krapez, 1999;
667 Rogers and Santosh, 2002, 2003; Condie, 2002; Zhao et al., 2002, 2004).

668 The Central Indian Tectonic zone (CITZ) is a linear Paleoproterozoic
669 orogenic belt that represents the locus of collision between the northern
670 Aravalli protocontinent (Aravalli-Delhi belt, Bundelkhand massif and Vindhyan
671 basin) and the southern Dharwar protocontinent (Bastar, Singhbhum,
672 Dharwar cratons and Southern Indian Granulite terrane; figure. 12a). The
673 connection between the Bastar, Singhbhum and Dharwar cratons of the South
674 Indian block is well established at least by 1.9 Ga (Ramchandra et al., 1995;
675 French et al., 2008). The temporal control on the collision between the Aravalli
676 and the Dharwar protocontinents is still contentious (Meert et al., 2010). Stein
677 et al. (2004) proposed an oblique collision between the northern and southern
678 blocks around 2.5 Ga with the initiation of the formation of CITZ at this time.
679 Other authors argue for a ~1.9-1.6 Ga collision between the two blocks
680 (Acharyya et al., 2003) or even much younger ~1.0 Ga (Bhowmik et al., 2011).

681 If we accept a pre-2.0 Ga age for the amalgamation between the northern
682 and southern Indian cratons, then we can use our new paleomagnetic data
683 from the ~2.0 Ga NW-SE trending mafic dykes intruding the Bundelkhand
684 craton combined with paleomagnetic data from the ~1.9 Ga mafic dykes of the
685 Bastar craton (Meert et al., 2010; French et al., 2008), Cuddapah trap
686 volcanics (Clark, 1982) and a dyke adjacent to the Cuddapah basin in the
687 Dharwar craton (Kumar and Bhalla, 1983) to provide some insight into the drift
688 history of the Aravalli and Dharwar protocontinents (figure 12b). The
689 combined result from the ~2.0 Ga NW-SE trending older suite of dykes from
690 the Bundelkhand craton yield a paleomagnetic pole for India at 58.5°N and
691 312.5°E ($dp = 4.9^\circ$; $dm = 9.7^\circ$) and places the Bundelkhand craton in an
692 equatorial position (figure 12b). The combined 1.9 Ga paleomagnetic pole for
693 the Dharwar and Bastar cratons falls at 31° N, 330°E ($dp = 6.3^\circ$; $dm = 12.2^\circ$)
694 and also places these cratonic nuclei at low latitudes (Meert et al., 2011). A
695 nearly equatorial position for the Bundelkhand craton is also indicated by the
696 paleomagnetic data from ~ 1.8 Ga Gwalior volcanics of the Bundelkhand craton
697 that generates a paleomagnetic pole for the cratonic nuclei at 15.4° S and
698 353.2°E ($dp = 5.6$; $dm = 11.2$; Pradhan et al., 2010). Utilizing the three
699 paleomagnetic poles from the Bundelkhand dykes, Bastar-Cuddapah dykes
700 and the Gwalior volcanics, an apparent polar wander (APW) path was
701 constructed for the Indian peninsular shield during the 2.0- 1.8 Ga interval
702 (figure 12b). The APWP indicates that India rotated through 80 degrees with
703 only slight changes in paleolatitude during this interval.

704 *Implications for Columbia*

705 The Paleo-Mesoproterozoic history of the Earth is punctuated by the
706 presence of globally distributed 2.1-1.8 Ga collisional orogens related to a
707 proposed pre-Rodinian supercontinent named Columbia (Zhao et al., 2002;
708 Zhao et al., 2004a, b; Condie, 2000, 2002; Rogers and Santosh, 2002; Kusky et
709 al., 2007a; French et al., 2010). In particular, the Columbia model by Zhao et
710 al. (2004) is based primarily on the geological connections between globally
711 distributed cratonic nuclei and the presence of the Paleo-Mesoproterozoic
712 orogenic belts (2.1-1.8 Ga; figure 13a).

713 Reliable paleomagnetic data provide a quantitative reference frame for
714 documenting the history and dynamics of the plate tectonic regime and
715 constraining the position of various cratonic blocks within the proposed
716 continental assemblies. Any attempt at global reconstructions in the
717 Precambrian is an arduous task due to the scarcity of well-dated
718 paleomagnetic data, polarity ambiguity and the absence of longitudinal control
719 in positioning of the continents (Van der Voo and Meert, 1991; Meert, 2002;
720 Meert et al., 2011). In addition, the majority of present day continents are an
721 amalgam of older Archean cratonic nuclei that were not fully welded until
722 Mesoproterozoic or later time.

723 The paleomagnetic database for the Paleoproterozoic has improved over
724 the past decade as reliable and well-dated poles are becoming more
725 commonplace. Below, we discuss the paleogeographic reconstruction of the

726 Paleoproterozoic Columbia supercontinent utilizing the most updated
727 paleomagnetic results from various cratonic blocks at ~2.0 Ga (figure 13b;
728 table 3a).

729 The ~ 2.0 Ga paleomagnetic pole calculated from the NW-SE trending
730 dyke suite of the Bundelkhand craton constrains the position of the North
731 Indian Block (Aravalli protocontinent) in our reconstruction. As noted above,
732 the North Indian and the South Indian blocks of the peninsular India were in
733 close proximity during 2.1 – 1.9 Ga (also see Meert et al., 2011; Stein et al.,
734 2004). Hence, we suggest that the ~ 2.0 Ga pole from the Bundelkhand dykes
735 is representative of a major portion of Peninsular India for this time period.

736 The palaeolatitudinal position of the Superior craton of the Laurentian
737 block is constrained at ~2.0 Ga via the paleomagnetic data from the diabase
738 dykes of the Minto block of the northeastern Superior Province (Buchan et al.,
739 2000). The Minto dykes paleomagnetic pole has a positive baked contact test
740 and is precisely dated at 1998 ± 2 Ma by U-Pb isotopic methods (Buchan et al.,
741 2000). Most of the other cratonic nuclei of Laurentia such as Slave-Rae-
742 Hearne and Wyoming blocks collided with the Superior craton during Trans-
743 Hudson orogeny (2.1-1.8 Ga), although the terminal collision was protracted
744 until ~1.78 Ga (Corrigan et al., 2005). Recent paleomagnetic studies on the
745 Lac de Gras diabase dykes across the Slave Province of the Canadian Shield
746 suggest that the Slave and Superior cratons were located at similar latitudes at
747 ~2.02 Ga but with different relative orientations than today (Buchan et al.,

748 2009). Due to the absence of coeval paleomagnetic data from other cratonic
749 blocks of Laurentia at ~2.0 Ga, we use the Minto dyke pole as representative
750 for Laurentia assuming that the other Laurentian nuclei were in close
751 proximity during this period.

752 A low to intermediate latitudinal position for the Fennoscandian shield
753 during Paleoproterozoic is based on paleomagnetic data between 2.2 and 1.97
754 Ga (Pisarevsky and Sokolov, 1999; Neuvonen et al., 1997; Mertanen and
755 Pesonen, 1994). The paleoposition of the Fennoscandia is constrained in our
756 reconstruction utilizing the only available paleomagnetic pole from the $1974 \pm$
757 27 Ma (Sm-Nd age) Konchozero peridotite sill (component I) of the
758 Fennoscandia (Pisarevsky and Sokolov, 1999).

759 According to Bogdanova et al. (1994) the Ukrainian shield was probably
760 attached to the Fennoscandia at ca. 2.0 Ga. However, the paleomagnetic data
761 for the Ukrainian shield between ca. 2.0 and 1.72 Ga suggest that the final
762 accretion of Fennoscandia to the Ukrainian shield took place sometimes after
763 ca. 1.8 Ga (Elming et al., 2001). The position of the Ukrainian shield at ~2.0 Ga
764 in our reconstruction is derived from the paleomagnetic data from the gabbro
765 diabase dyke of the southern Sarmatia province of Baltica (Elming et al., 2001).

766 The Kalahari craton of South Africa consists of the Kaapvaal and the
767 Zimbabwe blocks welded together along the Limpopo belt sometime between
768 1.9 Ga and 2.06 Ga (De Wit et al., 1992; Lubnina et al., 2010b; Hanson et al.,
769 2011). Paleomagnetic data for the Zimbabwe craton at ~2.0 Ga are lacking and

770 therefore its connection with the Bushveld complex of the Kaapvaal craton is
771 also ambiguous (Lubnina et al., 2010b; Soderlund et al., 2010). We use
772 updated paleomagnetic data from the ~2.02 Ga Vredefort dykes/impact
773 structures of the Kaapvaal craton to constrain its position at ~2.0 Ga in our
774 reconstruction (Salminen et al., 2009; Carporzen et al., 2006; Pesonen et al.,
775 2002).

776 The metamorphosed Uauã mafic dykes of São Fransisco provide the only
777 paleomagnetic pole for Congo-São Fransisco cratons at ~2.0 Ga (De'Agrella
778 Filho and Pacca, 1998). Paleomagnetic, petrographic and geochronological
779 evidence support a secondary origin of magnetization in these dykes, probably
780 acquired approximately at 2 Ga-1.9 Ga, during the uplift and regional cooling
781 of the Transamazonian cycle (De'Agrella Filho and Pacca, 1998).

782 Nomade et al. (2003, 2001) reported a paleomagnetic pole from the
783 Oyapok-Campoi river zone (OYA in their manuscript) of the French Guiana
784 shield of the Amazonian craton with a magnetization age of 2036 Ma. Other
785 paleomagnetic poles that exist for the Amazonian craton at ~2.0 Ga come from
786 the Encrucijada pluton of the Venezuela block (Onstott and Hargraves, 1981).
787 The statistical precision on the Rb-Sr ages of the Encrucijada granites are poor
788 and the ages are considered rather inconsistent. The two poles are
789 significantly different and, on the basis of the difference, it was argued that
790 there was northward movement along the Pisco Jurua fault zone during the
791 2036 - 2000 Ma period (Onstott and Hargraves, 1981; Nomade et al., 2001).

792 Although not united but lying in close association, we consider the OYA poles
793 to constrain the position of the Amazonia craton in our ~2.0 Ga reconstruction.

794 Utilizing all the available paleomagnetic data from the cratonic blocks
795 mentioned above, we attempt to test the proposed Columbia configuration of
796 Zhao et al. (2002, 2004a,b). Figure 13(a) represents the typical Columbia
797 configuration of Zhao et al. (2004) based on the correlation of the coeval
798 orogenic belts (2.1 - 1.8 Ga) within its constituent cratonic blocks. The Zhao et
799 al. (2004) configuration is not supported by the existing paleomagnetic
800 database at ca. 2.0 Ga (figure 13b; table 3a). The majority of these continental
801 nuclei occupy low to intermediate latitudinal positions as they did in the
802 Kenorland assembly at ca. 2.45 Ga (Salminen et al., 2009; Pesonen et al.,
803 2003). The only resemblance to the Columbia model by Zhao et al. (2004) is
804 exhibited by the juxtaposition of the parts of Amazonia and West-Africa (figure
805 13b; table 3a).

806 In the traditional Columbia configuration, India is placed adjacent to
807 East Antarctica and North China along the present day south-western margin
808 of Laurentia (Zhao et al., 2004). The Kalahari craton of South Africa, on the
809 other hand, is positioned along the north-western margin of Australia (figure
810 12a). In our reconstruction, the new paleomagnetic data from ~2.0 Ga
811 Bundelkhand dykes (this study) constrain the position of India at nearly
812 equatorial latitudes with Laurentia occupying low to intermediate latitudes.
813 The Kaapvaal block of the Kalahari craton can be placed at mid-latitudes either

814 north or south depending upon polarity choice. Baltica did not exist as a
815 coherent block at ~2.0 Ga and the available paleomagnetic data from the
816 Fennoscandian and the Ukrainian shield position these two blocks at mid-
817 latitudes with no obvious connection to Laurentia (Salminen et al., 2009).

818 The African and South-American continental fragments represent a loose
819 connection in the configuration at ~2.0 Ga and may show the only resemblance
820 to the archetypal Columbia model of Zhao et al. (2004). The low southerly
821 latitudinal positions indicated by the paleomagnetic data for Amazonia, West
822 Africa and Congo-Sao Fransisco blocks may indicate that these were
823 juxtaposed at ~2.0 Ga (Nomade et al., 2001, 2003). The presence of coeval
824 Trans-Amazonian and Eburnean orogenic events in Amazonia (Hartmann,
825 2002) and West Africa (Ledru et al., 1994) respectively, may lend additional
826 support to their connection at 2.1-1.9 Ga.

827 Although our reconstruction at ~2.0 Ga is based on limited number of
828 paleomagnetic poles from a small number of cratonic blocks, most of the poles
829 are reasonably constrained in both time and space. Thus, we cannot reject the
830 existence of a “Columbia-type” supercontinent during the Paleoproterozoic;
831 though the independent drift of most of the continental blocks at ~ 2.0 Ga
832 enables us to reject some of the relationships between cratonic blocks
833 suggested in the Columbia model by Zhao et al. (2004).

834

835 **Conclusions**

836 (1). The paleomagnetic and geochronological results on the mafic dyke
837 swarms intruding the Archean - Paleoproterozoic Bundelkhand craton
838 presented in this paper are significant not only in providing reliable age
839 constraints for these magmatic events, but also for improving our
840 understanding of the tectonic evolution of the Central Indian shield. The three
841 distinctive paleomagnetic directions obtained in this study for the mafic dyke
842 swarms suggest three different pulses of emplacement within the BC. The
843 precise U-Pb isotopic zircon age of ~1980 Ma for the NW-SE trending dyke
844 (sample I9GS-13) and 1113 Ma for the ESE-WSW trending great dyke of
845 Mahoba support our paleomagnetic analysis and the geologic correlations.

846 (2) This study provides a refined virtual geomagnetic pole for the Mahoba
847 suite of dykes at 37.8°S, 49.5°E ($dp/dm=10.8/18.3$). This geomagnetic pole
848 correlates well with the VGP generated for the Majhgawan kimberlite and the
849 poles from the Bhandar-Rewa Groups of the Upper Vindhyan sequence
850 (Gregory et al., 2006; Malone et al., 2008). Our interpretation of the Mahoba
851 paleomagnetic and geochronological results lend further support to the
852 argument that the closure age for the Upper Vindhyan rocks is older than 1000
853 Ma.

854 (3) The paleomagnetic results from the ~1980 Ma NW-SE trending dyke
855 suite of the Bundelkhand craton along with other published data from the
856 1800-2000 Ma interval indicates a close proximity between the major elements
857 of Peninsular India (Aravalli-Bundelkhand and Dharwar-Bastar and

858 Singhbhum cratons). This would suggest that the younger tectono-magmatic
859 events recorded in the CITZ represent crustal-scale reactivation along an
860 existing zone of weakness.

861 (4) We also provide paleogeographic reconstructions at 2.0 Ga and 1.1
862 Ga. Our ~2.0 Ga pole from the NW-SE trending Bundelkhand dykes favors a
863 low latitudinal position for India with mid latitudinal disposition of Laurentia
864 and the Kaapvaal block. The proposed connection of India to East Antarctica
865 and North China (Zhao et al., 2004) remains untested due to the absence of
866 paleomagnetic data from North China and East Antarctica cratons at ~2.0 Ga.
867 Laurentia and India can be placed in proximity to each other but in a vastly
868 different configuration than that suggested by Zhao et al. (2004) based on the
869 geometric relationships of the radiating dyke swarms. The global
870 paleogeography at ~2.0 Ga favors scattered independent continental blocks as
871 suggested by Pesonen et al. (2003; also see Salminen et al., 2009) and does not
872 support the Columbia model of Zhao et al. (2004).

873 (5) With reference to Rodinia, one of the interesting implications of our results
874 from ~1113 Ma Mahoba dyke pole in conjunction with the coeval Majhgawan
875 kimberlite and Bhandar-Rewa poles is that it infers a low latitudinal position
876 for India with Australia – Mawson blocks located at mid latitudes. The link
877 between India and East Antarctica remains paleomagnetically untested for this
878 interval due to the absence of any paleomagnetic data from the East Antarctica
879 block. However, the proposed geological coherence of the Mawson block with

880 Australia in post-1200 Ma configurations (Cawood and Korsch, 2008; Payne et
881 al., 2009; Wang et al., 2008; Kelly et al., 2002; Torsvik et al., 2001) and the
882 disposition of India at low latitudes (this study) might indicate a loose East
883 Gondwana fit, with India positioned further south of East Antarctica.

884

885 Acknowledgements

886 This work was supported by a grant from the US National Science
887 Foundation to J.G. Meert (EAR09-10888). We wish to thank Shawn Malone for
888 the careful proofreading of the manuscript. We would also like to thank Dr.
889 Rajesh Srivastava and an anonymous reviewer for the thorough and thoughtful
890 review of the manuscript.

891

892

893 References

894 Acharyya, S.K, 2003. The nature of the Mesoproterozoic Central Indian
895 Tectonic Zone with exhumed and reworked older granites. *Gondwana*
896 *Research* 6, 197-214.

897 Auden, J.B., 1933. Vindhyan sedimentation in the Son-Valley, Mirzapur
898 district, *Memoir of Geological Survey of India*, 141-250.

899

900 Azmi R.J., Joshi, D., Tiwari, B.N., Joshi, M.N., Srivastava, S.S., 2008. A
901 synoptic view on the current discordant geo- and biochronological ages of
902 the Vindhyan Supergroup, Central India. *Himalayan Geology* 29,177-191.

903 Basu, A. K., 1986. Geology of parts of Bundelkhand and Granite Massif,
904 Central India, *Geological Survey of India Records* 117, 61-124.

905

906 Bleeker, W., Ernst, R.E., 2006. Short-lived mantle generated magmatic events
907 and their dyke swarms: the key to unlocking Earth's paleogeographic
908 record back to 2.5 Ga. In: *Symposium Volume for Fifth International Dyke*
909 *Conference, July-August 2005. Balkema, Rotterdam.*

910

911 Bhowmik, S.K., Wilde, S.A., Bhandari, A., Pal, T., Pant, N.C., 2011. Growth of
912 the Greater Indian landmass and its assembly in Rodinia:
913 Geochronological evidence from the Central Indian Tectonic Zone,
914 *Gondwana Research*, doi:10.1016/j.gr.2011.09.008.

- 915
916 Boger, S.D., Carson, C.J., Wilson, C.J.L., Fanning, C.M., 2000. Neoproterozoic
917 deformation in the Radok Lake region of the northern Prince Charles
918 Mountains East Antarctica; evidence for a single protracted orogenic event.
919 *Precambrian Research* 104, 1–24.
920
- 921 Boger, S.D., Wilson, C.J.L., Fanning, C.M., 2001. Early Paleozoic tectonism
922 with the East Antarctic craton: the final suture between east and west
923 Gondwana. *Geology* 29, 463– 466.
924
- 925 Bogdanova, S.V., Bibikova, E.V., Gorbachev, R., 1994. Palaeoproterozoic U–Pb
926 zircon ages from Belorussia: new geodynamic implications for the East
927 European craton. *Precambrian Research* 68, 231–240.
928
- 929 Buchan, K.L., Mertanen, S., Park, R.G., Pesonen, L.J., Elming, S.-Å.,
930 Abrahamsen, N., Bylund, G., 2000. Comparing the drift of Laurentia and
931 Baltica in the Proterozoic: the importance of key poles. *Tectonophysics*
932 319, 167–198.
933
- 934 Buchan, K.L., Ernst, R.E., Hamilton, M.A., Mertanen, S., Pesonen, L.J.,
935 Elming, S.A., 2001. Rodinia: the evidence from integrated
936 palaeomagnetism and U–Pb geochronology. *Precambrian Research* 110, 9–
937 32.
938
- 939 Buchan, K.L., LeCheminant, A.N., Breemen, O.V., 2009. Paleomagnetism and
940 geochronology of Lac de Gras diabase dyke swarm, Slave Province,
941 Canada: Implications for relative drift of Slave and Superior provinces in
942 the Paleoproterozoic. *Canadian Journal of Earth Sciences* 46, 361–379.
943
- 944 Burke, K. and Dewey, J.F., 1972, Orogeny in Africa, in Dessauvagie, T.F.W.
945 and Whiteman, A.J., eds., *Proceedings of the Ibadan Conference on*
946 *African Geology*, December, 1970: Ibadan, Nigeria, 583–608.
947
- 948 Brown, L.L., McEnroe, S.A., 2004. Palaeomagnetism of the Egersund–Ogna
949 anorthosite, Rogaland, Norway, and the position of Fennoscandia in the
950 Late Proterozoic. *Geophysical Journal International* 158, 479 – 488.
951
- 952 Cawood, P.A., Korsch, R.J., 2008. Assembling Australia: Proterozoic building of
953 Australia. *Precambrian research* 166, 1–38.
954
- 955 Carporzen, L., Gilder, S.A., Hart, R.J., 2006. Origin and implications of Verwey
956 transitions in the basement rocks of the Vredefort meteorite crater, South
957 Africa. *Earth and Planetary Science Letters* 251, 305 - 317.
958

- 959 Chakrabarti, A., 1990. Traces and dubiotraces: examples from the so called
960 Late Proterozoic siliciclastic rocks of the Vindhyan SuperGroup around
961 Maihar, India. *Precambrian Research* 47, 141–153.
962
- 963 Clark, D.A., 1982. Preliminary paleomagnetic results from the Cuddapah traps
964 of Andhra Pradesh. *Monograph-2, On Evolution of the intracratonic*
965 *Cuddapah Basin, HPG, Hyderabad, India*, 47–51.
966
- 967 Condie, K.C., 2002. Breakup of a Paleoproterozoic supercontinent. *Gondwana*
968 *Research* 5, 41–43.
969
- 970 Corrigan, D., Hajnal, Z., Nemeth, B., Lucas, S. B., 2005. Tectonic framework of
971 a Palaeoproterozoic arc-continent to continent-continent collisional zone,
972 Trans-Hudson Orogen, from geological and seismic reflection studies.
973 *Canadian Journal of Earth Sciences* 42, 421–434.
974
- 975 Crawford, A. R., 1975. The Precambrian geochronology of Rajasthan and
976 Bundelkhand, northern India. *Canadian Journal of Earth Sciences* 7, 91-
977 110.
978
- 979 Crawford, A. R., Compston, W., 1970. The age of Vindhyan system of
980 peninsular India, *Quaternary Journal of Geological Society of London* 125,
981 351–371.
982
- 983 Dalziel, I.W.D., 1991. Pacific margins of Laurentia and East Antarctica–
984 Australia as a conjugate rift pair: evidence and implications for an
985 Eocambrian supercontinent. *Geology* 19, 598–601.
986
- 987 Dalziel, I.W.D., 1997. Neoproterozoic–Paleozoic geography and tectonics:
988 review, hypothesis and environmental speculation. *Bulletin of the*
989 *Geological Society of America* 109, 16–42.
990
- 991 Dalziel, I.W.D., Mosher, S., Gahagan, L.M., 2000. Laurentia – Kalahari collision
992 and the assembly of Rodinia. *Journal of Geology* 108, 499– 513.
993
- 994 D’Agrella-Filho, M.S., Pacca, I.G., 1998. Paleomagnetism of Paleoproterozoic
995 mafic dyke swarm from the Uauá region, Northeastern São Francisco
996 Craton, Brazil: tectonic implications. *Journal of South American Earth*
997 *Sciences* 11, 23–33.
998
- 999 Davis, D., and Sutcliffe, R., 1985, U-Pb ages from the Nipigon plate and
1000 northern Lake Superior: *Geological Society of America Bulletin* 96, 1572–
1001 1579.
1002

- 1003 De, C., 2003. Possible organisms similar to Ediacaran forms of the Bhandar
1004 Group, Vindhyan Super Group, Late Neoproterozoic of India. *Journal of*
1005 *Asian Earth Sciences* 21, 387–395.
- 1006 De, C., 2006. Ediacara fossil assemblage in the Upper Vindhyan of Central
1007 India and its significance. *Journal of Asian Earth Sciences* 27, 660–683.
1008
- 1009 Devaraju, T.C., Laajoki, L., Zozulya, D., Khanadali, S.D., Ugarkar, A.G., 1995.
1010 Neo-Proterozoic dyke swarms of southern Karnataka. Part II:
1011 Geochemistry, oxygen isotope composition, Rb–Sr age and petrogenesis.
1012 *Memoir Geological Society of India* 33, 267–306.
1013
- 1014 Dewey, J.F., Burke, K.C.A., 1973. Tibetan, Variscan and Precambrian
1015 basement reactivation: products of continental collision. *Journal of*
1016 *Geology* 81, 683–692.
1017
- 1018 De Wit, M.J., de Ronde, C.E.J., Tredoux, M., Roering, C., Hart, R.J.,
1019 Armstrong, R.A., Green, R.W.E., Peberdy, E., Hart, R.A., 1992. Formation
1020 of an Archean continent. *Nature* 357, 553–562.
1021
- 1022 Drury, S.A., 1984. A Proterozoic intracratonic basin, dyke swarms and thermal
1023 evolution in south India. *Journal of Geological Society of India* 25, 437–
1024 444.
1025
- 1026 Elming, S.-Å., Mattsson, H., 2001. Post Jotnian basic intrusion in the
1027 Fennoscandian Shield, and the breakup of Baltica from Laurentia: a
1028 palaeomagnetic and AMS study. *Precambrian Research* 108, 215–236.
1029
- 1030 Ernst, R.E., Srivastava, R.K., 2008. India's place in the Proterozoic world:
1031 constraints from the large igneous provinces (LIP) record. In: Srivastava,
1032 R.K., Sivaji, Ch., Chalapathi Rao, N.V. (Eds.), *Indian Dykes: Geochemistry,*
1033 *Geophysics, and Geochronology*. Narosa Publishing House Pvt. Ltd., New
1034 Delhi, India, pp. 41–56.
1035
- 1036 Ernst, R.E., Wingate, M.T.D., Buchan, K.L., Li, Z.X., 2008. Global record of
1037 1600–700 Ma Large Igneous Provinces (LIPs): Implications for the
1038 reconstruction of the proposed Nuna (Columbia) and Rodinia
1039 supercontinents. *Precambrian Research* 160, 159–178.
1040
- 1041 Ernst, R.E., Bleeker, W., 2010. Large igneous provinces (LIPs), giant dyke
1042 swarms, and mantle plumes: significance for breakup events within
1043 Canada from 2.5 Ga to the present. *Canadian Journal of Earth Sciences*
1044 47, 695–739, doi:10.1139/E10-025.
1045

- 1046 Fitzsimons, I.C.W., 2000a. A review of tectonic events in the East Antarctic
1047 shield, and their implications for Gondwana and earlier supercontinents.
1048 *Journal of African Earth Sciences* 31, 3– 23.
1049
- 1050 Fitzsimons, I.C.W., 2000b. Grenville-age basement provinces in East
1051 Antarctica: evidence for three separate collisional orogens. *Geology* 28,
1052 879– 882.
1053
- 1054 French, J.E., 2007. U–Pb Dating of Paleoproterozoic mafic dyke swarms of the
1055 South Indian shield: implications for paleocontinental reconstructions and
1056 identifying ancient mantle plume events. Ph.D. Thesis. University of
1057 Alberta, Edmonton, Alberta, 373.
1058
- 1059 French, J.E., Heaman, L.M., Chacko, T., Srivastava, R.K., 2008. 1891-1883 a
1060 southern Bastar craton-Cuddapah mafic igneous events, India: A newly
1061 recognized large igneous province. *Precambrian Research* 160, 308-322.
1062
- 1063 French, J.E., Heaman, L.M., 2010. Precise U-Pb dating of Paleoproterozoic
1064 mafic dyke swarms of the Dharwar craton, India: Implications for the
1065 existence of the Neoproterozoic supercraton Sclavia. *Precambrian Research*
1066 183, 416-441.
1067
- 1068 Gallet, Y., Pavlov, V.E., Semikhatov, M.A., Petrov, P.Y., 2000. Late
1069 Mesoproterozoic magnetostratigraphic results from Siberia:
1070 paleogeographic implications and magnetic field behavior. *Journal of*
1071 *Geophysical Research* 105, 16,481– 16,500.
1072
- 1073 Gopalan, K., MacDougall, J.D., Roy, A.B., Murali, A.K., 1990. Sm–Nd evidence
1074 for 3.3 Ga old rocks in Rajasthan, northwestern India. *Precambrian*
1075 *Research* 48, 287–297.
1076
- 1077 Goodge, J.W., Vervoort, J.D., Fanning, C.M., Brecke, D.M., Farmer, G.L.,
1078 Williams, I.S., Myrow, P.M., DePaolo, D.J., 2008. A Positive Test of East
1079 Antarctica - Laurentia Juxtaposition within the Rodinia Supercontinent.
1080 *Science* 321, 235-240.
1081
- 1082 Goodwin, A.M., 1991. *Precambrian Geology: The Dynamic Evolution of the*
1083 *Continental Crust*. Academic Press, London, pp. 666.
1084
- 1085 Gose, W.A., Helper, M.A., Connelly, J.N., Hutson, F.E., Dalziel, I.W.D., 1997.
1086 Paleomagnetic data and U–Pb isotopic age determinations from Coats
1087 Land, Antarctica: implications for late Proterozoic plate reconstructions.
1088 *Journal of Geophysical Research* 102, 7887– 7902.
1089

- 1090 Gose, W.A., Johnston, S.T., Thomas, R.J., 2004. Age of magnetization of
1091 Mesoproterozoic rocks from the Natal sector of the Namaqua–Natal belt,
1092 South Africa. *Journal of African Earth Sciences* 40, 137–145.
1093
- 1094 Gose, W.A., Hanson, R.E., Dalziel, I.W.D., Pancake, J.A., Seidel, E.K., 2006.
1095 Paleomagnetism of the 1.1Ga Umkondo large igneous province in southern
1096 African *Journal of Geophysical Research* 111, B09101,
1097 doi:10.1029/2005JB003897.
1098
- 1099 Gower, C.F., Ryan, A.B., Rivers, T., 1990. Mid-Proterozoic Laurentia-Baltica: an
1100 overview of its geological evolution and summary of the contributions by
1101 this volume. In: Gower, C.F., Rivers, T., Ryan, B., (Eds.), *Mid-Proterozoic*
1102 *Laurentia- Baltica*. Geological Association of Canada Special paper 38, 1-
1103 20.
1104
- 1105 Gower, C. F., Schärer, U., Heaman, L. M., 1992. The Labradorian Orogeny in
1106 the Grenville Province, eastern Labrador. *Canadian Journal of Earth*
1107 *Sciences* 29, 1944–1957.
1108
- 1109 Gregory, L.C., Meert, J.G., Pradhan, V., Pandit, M.K., Tamrat, E., Malone, S.J.,
1110 2006. A paleomagnetic and geochronological study of the Majhgawan
1111 Kimberlite, India: implications for the age of the Vindhyan SuperGroup.
1112 *Precambrian Research* 149, 65–75.
1113
- 1114 Halls, H.C., 1982. The importance of potential of mafic dyke swarms in studies
1115 of geodynamic process. *Geoscience Canada* 9, 129–143.
1116
- 1117 Halls, H. C., 1987. Dyke swarms and continental rifting some concluding
1118 remarks. In: H. C. Halls and W. F. Fahrig (Eds.), *Mafic Dyke Swarms*.
1119 Geological Association of Canada Special paper 34, 5-24.
1120
- 1121 Halls, H.C., Pesonen, L.J., 1982. Paleomagnetism of Keweenawan rocks.
1122 Geological Society of America, *Memoir* 156, 173–201.
1123
- 1124 Halls, H.C. Zhang, B., 1995. Tectonic implications of clouded feldspar in
1125 Proterozoic mafic dykes. In *Dyke Swarms of Peninsular India*, edited by
1126 Devaraju, T.C., *Memoir Geological Society of India* 33, 65- 80.
1127
- 1128 Halls, H.C., Kumar, A., Srinivasan, R., Hamilton, M.A., 2007. Paleomagnetism
1129 and U–Pb geochronology of easterly trending dykes in the Dharwar craton,
1130 India: feldspar clouding, radiating dyke swarms and the position of India
1131 at 2.37 Ga. *Precambrian Research* 155, 47–68.
1132
- 1133 Hanson, R.E., Gose, W.A., Crowley, J.L., Ramezani, J., Bowring, S.A., Bullen,
1134 D.S., Hall, R.P., Pancake, J.A., Mukwakwami, J., 2004a. Paleoproterozoic
1135 intraplatemagmatism and basin development on the Kaapvaal Craton: age,

- 1136 paleomagnetism and geochemistry of ~1.93 to ~1.87 Ga post-Waterberg
1137 dolerites. *South African Journal of Geology* 107, 233–254.
- 1138
- 1139 Hanson, R.E., Rioux, M., Gose, W.A., Blackburn, T.J., Bowring, S.A.,
1140 Mukwakwami, J., Jones, D.L., 2011. Paleomagnetic and
1141 geochronological evidence for large-scale post-1.88 Ga displacement
1142 between the Zimbabwe and Kaapvaal cratons along the Limpopo belt.
1143 *Geology* 39 (5), 487–490.
- 1144
- 1145 Hargraves, R.B., Hattingh, P.J., Onstott, T.C., 1994. Palaeomagnetic results
1146 from the Timbavati gabbros in the Kruger National Park, South Africa.
1147 *South African Journal of Geology* 97, 114 – 118.
- 1148
- 1149 Hartmann, L.A., 2002. The mesoproterozoic supercontinent Atlantica in the
1150 Brazilian Shield; review of geological and U–Pb zircon and Sm–Nd isotopic
1151 evidence. In: Rogers, J.W., Santosh, M. (Eds.), *Mesoproterozoic*
1152 *Supercontinent. Gondwana Research* 5, 157– 163.
- 1153
- 1154 Hoffman, P.F., 1988. United plates of America, the birth of a craton. *Annual*
1155 *Review of Earth and Planetary Science* 16, 543–603.
- 1156
- 1157 Hoffman, P.F., 1991. Did the breakout of Laurentia turn Gondwanaland inside
1158 out? *Science* 252, 1409–1412.
- 1159
- 1160 Jacobs, J., Pisarevsky, S., Thomas, R.J., Becker, T., 2008. The Kalahari Craton
1161 during the assembly and dispersal of Rodinia. *Precambrian Research* 160,
1162 142–158
- 1163
- 1164 Jayananda, M., Moyen, J.F., Martin, H., Peucat, J.-J., Auvray, B.,
1165 Mahabaleswar, B., 2000. Late Archaean (2550–2520 Ma) juvenile
1166 magmatism in the Eastern Dharwar craton, southern India: constraints
1167 from geochronology, Nd–Sr isotopes and whole rock geochemistry.
1168 *Precambrian Research* 99, 225–254.
- 1169
- 1170 Jones, D.L., McElhinny, M.W., 1966. Paleomagnetic correlation of basic
1171 intrusions in the Precambrian of southern Africa. *Journal of Geophysical*
1172 *Research* 71, 543– 552.
- 1173
- 1174 Jones, D.L., Powell, C. McA., 2001. Palaeomagnetic results from the Umkondo
1175 Large Igneous Province and their relevance to Rodinia. Fourth
1176 International Dyke Conference, South Africa 26– 29 June, 2001, Program
1177 and Abstracts, 34.
- 1178
- 1179 Karlstrom, K.E., Harlan, S.S., Williams, M.L., McClelland, J., Geissman, J.W.,
1180 Å häll, K. I., 1999. Refining Rodinia: geologic evidence for the Australia–
1181 western US connection in the Proterozoic. *GSA Today* 9 (10), 1 – 7.

- 1182
1183 Kelly, N. M., Clarke, G. L., Fanning, C. M., 2002. A two-stage evolution of the
1184 Neoproterozoic Rayner Structural Episode: new U–Pb sensitive high
1185 resolution ion microprobe constraints from the Oygarden Group, Kemp
1186 Land, East Antarctica. *Precambrian Research* 116, 307–330.
1187
- 1188 Klootwijk, C.T., Nazirullah, R., de Jong, K.A., 1986. Paleomagnetic constraints
1189 on formation of the Mianwali re-entrant, Trans-Indus and Western Salt
1190 Range, Pakistan. *Earth and Planetary Science Letters* 80, 394–414.
1191
- 1192 Krapez, B., 1999. Stratigraphic record of an Atlantic-type global tectonic cycle
1193 in the Palaeoproterozoic Ashburton Province of Western Australia.
1194 *Australian Journal of Earth Sciences* 46, 71–87.
1195
- 1196 Kumar, B., Das Sharma, S., Sreenivas, B., Dayal, A.M., Rao, M.N., Dubey, N.,
1197 Chawla, B.R., 2002. Carbon, oxygen and strontium isotope geochemistry
1198 of Proterozoic carbonate rocks of the Vindhyan Basin, central India.
1199 *Precambrian Research* 113, 43–63.
1200
- 1201 Kumar, S., Srivastava, P., 1997. A note on the carbonaceous megafossils from
1202 the Neoproterozoic Bhandar Group, Maihar area, Madhya Pradesh.
1203 *Journal of Paleontological Society of India* 42, 141–146.
1204
- 1205 Kumar, S., 2001. Mesoproterozoic megafossil Chuaria-Tawuia association may
1206 represent parts of a multicellular plant, Vindhyan Supergroup, central
1207 India. *Precambrian Research* 106, 187–211.
1208
- 1209 Kumar, A., Bhalla, M.S., 1983. Paleomagnetism and igneous activity of the area
1210 adjoining the south-western margin of the Cuddapah basin, India.
1211 *Geophysical Journal of Royal Astronomical Society* 73, 27–37.
1212
- 1213 Kusky, T.M., Li, J.H., Santosh, M., 2007. The Paleoproterozoic North Hebei
1214 Orogen: North China craton's collisional suture with the Columbia
1215 supercontinent. *Gondwana Research* 12, 4–28.
1216
- 1217 Lauerma, R., 1995. Kursun ja Sallan kartta-alueiden kalliopera. Summary:
1218 Pre-Quaternary rocks of the Kursu and Salla map-sheet areas. Geological
1219 map of Finland 1:100000, Explanation to the map of Pre-Quaternary
1220 Rocks, Sheets 3643,4621 +4623, pp. 40.
1221
- 1222 Ledru, P., Johan, V., Milesi, P., Tegye, M., 1994. Markers of the last stages of
1223 the Palaeoproterozoic collision: evidence for a 2 Ga continent involving
1224 circum- South Atlantic provinces. *Precambrian Research* 69, 169–191.
1225
- 1226 Li, Z.X., Bogdanova, S.V., Collins A.S., Davidson A., De Waele B., Ernst R.E.,
1227 Fitzsimons I.C.W., Fuck R.A., Gladkochub D.P., Jacobs J., Karlstrom K.E.,

- 1228 Lu S., Natapov L.M., Pease V., Pisarevsky S.A., Thrane K., Vernikovsky V.,
1229 2008. Assembly, configuration, and break-up history of Rodinia: A
1230 synthesis. *Precambrian Research* 160, 179-210.
1231
- 1232 Lubnina, N.V., Ernst, R., Klausen, M., Söderlund, U., 2010. Paleomagnetic
1233 study of NeoArchean- Paleoproterozoic dykes in the Kaapvaal craton,
1234 *Precambrian Research* 183, 523-552.
1235
- 1236 Ludwig, K.R., 1999. User's Manual for Isoplot/Ex Version 2.02, A
1237 Geochronological Toolkit for Microsoft Excel. Berkeley Geochronology
1238 Center Special publication 1a, Berkeley, CA, USA.
1239
- 1240 Malone, S.J., Meert, J.G., Banerjee, D.M., Pandit, M.K., Tamrat, E., Kamenov,
1241 G.D., Pradhan, V.R., Sohl, L.E., 2008. Paleomagnetism and detrital zircon
1242 geochronology of the Upper Vindhyan sequence, Son Valley and
1243 Rajasthan, India: a ca. 1000Ma closure age for the Purana basins?
1244 *Precambrian Research* 164, 137-159.
1245
- 1246 Malviya, V. P., Arima, M., Pati, J. K., Kaneko, Y., 2004. First report of
1247 metamorphosed basaltic pillow lava from central part of Bundelkhand
1248 craton, India: An Island arc setting of possible Late Archaean age,
1249 *Gondwana Research* 7, 1338-1340.
1250
- 1251 Malviya, V.P., Arima, M., Pati, J.K., Kaneko, Y., 2006. Petrology and
1252 geochemistry of metamorphosed basaltic pillow lava and basaltic komatiite
1253 in Mauraipur area: subduction related volcanism in Archean
1254 Bundelkhand craton, Central India. *Journal of Mineralogical and
1255 Petrological Sciences* 101, 199-217.
1256
- 1257 Mazumdar, R., Banerjee, D.M., 2001. Regional variations in the carbon isotopic
1258 composition of phosphorite from the Early Cambrian Lower Tal formation,
1259 Mussoorie Hills, India. *Chemical Geology* 175, 5-15.
1260
- 1261 McElhinny, M.W., Cowley, J.A., Edwards, D.J., 1978. Palaeomagnetism of
1262 some rocks from peninsular India and Kashmir. *Tectonophysics* 50, 41-
1263 54.
1264
- 1265 McMenamin, M.A.S., McMenamin, D.L.S., 1990. *The Emergence of Animals:
1266 The Cambrian Breakthrough*. Columbia Univ. Press, New York, 217.
1267
- 1268 Meert, J.G., 2001. Growing Gondwana and rethinking Rodinia. *Gondwana
1269 Research* 4, 279-288.
1270
- 1271 Meert, J.G., 2002. Paleomagnetic evidence for a Paleo-Mesoproterozoic
1272 supercontinent Columbia. *Gondwana Research* 5, 207-216.
1273

- 1274 Meert, J.G., 2003. A synopsis of events related to the assembly of eastern
1275 Gondwana. *Tectonophysics* 362, 1–40.
1276
- 1277 Meert, J.G., 2009. In GAD we trust. *Nature Geosciences news and views* 2,
1278 673-674.
1279
- 1280 Meert, J.G., Pandit, M.K., Pradhan, V.R., Banks, J.C., Sirianni, R., Stroud, M.,
1281 Newstead, B., Gifford, J., 2010. The Precambrian tectonic evolution of
1282 India: A 3.0 billion year odyssey, *Journal of Asian Earth Sciences* 39, 483-
1283 515.
1284
- 1285 Meert, J.G., Pandit, M.K., Pradhan, V.R., 2011. Preliminary report on the
1286 paleomagnetism of 1.88 Ga dykes from the Bastar and Dharwar cratons,
1287 Peninsular India. *Gondwana Research*, doi10.1016/j.gr.2011.03.005
1288
- 1289 Meert, J.G., Van der Voo, R., Ayub, S., 1995. Paleomagnetic investigation of the
1290 Gagwe lavas and Mbozi Complex, Tanzania and the assembly of
1291 Gondwana. *Precambrian Research* 74, 225– 244.
1292
- 1293 Meert, J.G., Van der Voo, R. 1996. Paleomagnetic and $^{40}\text{Ar}/^{39}\text{Ar}$ study of the
1294 Sinyai dolerite, Kenya: implications for Gondwana assembly. *Journal of*
1295 *Geology* 104, 131–142.
1296
- 1297 Meert, J.G., Powell, C.McA. 2001. Assembly and Breakup of Rodinia.
1298 *Precambrian Research* 110, 1–8.
1299
- 1300 Meert, J.G., Stuckey, W. 2002. Revisiting the paleomagnetism of the 1.476 Ga
1301 St. Francois Mountains igneous province, *Missouri Tectonics*, 21(2), pp.
1302 19.
1303
- 1304 Meert, J.G., Torsvik, T.H., 2003. The making and unmaking of a
1305 supercontinent: Rodinia revisited. *Tectonophysics* 375, 261–288.
1306
- 1307 Mertanen, S., Pesonen, L.J., 1994. Preliminary results of the palaeomagnetic
1308 and rock magnetic study of the Early Proterozoic Tsuomasvarri ultramafic
1309 and gabbrodiorite intrusion, northern Fennoscandia. *Precambrian*
1310 *Research* 69, 25– 50.
1311
- 1312 Mertanen, S., Pesonen, L.J., Huhma, H., 1996. Palaeomagnetism and Sm–Nd
1313 ages of the Neoproterozoic diabase dykes in Laanila and Kautokeino,
1314 northern Fennoscandia. In: Brewer, T.S. (Ed.), *Precambrian Crustal*
1315 *Evolution in the North Atlantic Region*. Geological Society of London
1316 special publication 112, 331– 358.
1317
- 1318 Miller, K.C., Hargraves, R.B., 1994. Paleomagnetism of some Indian kimberlites
1319 and lamproites. *Precambrian Research* 69, 259–267.

- 1320
1321 Mondal, M.E.A., Zainuddin, S.M., 1996. Evolution of Archean-
1322 Palaeoproterozoic Bundelkhand massif, Central India—evidence from
1323 granitoid geochemistry. *Terra Nova* 8, 532–539.
1324
- 1325 Mondal, M. E. A., Deomurari, M. P., Goswami, J. N., Rahman, A. and Sharma,
1326 K. K., 1997. $^{207}\text{Pb}/^{206}\text{Pb}$ zircon ages of samples from Bundelkhand massif,
1327 Central India; Abstract in International Conference on Isotopes in Solar
1328 System 80-81.
1329
- 1330 Mondal, M.E.A., Sharma, K.K., Rahman, A., Goswami, J.N., 1998. Ion
1331 microprobe $^{207}\text{Pb}/^{206}\text{Pb}$ zircon ages for gneiss-granitoid rocks from
1332 Bundelkhand massif: evidence for Archean components. *Current Science*
1333 74, 70–75.
1334
- 1335 Mondal, M.E.A., Goswami, J.N., Deomurari, M.P., Sharma, K.K., 2002. Ion
1336 microprobe $^{207}\text{Pb}/^{206}\text{Pb}$ ages of zircons from the Bundelkhand Massif,
1337 northern India: implications for crustal evolution of the Bundelkhand-
1338 Aravalli supercontinent. *Precambrian Research* 117, 85–100.
1339
- 1340 Moores, E.M., 1991. Southwest U.S. –East Antarctic (SWEAT) connection: a
1341 hypothesis. *Geology* 19, 425– 428.
1342
- 1343 Mueller, P.A., Kamenov, G.D., Heatherington, A.L., Richards, J., 2008. Crustal
1344 evolution in the Southern Appalachian Orogen; evidence from Hf isotopes
1345 in detrital zircons. *Journal of Geology* 116, 414–422.
1346
- 1347 Murthy, N.G.K., 1995. Proterozoic mafic dykes in southern peninsular India: a
1348 review. In: Devaraju, T.C. (Ed.), *Mafic Dyke Swarms of Peninsular India*,
1349 vol. 33. Geological Society of India, Memoir, pp. 81–98.
1350
- 1351 Murthy, Y.G.K., Babu Rao, V., Guptasarma, D., Rao, J.M., Rao, M.N.,
1352 Bhattacharji, S., 1987. Tectonic, petrochemical and geophysical studies of
1353 mafic dyke swarms around the Proterozoic Cuddapah Basin, south India.
1354 In: Halls, H.C., Fahrig, W. (Eds.), *Mafic Dyke Swarms*, Geology Association
1355 of Canada Special Paper 34, 303–316.
1356
- 1357 Naqvi, S.M., Rogers, J.J.W., 1987. *Precambrian Geology of India*. Oxford
1358 University Press Inc, pp. 223.
1359
- 1360 Neuvonen, K.J., Pesonen, L.J., Pietarinen, H., 1997. Remanent magnetization
1361 in the Archaean basement and cutting dykes in Finland, Fennoscandian
1362 shield. In: Pesonen, L.J. (Ed.), *The Lithosphere of Finland—a Special Issue*
1363 of the Finnish Lithosphere Programme. *Geophysica* 33, 111 –146.
1364

- 1365 Nomade, S., Chen, Y., Feraud, G., Pouclet, A., Theveniaut, H., 2001. First
 1366 paleomagnetic and $^{40}\text{Ar}/^{39}\text{Ar}$ study of Paleoproterozoic rocks from the
 1367 French Guayana (Camopi and Oypok rivers), northeastern Guyana Shield.
 1368 Precambrian Research 109, 230– 256.
 1369
- 1370 Nomade, S., Chen, Y., Pouclet, A., Feraud, G., Theveniaut, H., Daouda,
 1371 B.Y., Vidal, M., Rigolet, C., 2003. The Guiana and the West African Shield
 1372 Palaeoproterozoic grouping: new palaeomagnetic data for French Guiana
 1373 and the Ivory Coast. Geophysical Journal International 154, 677– 694.
 1374
- 1375 Oldham, R D., 1893. Manual of Geology, second ed. Calcutta, India.
 1376
- 1377 Onstott, T.C., Hargraves, R.B., 1981. Proterozoic transcurrent tectonics:
 1378 palaeomagnetic evidence from Venezuela and Africa. Nature 289, 131–
 1379 136.
 1380
- 1381 Onstott, T.C., Dorbor, J., 1987. $^{40}\text{Ar}/^{39}\text{Ar}$ and paleomagnetic results from
 1382 Liberia and the Precambrian APW database for the West African Shield.
 1383 Journal of African Earth Sciences 6, 537– 552.
 1384
- 1385 Park, J. K., Buchan, K. L. and Harlan, S. S., 1995. A proposed giant radiating
 1386 dyke swarm fragmented by the separation of Laurentia and Australia
 1387 based on paleomagnetism of ca. 780 Ma mafic intrusions in western North
 1388 America. Earth and Planetary Science Letters 132, 129–139.
 1389
- 1390 Patchett, P.J., Bylund, G., 1977. Age of Grenville Belt magnetization: Rb–Sr
 1391 and paleomagnetic evidence from Swedish dolerites. Earth and Planetary
 1392 Science Letters 35, 92 – 104.
 1393
- 1394 Pati, J. K., Raju, S., Mangain, V. D., Shankar, R., 1997. Record of gold
 1395 mineralization in parts of Bundelkhand Granitoid Complex (BGC), Journal
 1396 of Geological Society of India 50, 601–606.
 1397
- 1398 Pati, J. K., 1999. Study of granitoid mylonites and reef/vein quartz in parts of
 1399 Bundelkhand Granitoid Complex (BGC), Records Geological Survey of India
 1400 131 (8), 95–96.
 1401
- 1402 Pati, J. K., Patel, S. C., Pruseth, K. L., Malviya, V. P., Arima, M., Raju, S., Pati,
 1403 P. and Prakash, K., 2007. Geochemistry of giant quartz veins from the
 1404 Bundelkhand craton, Central India and its implications, Journal of Earth
 1405 System Science, 116, 697–510.
 1406
- 1407 Pati, J.K., Raju, S., Malviya, V.P., Bhushan, R., Prakash, K., Patel, S.C., 2008.
 1408 Mafic dykes of Bundelkhand craton, Central India: Field, Petrological and
 1409 Geochemical characteristics. In: Srivastava, R et al (eds) Indian dykes:

- 1410 geochemistry, geophysics and geochronology. Narosa Publishing House,
1411 New Delhi, pp 547–569.
1412
- 1413 Patranabis-Deb, S., Bickford, M.E., Hill, B., Chaudhuri, A.K., Basu, A., 2007.
1414 SHRIMP ages of zircon in the uppermost tuff in Chattisgarh Basin in
1415 central India require up to 500 Ma adjustment in Indian Proterozoic
1416 stratigraphy. *Journal of Geology* 115, 407–416.
1417
- 1418 Paul, D.K., Potts, P.J., Gibson, I.L., Harris, P.G., 1975. Rare-earth abundances
1419 in Indian kimberlites. *Earth and Planetary Science Letters* 25, 151–158.
1420
- 1421 Payne, J.L., Hand, M., Barovich, K.M., Reid, A., Evans, D.A.D., 2009.
1422 Correlations and reconstruction models for the 2500 – 1500 Ma evolution
1423 of the Mawson continent. *Geological society of London, special publication*
1424 323, 319–355.
1425
- 1426 Pesonen, L.J., Neuvonen, K.J., 1981. Paleomagnetism of the Baltic shield-
1427 implications for Precambrian tectonics. In: Kroöner, A. (Ed.), *Precambrian*
1428 *Plate Tectonics*. Elsevier, Amsterdam, pp. 623– 648.
1429
- 1430 Pesonen, L.J., Reimold, W.U., Gibson, R.L., 2002. Preliminary paleomagnetic
1431 and rock magnetic data of the Vredefort structure, South Africa. *Abstracts*
1432 *of the 33rd LPSC, Houston, March 4– 8, 2002 CD-ROM*.
1433
- 1434 Pesonen, L.J., Elming, S.A., Mertanen, S., Pisarevsky, S., D'Agrella, M.S.,
1435 Meert, J.G., Schmidt, P.W., Abrahamsen, N., Bylund, G., 2003.
1436 Palaeomagnetic configuration of continents during the Proterozoic.
1437 *Tectonophysics* 375, 289–324.
1438
- 1439 Piispa, E.J., Smirnov, A.V., Pesonen, L.J., Lingadevaru, M., Ananthar-Murthy,
1440 K.J., Devaraju, T.C., 2011. An integrated study of Proterozoic dykes,
1441 Dharwar craton, southern India, in: Srivastava, R.K. (ed) *Dyke Swarms:*
1442 *Keys for Geodynamic Interpretation*, Springer-Verlag, Heidelberg, pp. 33-
1443 45.
1444
- 1445 Pisarevsky, S.A., Sokolov, S.J., 1999. Palaeomagnetism of the Palaeoproterozoic
1446 ultramafic intrusion near Lake Konchozero, Southern Karelia, Russia.
1447 *Precambrian Research* 93, 201– 213.
1448
- 1449 Pisarevsky, S.A., Natapov, L.M., 2003. Siberia and Rodinia. *Tectonophysics*
1450 375, 221–245.
1451
- 1452 Pisarevsky, S.A., Murphy, J.B., Cawood, P.A., Collins, A.S., 2008. Late
1453 Neoproterozoic and Early Cambrian paleogeography: models and
1454 problems. *Geological society of London* 294, 9–31.
1455

- 1456
1457 Poitou, C., Kumar, A., Valet, J., Mamila, V., Besse, J., Rao, M., Rao, P., 2008.
1458 Paleomagnetism of the Bundelkhand Dyke swarms, Madhya Pradesh,
1459 Central India. Abstract, AGU, Fall meeting.
1460
1461 Poorter, R.P.E., 1975. Palaeomagnetism of Precambrian rocks from southeast
1462 Norway and south Sweden. *Physical Earth and Planetary International* 10,
1463 74– 87.
1464
1465 Powell, C.McA., Jones, D.L., Pisarevsky, S.A., Wingate, M.T.D., 2001.
1466 Paleomagnetic constraints on the position of the Kalahari craton in
1467 Rodinia. *Precambrian Research* 110, 33– 46.
1468
1469 Powell, C. McA., Pisarevsky, S.A., 2002. Late Neoproterozoic assembly of east
1470 Gondwana. *Geology* 3, 3–6.
1471
1472 Pradhan, V.R., Pandit, M.K., Meert, J.G., 2008. A cautionary note on the age of
1473 the Paleomagnetic pole obtained from the Harohalli Dyke swarms,
1474 Dharwar Craton, Southern India. In: Srivastava, et al. (Eds.), *Indian*
1475 *Dykes: Geochemistry, Geophysics and Geochronology*. Narosa Publishing
1476 House, India, pp. 339-351.
1477
1478 Pradhan, V.R., Meert, J.G., Pandit, M.K., Kamenov, G., Gregory, L.C., Malone,
1479 S., 2010. India's changing place in global Proterozoic reconstructions: new
1480 geochronologic constraints on key paleomagnetic poles from the Dharwar
1481 and Aravalli/Bundelkhand Cratons. *Journal of Geodynamics* 50, 224-242.
1482
1483 Rai, V., Shukla, M., Gautam Vibhuti, R., 1997. Discovery of carbonaceous
1484 megafossils (Chuarina-Tawuia assemblage) from the Neoproterozoic
1485 Vindhyan succession (Rewa Group), Allahabad, India. *Current Science* 73,
1486 783–788.
1487
1488 Rainbird, R.H., Stern, R.A., Khudoley, A.K., Kropachev, A.P., Heaman, L.M.,
1489 Sukhorukov, V.I., 1998. U–Pb geochronology of Riphean sandstone and
1490 gabbro from Southeast Siberia and its bearing on the Laurentia–Siberia
1491 connection. *Earth and Planetary Science Letters* 164, 409–420.
1492
1493 Ramchandra, H.M., Mishra, V.P., Deshmukh, S.S. 1995. Mafic dykes in the
1494 Bastar Precambrian: study of the Bhanupratappur – Keskhal mafic dyke
1495 swarm. In: Devaraju, T.C., *Mafic Dyke Swarms of Peninsular India.*,
1496 *Memoirs Geological Society of India* 33, 183-207.
1497
1498 Rao, J.M., Rao, G.V.S.P., Widdowson, M., Kelley, S.P., 2005. Evolution of
1499 Proterozoic mafic dyke swarms of the Bundelkhand Granite Massif,
1500 Central India. *Current Science* 88, 502-506.
1501

- 1502 Rao, J.M., 2004. The wide-spread 2Ga dyke activity in the Indian shield—
1503 evidences from Bundelkhand mafic dyke swarm, Central India and their
1504 tectonic implications. *Gondwana Research* 7, 1219–1228.
1505
- 1506 Rasmussen, B., Bose, P.K., Sakar, S., Banerjee, S., Fletcher, I.R., McNaughton,
1507 N.J., 2002a. 1.6Ga U–Pb zircon age for the Chorhat Sandstone, Lower
1508 Vindhyan, India: possible implications for the early evolution of animals.
1509 *Geology* 20, 103–106.
1510
- 1511 Rasmussen, B., Fletcher, I.R., Bengtson, S., McNaughton, N.J., 2002b.
1512 Discoidal impressions and trace-like fossils more than 1200 million years
1513 old. *Science* 296, 1112–1115.
1514
- 1515 Ratre, K, Waele, B.D., Biswal, T.K., Sinha, S., 2010. SHRIMP geochronology for
1516 the 1450 Ma Lakhna dyke swarm: its implication for the presence of
1517 Eoarchean crust in the Bastar craton and 1450-570 Ma depositional age
1518 for Purana basin (Khariar) Eastern Indian Peninsula. *Journal of Asian
1519 Earth Sciences*, 39 563-577.
1520
- 1521 Ray, J.S., Martin, M.W., Veizer, J., Bowring, S.A., 2002. U–Pb Zircon dating
1522 and Sr isotope systematic of the Vindhyan SuperGroup, India. *Geology* 30,
1523 131–134.
1524
- 1525 Ray, J.S., Veizer, J., Davis, W.J., 2003. C, O, Sr and Pb isotope systematics of
1526 carbonate sequences of the Vindhyan SuperGroup, India: Age, diagenesis,
1527 correlations, and implications for global events. *Precambrian Research*
1528 121, 103–140.
1529
- 1530 Renne, P.R., Onstott, T.C., D’Agrella-Filho, M.S., Pacca, I.G., Teixeira, W.,
1531 1990. $^{40}\text{Ar}/^{39}\text{Ar}$ dating of 1.0–1.1 Ga magnetizations from the São
1532 Francisco and Kaapvaal Cratons: tectonic implications for Pan-African and
1533 Brasiliano mobile belts. *Earth and Planetary Science Letters* 101, 349–
1534 366.
1535
- 1536 Rogers, J.J.W., 1996. A history of the continents in the past three billion years.
1537 *Journal of Geology* 104, 91–107.
1538
- 1539 Rogers, J.J.W., Santosh, M., 2002. Configuration of Columbia, a
1540 Mesoproterozoic supercontinent. *Gondwana Research* 5, 5–22.
1541
- 1542 Rogers, J. J. W., Santosh, M., 2003. Supercontinent in Earth history,
1543 *Gondwana Research* 6, 417–434.
1544
- 1545 Roy, A.B., Paliwal, B.S., Shekhawat, S.S., Nagori, D.K., Golani, P.R., Bejarniya
1546 B.R., 1988. Stratigraphy of the Aravalli Supergroup in the type area; In:

- 1547 Precambrian of the Aravalli Mountain, Rajasthan, India (eds.) Roy A B;
1548 Geological Society of India Memoir 7,121-138.
1549
- 1550 Roy, A.B., Kröner, A., 1996. Single zircon evaporation ages constraining the
1551 growth of the Archean Aravalli craton, northwestern Indian shield. *Geology*
1552 *Magazine* 133, 333-342.
1553
- 1554 Salminen, J., Pesonen, L.J., Reimold, W.U., Donadini, F., Gibson, R.L., 2009.
1555 Paleomagnetic and rock magnetic study of the Vredefort impact structure
1556 and the Johannesburg Dome, Kaapvaal Craton, South Africa-Implications
1557 for the apparent polar wander path of the Kaapvaal Craton during the
1558 Mesoproterozoic. *Precambrian Research* 168, 167-184.
1559
- 1560 Santosh, M., Yokoyama, K., Biju-Shekhar, S., Rogers, J.J.W., 2003. Multiple
1561 tectonothermal events in the granulite blocks of southern India revealed
1562 from EPMA dating: implications on the history of supercontinents.
1563 *Gondwana Research* 6, 29-63.
1564
- 1565 Sarangi, S., Gopalan, K., Kumar, S., 2004. Pb-Pb age of earliest megascopic,
1566 eukaryotic alga bearing Rhotas formation, Vindhyan SuperGroup, India:
1567 implications for Precambrian atmospheric oxygen evolution. *Precambrian*
1568 *Research* 121, 107-121.
1569
- 1570 Sarkar, A., Paul, D.K., Potts, P.J., 1996. Geochronology and geochemistry of
1571 Mid-Archaean trondhjemitic gneisses from the Bundelkhand craton,
1572 central India. *Records Research in Geology and Geophysics of*
1573 *Precambrians* 16, 76-92.
1574
- 1575 Sarkar, A., Ghosh, S., Singhai, R. K., Gupta, S. N., 1997. Rb-Sr geochronology
1576 of the Dargawan sill: constraint on the age of the type Bijawar sequence of
1577 Central India. *International Conf. on isotopes in Solar System.*, Nov.11-4,
1578 5,100-101.
1579
- 1580 Sarkar, G., Corfu, F., Paul, D.K., McNaughton, N.J., Gupta, S.N., Bishui, P.K.
1581 1993. Early Archean crust in Bastar craton, Central India – a geochemical
1582 and isotopic study. *Precambrian Research* 62, 127-137.
1583
- 1584 Sears, J.W., Price, R.A., 2000. New look at the Siberian connection: no SWEAT.
1585 *Geology* 28, 423- 426.
1586
- 1587 Sears, J.W., Price, R.A., 2003. Tightening the Siberian connection to western
1588 Laurentia. *GSA Bulletin* 115, 943 – 953.
1589
- 1590 Sharma, K. K., 1998. Geological evolution and crustal growth of Bundelkhand
1591 craton and its relict in the surrounding regions, North Indian Shield. In

- 1592 The Indian Precambrian (ed. Paliwal, B. S.), Scientific Publishers, Jodhpur,
1593 33–43.
1594
- 1595 Sharma, K. K., Rahman, A., 1996. Mafic dykes in Bundelkhand granitoids and
1596 mafic volcanics in Supra-batholithic volcanosedimentaries (Bijawar). DST
1597 Newsletters 15, 17–19.
1598
- 1599 Sharma, K.K., Rahman, A., 2000. The early Archaean–Paleoproterozoic crustal
1600 growth of the Bundelkhand craton, northern Indian shield. In: Deb, M.
1601 (Ed.), Crustal Evolution and Metallogeny in the Northwestern Indian
1602 Shield. Narosa Publishing House, New Delhi, pp. 51–72.
1603
- 1604 Sinha Roy, S., Malhotra, G., Mohanty, M., 1998. Geology of Rajasthan.
1605 Geological Society of India, Bangalore, 278.
1606
- 1607 Smith, C.B., 1992. The age of the Majhgawan pipe, India. Scott Smith
1608 Petrology, 9.
- 1609 Söderlund, U., Hofmann, A., Klausen, M.B., Olsson, J.R., Ernst, R.C., Persson,
1610 P., 2010. Towards a complete magmatic barcode for the Zimbabwe craton:
1611 Baddeleyite U-Pb dating of regional dolerite dyke swarms and sill
1612 complexes, Precambrian Research 183, 388–398.
- 1613 Srivastava, A.P., Rajagopalan, G., 1988. F-T Ages of the Vindhyan Glauconitic
1614 sandstone beds exposed around the Rawatbhata area, Rajasthan. Journal
1615 of Geological Society of India 32, 527–529.
1616
- 1617 Srivastava, R.K., Chalapathi, S., Chalapathi R.N.V., 2008. Dyke swarms of
1618 Indian shield in space and time. In: Indian Dykes: Geochemistry,
1619 Geophysics, and Geochronology. Narosa Publishing Ltd., New Delhi, India,
1620 pp.650.
1621
- 1622 Srivastava, R.K., Gautam, G.C., 2008. Precambrian mafic dyke swarms from
1623 the southern Bastar Central India craton: present and future perspectives.
1624 In: Srivastava, R.K., Sivaji, Ch., Chalapati Rao, N.V. (Eds.), Indian Dykes:
1625 Geochemistry, Geophysics, and Geochronology. Narosa Publishing Ltd.,
1626 New Delhi, India, pp. 367–376.
1627
- 1628 Stearn, J.E.F., Piper, J.D.A., 1984. Palaeomagnetism of the Sveconorwegian
1629 mobile belt of the Fennoscandian Shield. Precambrian Research 23, 201–
1630 246.
1631
- 1632 Stein, H. J., Hannah, J. L., Zimmerman, A., Markey, R. J., Sarkar, S. C., Pal,
1633 A. B., 2004. A 2.5 ga porphyry Cu-Mo-Au deposit at Malanjhand,
1634 central India; implications for late Archean continental assembly.
1635 Precambrian Research 134, 189–226.

- 1636
1637 Swanson-Hysell, N. L., Maloof, A. C., Weiss, B. P., Evans, D.A.D., 2009. *Nature*
1638 *Geosciences* 2, 713–717.
- 1639
1640 Torsvik, T.H., Briden, J.C., Smethurst, M.A., 2000. IAPD 2000. Norwegian
1641 Geophysical Union.
- 1642
1643 Van der Voo, R., 1990. The reliability of paleomagnetic data. *Tectonophysics*
1644 184, 1–9.
- 1645
1646 Van der Voo, R., Meert, J. G., 1991. Late Proterozoic paleomagnetism and
1647 tectonic models: A critical appraisal. *Precambrian Research*, 53, 149 –
1648 163.
- 1649
1650 Venkatachala, B.S., Mukund, S., Shukla, M., 1996. Age and Life of the
1651 Vindhyan- Facts and Conjectures. *Memoir Geological Society of India* 36,
1652 137–155.
- 1653
1654 Vinogradov, A.P., Tugarinov, A.I., Zhikov, C.I., Stanikova, N.I., Bibikova, E.V.,
1655 Khorre, K., 1964. Geochronology of the Indian Precambrian. Report of the
1656 22nd International Congress, New Delhi, 10, pp. 553–567.
- 1657
1658 Wang, Y., Liu, D., Chung, S.L., Tong, L., Ren, L., 2008. SHRIMP zircon age
1659 constraints from the Larsemann Hills region, Prydz Bay, for a late
1660 Mesoproterozoic to early Neoproterozoic tectono-thermal event in East
1661 Antarctica. *American Journal of Science* 308, 573–617.
- 1662
1663 Wiedenbeck, M., Goswami, J.N., 1994. High precision $^{207}\text{Pb}/^{206}\text{Pb}$ zircon
1664 geochronology using a small ion probe. *Geochimica Cosmochimica Acta*
1665 58, 2135–2141.
- 1666
1667 Wiedenbeck, M., Goswami, J.N., Roy, A.B., 1996. Stabilization of the Aravalli
1668 Craton of northwestern India at 2.5 Ga: an ion microprobe zircon study.
1669 *Chemical Geology* 129, 325–340.
- 1670
1671 Weil, A.B., Van der Voo, R., MacNiocall, C., Meert, J.G., 1998. The Proterozoic
1672 supercontinent Rodinia: paleomagnetically derived reconstructions for
1673 1100–800 Ma. *Earth and Planetary Science Letters* 154, 13–24.
- 1674
1675 Wingate, M.T.D., Giddings, J.W., 2000. Age and palaeomagnetism of the
1676 Mundine Well dyke swarm, Western Australia: implications for an
1677 Australia–Laurentia connection at 550 Ma. *Precambrian Research* 100,
1678 335–357.
- 1679

- 1680 Wingate, M.T.D., Pisarevsky, S.A., Evans, D.A.D., 2002. Rodinia connection
1681 between Australia and Laurentia; no SWEAT, no AUSWUS? *Terra Nova* 14,
1682 121–128.
1683
- 1684 Yoshida, M., Upreti, B.N., 2006. Neoproterozoic India within East Gondwana:
1685 Constraints from recent geochronologic data from Himalaya. *Gondwana*
1686 *Research* 10, 349–356.
1687
- 1688 Young, G.M., 1995. Are Neoproterozoic glacial deposits preserved on the
1689 margins of Laurentia related to the fragmentation of two supercontinents?
1690 *Geology* 23, 153– 156.
1691
- 1692 Zhang, S. H., Li, Z. X., Wu, H. C., 2006. New Precambrian palaeomagnetic
1693 constraints on the position of the North China Block in Rodinia,
1694 *Precambrian Research* 144, 213–238.
1695
- 1696 Zhao, G.C., Cawood, P.A., Wilde, S.A., Sun, M., 2002. Review of global 2.1–1.8
1697 Ga orogens: implications for a pre-Rodinia supercontinent. *Earth Science*
1698 *Reviews* 59, 125–162.
1699
- 1700 Zhao, G.C., Sun, M., Wilde, S.A., Li, S.Z., 2004a. A Paleo-Mesoproterozoic
1701 supercontinent: assembly, growth and breakup. *Earth Science Reviews* 67,
1702 91–123.
1703
- 1704 Zhao, T.P., Zhai, M.G., Xia, B., Li, H.M., Zhang, Y.X., Wan, Y.S., 2004b. Zircon
1705 U–Pb SHRIMP dating for the volcanic rocks of the Xiong'er Group:
1706 constraints on the initial formation age of the cover of the North China
1707 Craton. *Chinese Science Bulletin* 49, 2495–2502.
1708
1709
1710
1711
1712
1713
1714
1715
1716
1717

1718 Figure Legends

1719 **Figure 1:** Generalized geological and tectonic map of the Indian sub-continent
 1720 with the Precambrian mafic dyke swarms cross-cutting various Archean
 1721 cratonic blocks. C: Cuddapah basin; Ch: Chattisgarh Basin; CIS: Central
 1722 Indian Shear Zone; GR: Godavari Rift; M: Madras Block; Mk: Malanjkhand;
 1723 MR: Mahanadi Rift; N: Nilgiri Block; NS: Narmada-Son Fault Zone; PC: Palghat-
 1724 Cauvery Shear Zone; R: Rengali Province and Kerajang Shear Zone; S:
 1725 Singhbhum Shear Zone; V: Vindhyan Basin (modified after French et al., 2008)

1726 **Figure 2:** Sketch map of the major units in the Bundelkhand craton, NW India
 1727 (modified after Malviya et al., 2006). The asterisks on the map show the sites
 1728 sampled for both paleomagnetic and geochronological analysis (NW-SE
 1729 trending dyke I9GS_13 and ENE-WSW trending Great Dyke of Mahoba).

1730 **Figure 3:** (a) NW-SE trending dyke (I925) exposed in an outcrop ~50 km away
 1731 from Mauranipur, M.P. (b) granitic host rock at the same site I925 trellised by
 1732 numerous mafic dykelets. (c & d) ENE-WSW trending dyke I923 exposed in a
 1733 quarry in Mahoba district, Madhya Pradesh, Central India.

1734
 1735 **Figure 4:** (a) Backscattered electron (BSE) and cathodoluminescence (CL)
 1736 images of selected zircons/uranium bearing minerals from ENE-WSW trending
 1737 Mahoba dykes. Scale bars in μm . (b) Backscattered electron (BSE) and
 1738 cathodoluminescence (CL) images of selected zircons/uranium bearing
 1739 minerals from NW-SE trending dykes. Bar length corresponds to 10-100 μm .

1740
 1741 **Figure 5:** a) Concordia diagram for the eleven spots from five concordant
 1742 zircon/baddeleyite grains and tips from sample I9GS_13 yielding an age of
 1743 $1979.1 \pm 7.9 \text{ Ma}$ (2σ ; MSWD=0.63; Probability=0.90). (b) Tera-Wasserburg plot
 1744 obtained from 10 analyses on a population of four fragmentary
 1745 zircons/baddeleyites from NW-SE trending dyke sample I9GS_13 yielding
 1746 moderately discordant $^{207}\text{Pb}/^{206}\text{Pb}$ dates between 2777 Ma and 2686 Ma (2σ ;
 1747 MSWD=4.5) (c) Tera-Wasserburg concordia intercept age of $1096 \pm 19 \text{ Ma}$ (2σ ;
 1748 MSWD=0.3) derived from the regression through the uncorrected data from the
 1749 $^{207}\text{Pb}/^{206}\text{Pb}$ for the five analysis on three zircon grains and tips from sample
 1750 GDM & GDM1 (d) The weighted mean $^{207}\text{Pb}^*/^{206}\text{Pb}^*$ age for the five analysis
 1751 from sample GDM & GDM1 yielded an age of 1113 ± 7 (2σ ; MSWD=0.75;
 1752 probability of concordance=0.56).

1753 **Figure 6:** Orthogonal vector plots from the NW-SE and ENE-WSW trending
 1754 dykes of the Bundelkhand craton showing typical characteristic remanent

1755 magnetization directions. (a) Thermal demagnetization behavior of ENE-WSW
 1756 trending dyke sample I923-1A. (b) Alternating field demagnetization behavior of
 1757 ENE-WSW trending dyke specimen I923-4B. (c) Thermal demagnetization
 1758 behavior of NW-SE trending dyke sample I925-22A. (d) Alternating field
 1759 demagnetization behavior of NW-SE trending dyke sample I925-7B. Solid
 1760 squares represent projections on the horizontal plane indicated by 'H'; open
 1761 squares represent projection onto a vertical plane indicated by 'V'.

1762

1763 **Figure 7:** Baked contact test on NW-SE trending dyke I925. (a) Thermal
 1764 demagnetization behavior of the dyke specimen I925-7A (b) Thermal
 1765 demagnetization behavior of the granitic host rock specimen I925-39A about
 1766 1.5 m away from the main dyke showing similar directions as the main dyke.

1767

1768 **Figure 8:** (a -b) Curie temperature runs for ENE-WSW trending dyke samples
 1769 I923-5 & 6. Sample I923-5a shows Heating curie temperature (TcH) of 575.1 °C
 1770 and Cooling curie temperature (TcC) of 578.5 °C and I923-6 shows TcH =
 1771 562.1°C & TcC = 550.5°C. (c - d) Curie temperature runs for the NW-SE
 1772 trending older dyke suite samples I925-26 (TcH = 548.2°C & TcC = 525.5°C)
 1773 and I927-12 (TcH = 572.8°C & TcC = 567.5°C). (e) Isothermal Remanence
 1774 Magnetization (IRM) acquisition and back field demagnetization behavior of the
 1775 two ENE-WSW dyke specimens I923-4B and 8B. (f) Isothermal Remanence
 1776 Magnetization (IRM) acquisition and back field demagnetization behavior of two
 1777 NW-SE dyke samples I925-6B and 11B. All samples saturate at about 0.25-0.3
 1778 T. Coercivity of remanence values ranged from 0.07 to 0.1 Tesla.

1779

1780 **Figure 9:** (a) Stereoplot of site mean directions from the 12 NW-SE trending
 1781 dykes from the older suite (Dec = 155.3° and Inc = -7.8°). (b) Stereoplot of site
 1782 mean directions from ENE-WSW Mahoba suite of dykes (Dec = 24.7° and Inc =
 1783 -37.9°). (c) Stereoplot of site mean directions from NE-SW trending third set of
 1784 dykes (Dec = 189.3° and Inc = 64.5°) with a palaeolatitude of 46.4°N.

1785 **Figure 10:** Schmidt projection of virtual geomagnetic poles (VGP) from the
 1786 Mahoba dykes (this study) and the Majhgawan kimberlite (Gregory et al., 2006)
 1787 correlated to the mean paleomagnetic pole of the Bhandar-Rewa Groups of the
 1788 Upper Vindhyan Sequence (Malone et al., 2008). The locations of these sites
 1789 are shown in the inset map of India (red square = Mahoba dykes; magenta
 1790 square = Majhgawan kimberlite; and green square = Bhandar-Rewa).

1791

1792 **Figure 11:** Paleomagnetically based reconstruction at ~1.1 Ga based on our
1793 combined virtual geomagnetic pole (VGP) from ~1113 Ma Mahoba dykes of the
1794 Bundelkhand craton (this study); Majhgawan kimberlite pole (~1073 Ma;
1795 Gregory et al., 2006) and Bhandar-Rewa pole (Malone et al., 2008) and data
1796 reported in Pesonen et al. (2003) that places India at low latitudinal position to
1797 ~ mid latitudinal positions for Australia (Bangemall sill pole) (Paleolongitudes
1798 are unconstrained; see table 3a).

1799 **Figure 12:** (a) Generalized tectonic map of India showing the North Indian
1800 Block (Aravalli protocontinent) and South Indian Block (Dharwar
1801 protocontinent) docked together along Central Indian Tectonic Zone (CITZ). (b)
1802 Positions of northern Aravalli-Bundelkhand protocontinent (~2.0 Ga) and
1803 southern Dharwar protocontinent (~1.9 Ga) of the Indian peninsular shield
1804 based on the paleomagnetic poles from the ~2.0 Ga NW-SE trending
1805 Bundelkhand dyke suite, ~1.9 Ma Bastar dykes/Cuddapah dykes of the
1806 Bastar/Dharwar cratons and ~1.8 Ga Gwalior volcanics. The figure also shows
1807 the APW path for India utilizing the paleopoles from ~ 2.0 Ga – 1.8 Ga.

1808 **Figure 13:** Paleomagnetically-based reconstruction at ~2.0 Ga (after Pesonen
1809 et al., 2003). The Bundelkhand craton is positioned according to paleomagnetic
1810 data from the ~1980 Ma NW-SE trending dykes reported in this paper. The
1811 reconstruction places India at the equatorial positions with mid latitudinally
1812 located Laurentia (Sl: Slave and Wy: Wyoming cratons). The other continental
1813 blocks used in the reconstruction are Amazonia, Congo-SF, Kp: Kaapvaal,
1814 Fennoscandia, Ukraine, WA: West Africa (Palaeolongitudes are unconstrained;
1815 see table 3b).

Table 1: Bundelkhand paleomagnetic results

Site/Study	Latitude/Longitude	N/n	Dec	Inc	Kappa (k)	α_{95}	VGP latitude	VGP longitude	dp/dm
Older Suite (NW-SE)									
Site I442	25.717°N, 78.536°E	5	141.0°	-0.9°	11.3	7.2°	47.2°N	325.7°E	3.7/7.3
Site I443*									
Dyke A	25.425°N, 78.672°E	2	139.0°	-12.6°	70.0	11.1°	46.5°N	329.8°E	5.8/11.3
Dyke B	25.425°N, 78.672°E	4	141.4°	5.8°	70.0	11.1°	43.2°S	137.1°E	5.6/11.1
Dyke C**	25.425°N, 78.672°E	2	339.0°	-21°	70.0	11.1°	48.5°S	110.5°E	6.1/11.7
Site I444	25.408°N, 78.669°E	7	174.0°	-14.8°	16.0	15.5°	71.4°N	277.3°E	8.1/15.9
Site I454	25.147°N, 80.050°E	7	156.5°	-17.3°	50.0	8.6°	62.4°N	318.2°E	4.6/8.9
Site I455	24.935°N, 79.902°E	18	149.0°	-21°	47.3	5.1°	57.6°N	330.6°E	2.8/5.5
Site I925	24.946°N, 79.911°E	34	151.3°	-19.5°	34.0	4.3°	59.1°N	326.5°E	2.3/4.5
Site I927	25.017°N, 80.475°E	27	167.5°	-15.9°	42.0	4.3°	69.3°N	297.6°E	2.3/4.4
Site I929	25.192°N, 80.464°E	9	168.2°	-10.3°	107	5.0°	67.1°N	291.8°E	2.6/5.1
Site I930	25.189°N, 80.469°E	16	164.0°	-13.2°	71.3	4.4°	66.1°N	302.7°E	2.3/4.5
Site I931	25.286°N, 79.919°E	10	152.9°	-8.8°	46.2	7.2°	56.8°N	315.3°E	3.7/7.3
Mahoba Dykes (ENE-WSW)									
Site I451	25.284°N, 79.851°E	23	14.6°	-31.7°	25.0	6.1°	45.3°S	59.5°E	3.8/6.9
Site I452	25.284°N, 79.851°E	13	27.6°	-48.7°	232.0	2.7°	29.1°S	52.1°E	2.3/3.6
Site I923	25.184°N, 79.401°E	20	14.2°	-37.0°	125.0	3.3°	42.2°S	61.2°E	2.3/3.9
Site I924 (Great circles)	25.301°N, 79.934°E	10	40.7°	-29.2°	-	2.8°	33.1°S	31.0°E	1.7/3.1
NE-SW (third dyke suite)									
Site I448	25.134°N, 79.750°E	20	200.0°	60.0°	42.4	14.3°	21.5°S	63.3°E	16.3/21.6
Site I928	25.052°N, 80.486°E	20	175.0°	68.0°	48.6	4.7°	13.8°S	83.5°E	6.6/7.9
Overall Mean - Older (NW-SE)									
	25.00°N, 80°E	141/12	155.3°	-7.8°	21.4	9.6°	58.5°N	312.5°E	4.9/9.7
Overall Mean – Mahoba (ENE-WSW)									
	25.17°N, 79.5°E	76/4	24.7°	-37.9°	35.9	15.5°	38.7°S	49.5°E	9.5/16.3

N=Number of samples used; n=Number of Dykes/sites; Dec=Declination; Inc=Inclination; k=kappa precision parameter; α_{95} = cone of 95% confidence about the mean direction; VGP=Virtual Geomagnetic Pole. *Dyke A, B and C are 3 small dykes from Site I443 with Dyke C** showing reverse polarity.

Table 2a: Geochronological Results from the Bundelkhand older suite of dykes (I9GS_13)

Grain	Ratios						Ages						% Disc	RHO
	$^{207}\text{Pb}/^{206}\text{Pb}$	$\pm 2\sigma$	$^{206}\text{Pb}/^{238}\text{U}$	$\pm 2\sigma$	$^{*207}\text{Pb}/^{235}\text{U}$	$\pm 2\sigma$	$^{206}\text{Pb}/^{238}\text{U}$ (Ma)	$\pm 2\sigma$	$^{207}\text{Pb}/^{235}\text{U}$ (Ma)	$\pm 2\sigma$	$^{207}\text{Pb}/^{206}\text{Pb}$ (Ma)	$\pm 2\sigma$		
I9GS_13_2	0.1222	0.0012	0.34907	0.0179	5.88	0.30	1930	43	1959	22	1989	8	3	0.98
I9GS_13_6	0.1230	0.0016	0.35774	0.0239	6.07	0.42	1971	57	1985	30	2000	12	1	0.98
I9GS_13_7	0.1218	0.0026	0.36297	0.0223	6.10	0.40	1996	53	1990	28	1983	19	-1	0.95
I9GS_13_8	0.1210	0.0014	0.36787	0.0208	6.14	0.36	2019	49	1995	25	1970	10	-3	0.98
I9GS_13_9	0.1212	0.0012	0.37220	0.0221	6.22	0.38	2040	52	2007	26	1975	9	-3	0.98
I9GS_13_10	0.1220	0.0016	0.36876	0.0188	6.20	0.32	2023	44	2004	23	1985	11	-2	0.97
I9GS_13_11	0.1215	0.0012	0.35601	0.0164	5.96	0.28	1963	39	1970	20	1978	9	1	0.98
I9GS_13_14	0.1218	0.0012	0.35741	0.0198	6.00	0.34	1970	47	1976	24	1983	9	1	0.98
I9GS_13_15	0.1214	0.0012	0.35357	0.0157	5.92	0.26	1952	37	1964	20	1977	9	1	0.98
I9GS_13_16	0.1211	0.0014	0.35077	0.0178	5.86	0.28	1938	39	1955	21	1972	10	2	0.97
I9GS_13_17	0.1213	0.0012	0.35355	0.0163	5.91	0.30	1951	42	1963	22	1975	9	1	0.98
I9GS_13_21	0.1883	0.0008	0.45398	0.0221	11.79	0.58	2413	98	2588	45	2728	7	12	0.99
I9GS_13_23	0.1928	0.0007	0.47373	0.0190	12.59	0.51	2500	83	2649	38	2766	6	10	0.99
I9GS_13_24	0.1939	0.0008	0.46927	0.0187	12.55	0.50	2480	82	2646	37	2776	6	11	0.99
I9GS_13_26	0.2572	0.0020	0.47423	0.0696	16.82	2.47	2502	301	2924	136	3230	12	23	1.00
I9GS_13_27	0.2611	0.0007	0.63422	0.0162	22.83	0.59	3166	64	3220	25	3253	4	3	0.99
I9GS_13_28	0.2615	0.0008	0.56674	0.0566	20.44	2.04	2894	231	3112	95	3256	5	11	1.00
I9GS_13_30	0.1941	0.0007	0.50044	0.0099	13.39	0.27	2616	43	2708	19	2777	6	6	0.98
I9GS_13_31	0.1900	0.0007	0.48971	0.0130	12.83	0.34	2569	56	2667	25	2743	6	6	0.99
I9GS_13_33	0.1864	0.0008	0.48857	0.0105	12.56	0.28	2564	45	2647	21	2711	7	5	0.98
I9GS_13_34	0.1896	0.0012	0.45310	0.0204	11.85	0.54	2409	90	2592	42	2739	10	12	0.99
I9GS_13_35	0.1837	0.0006	0.46585	0.0121	11.80	0.31	2465	53	2588	24	2686	6	8	0.99
I9GS_13_37	0.1852	0.0009	0.47595	0.0122	12.16	0.32	2510	53	2616	24	2700	8	7	0.98
I9GS_13_38	0.1888	0.0016	0.49585	0.0112	12.91	0.31	2596	48	2673	23	2732	14	5	0.98

Table 2b: Geochronological Results from the Mahoba dykes (GDM and GDM1)

Grain	Ratios						Ages						% Disc	RHO
	$^{207}\text{Pb}/^{206}\text{Pb}$	$\pm 2\sigma$	$^{206}\text{Pb}/^{238}\text{U}$	$\pm 2\sigma$	$^{207}\text{Pb}/^{235}\text{U}$	$\pm 2\sigma$	$^{206}\text{Pb}/^{238}\text{U}$ (Ma)	$\pm 2\sigma$	$^{207}\text{Pb}/^{235}\text{U}$ (Ma)	$\pm 2\sigma$	$^{207}\text{Pb}/^{206}\text{Pb}$ (Ma)	$\pm 2\sigma$		
GDM_5a	0.07697	0.0006	0.17605	0.0051	1.868	0.06	1046	28	1070	20	1120	17	7	0.96
GDM_6a	0.07697	0.0007	0.17509	0.0040	1.858	0.05	1041	22	1066	16	1120	18	7	0.93
GDM_7a	0.07671	0.0006	0.17551	0.0041	1.856	0.05	1043	23	1066	16	1114	16	6	0.95
GDM_8a	0.07654	0.0006	0.17623	0.0041	1.860	0.05	1047	23	1067	16	1109	17	6	0.94
GDM_18a	0.07631	0.0006	0.18242	0.0041	1.919	0.05	1081	22	1088	16	1103	16	2	0.94

Table 3(a) Paleomagnetic poles at ca. ~1.1 Ga

Continent	Pole name	Age	Plat	Plong	A95	Reference
India	Mahoba dykes	1113 ±7 Ma	37.8°S	49.5°E	15.5°	This study
Laurentia	Keweenawan dykes mean + Portage volcanics	1099 Ma	36°N	188°E	3°	Swanson-Hysell et al., 2009; Pesonen et al., 2003
Baltica	Mean Baltica	1093 Ma	1°N	208°E	16°	Pesonen et al., 2003
Australia	Bangemall sill pole	1070 Ma	83.7°S	129°E	8.3°	Wingate et al., 2002
Kalahari	Mean Kalahari	1096 Ma	65°S	225°E	5°	Gose et al., 2006; Pesonen et al., 2003
Siberia	Malgina +Linok Formation	1078 Ma	25°S	231°E	3°	Gallet et al., 2000

Table 3(b). Paleomagnetic poles at ca. ~2.0 Ga

Continent	Pole name	Age	Plat	Plong	A95	Reference
India	NW-SE Bundelkhand dykes	1980 ± 9 Ma	58.5°N	312.5°E	9.6°	This study
Superior craton (Laurentia)	Minto Dykes	1998 ± 2 Ma	38°N	174°E	10.0°	Buchan et al., 1998
Fennoscandia	Konchozero sill, Karelia	1974 ± 27 Ma	14.2°S	282°E	11.0°	Pisarevsky and Sokolov, 1999
Ukraine	Gabbro Monzonite + Gabbro diabase	2000 Ma	53°N	142°E	-	Pesonen et al., 2003; Elming et al., 2001a
Amazonia	Oyapok tonalites + Encrucijada pluton	2019 Ma	42°N	181°E	4.0°	Pesonen et al., 2003
Congo-SF	Uauá dykes	1983 ± 31 Ma	24°N	331°E	4.0°	D'Agrella-Filho and Pacca, 1998
Kalahari	Vredefort dykes	2023 Ma	27°N	31°E	7.0°	Salminen et al., 2009; Pesonen et al., 2002
West-Africa	Liberia M	2050 ± 6 Ma	18°S	89°E	13.0°	Onstott and Dorbor, 1987

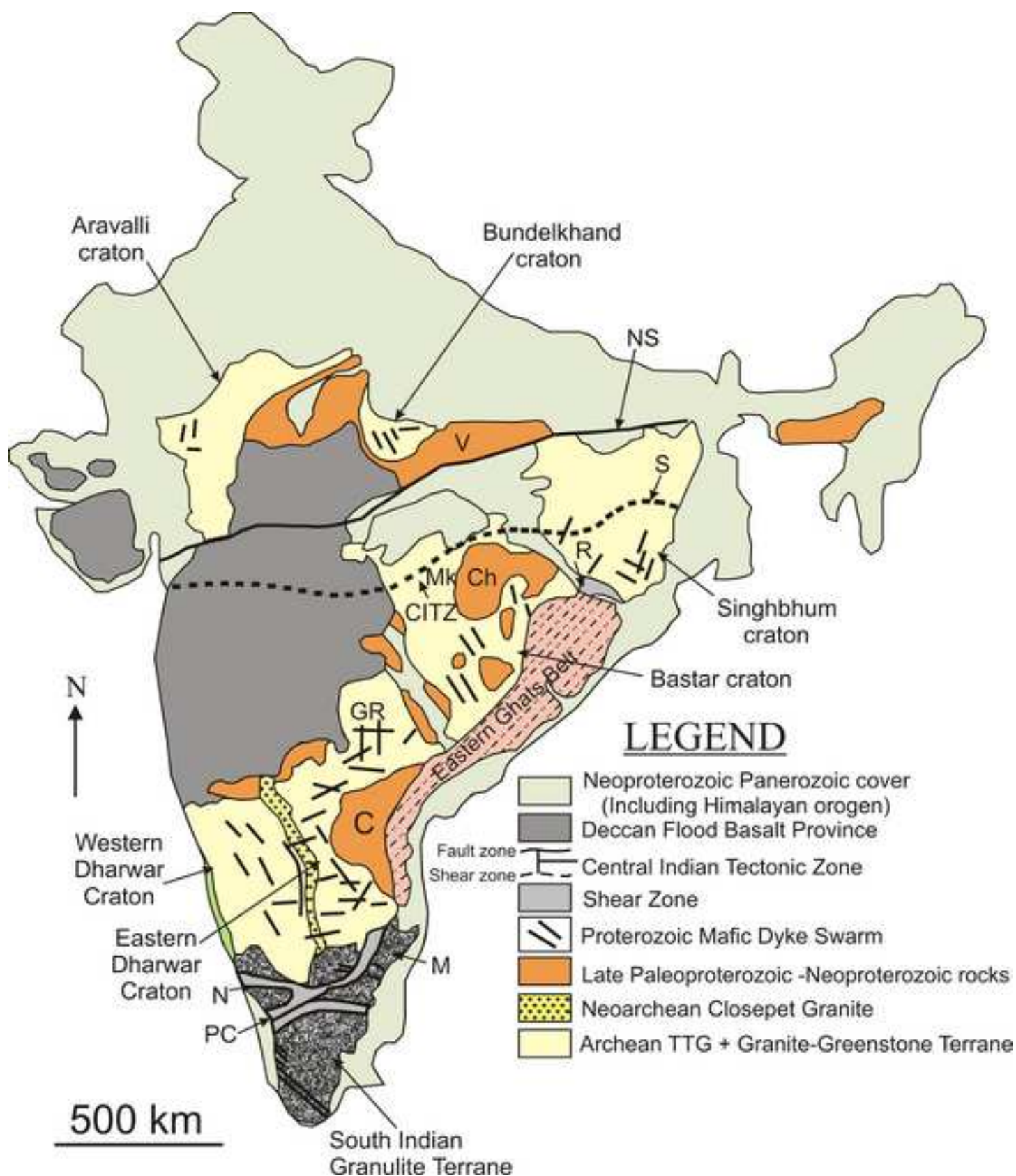


Figure-2

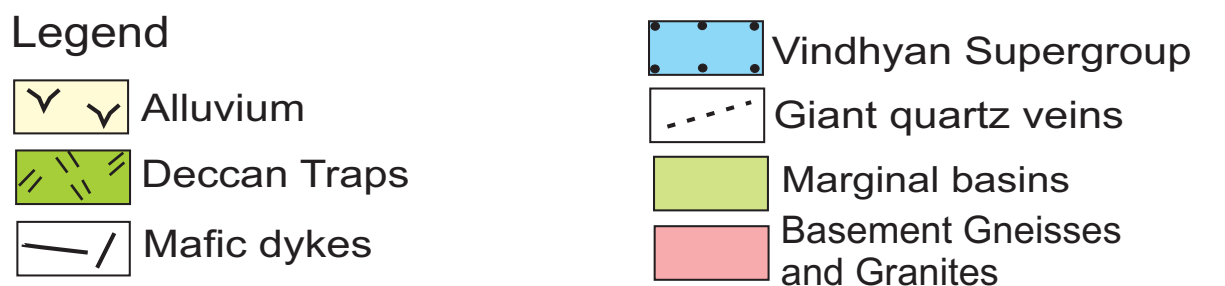
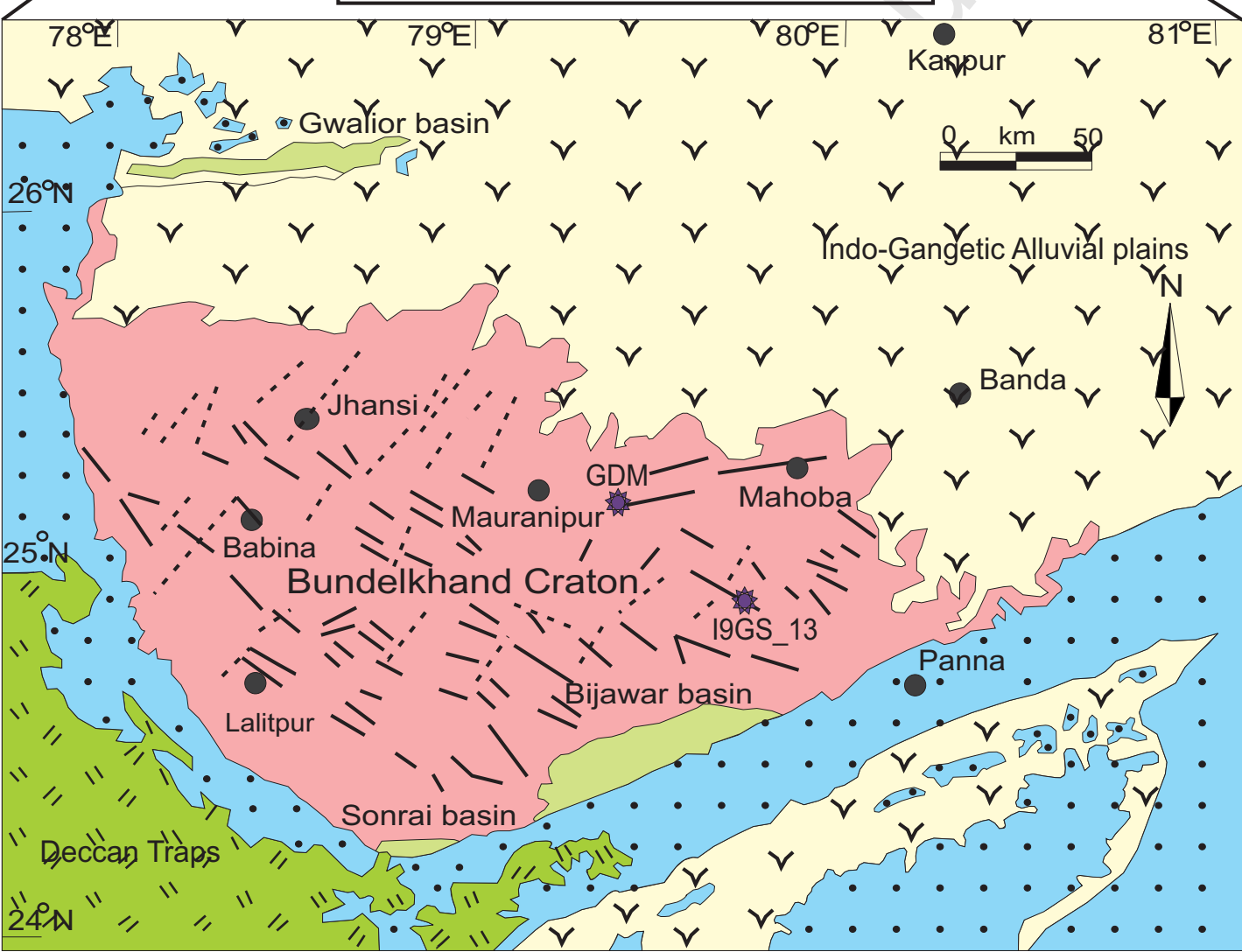
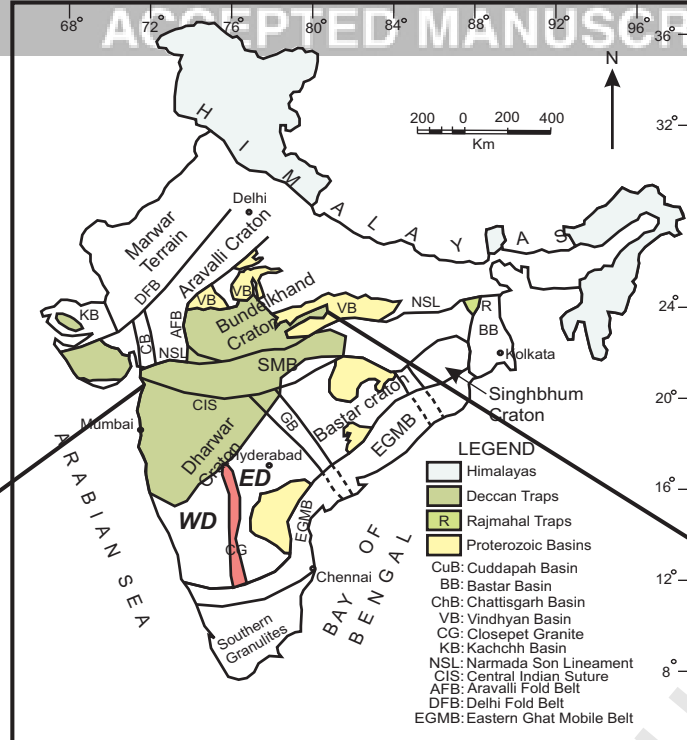
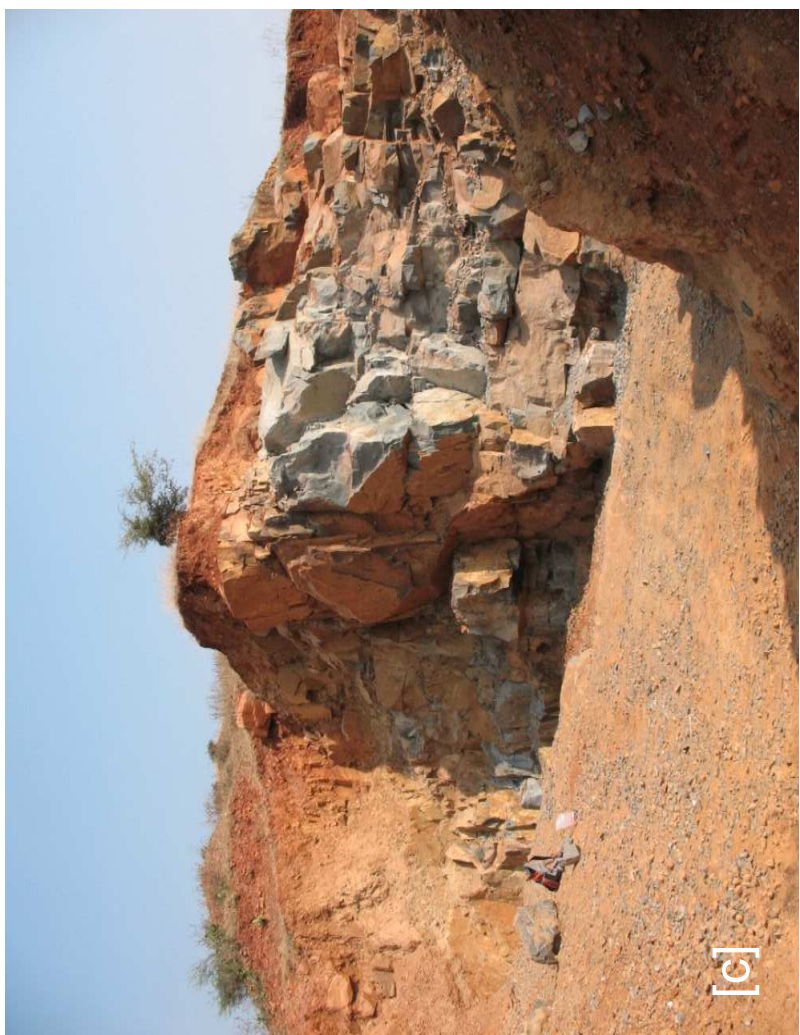
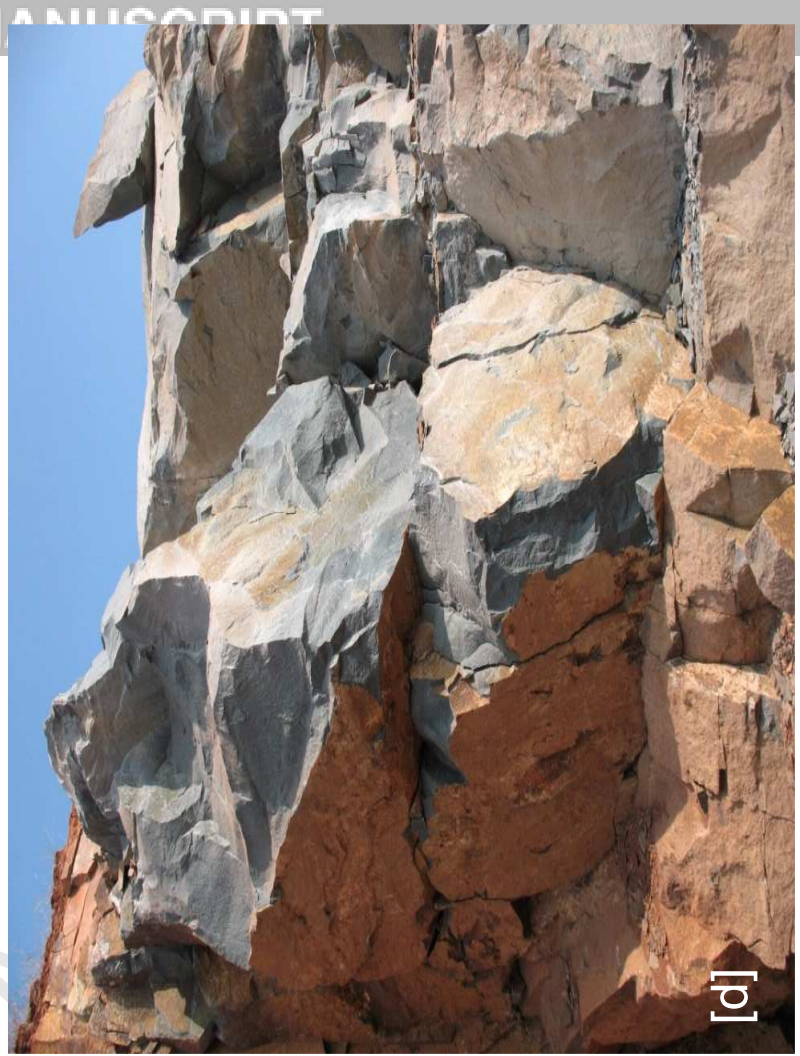
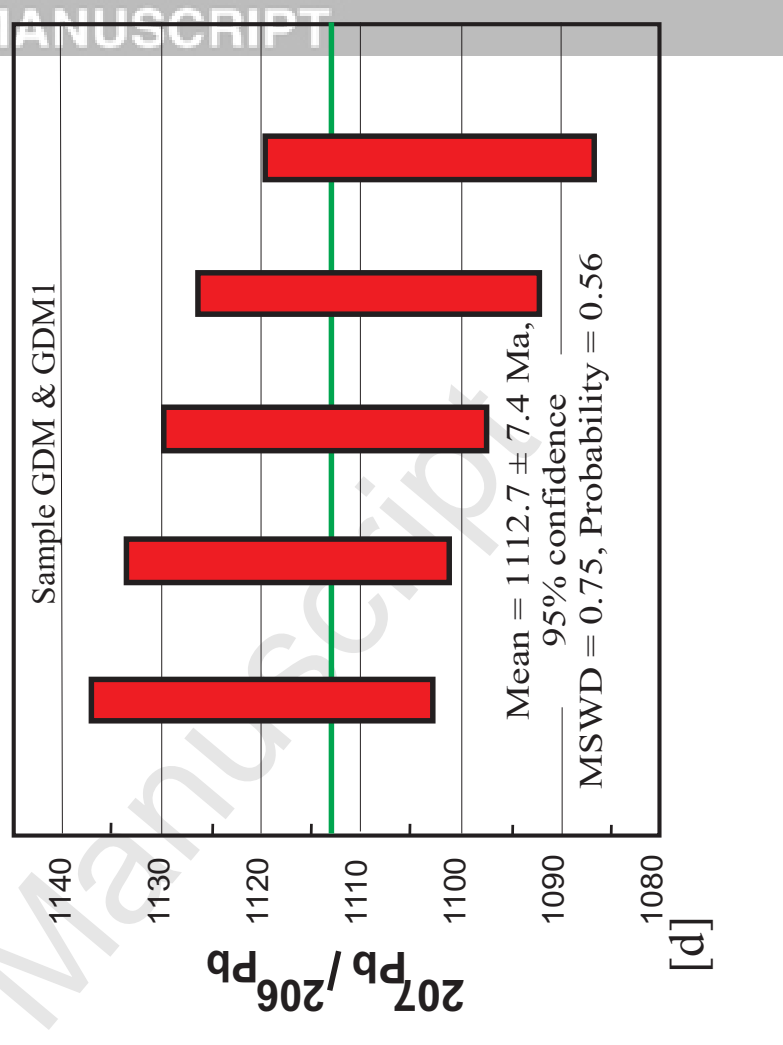
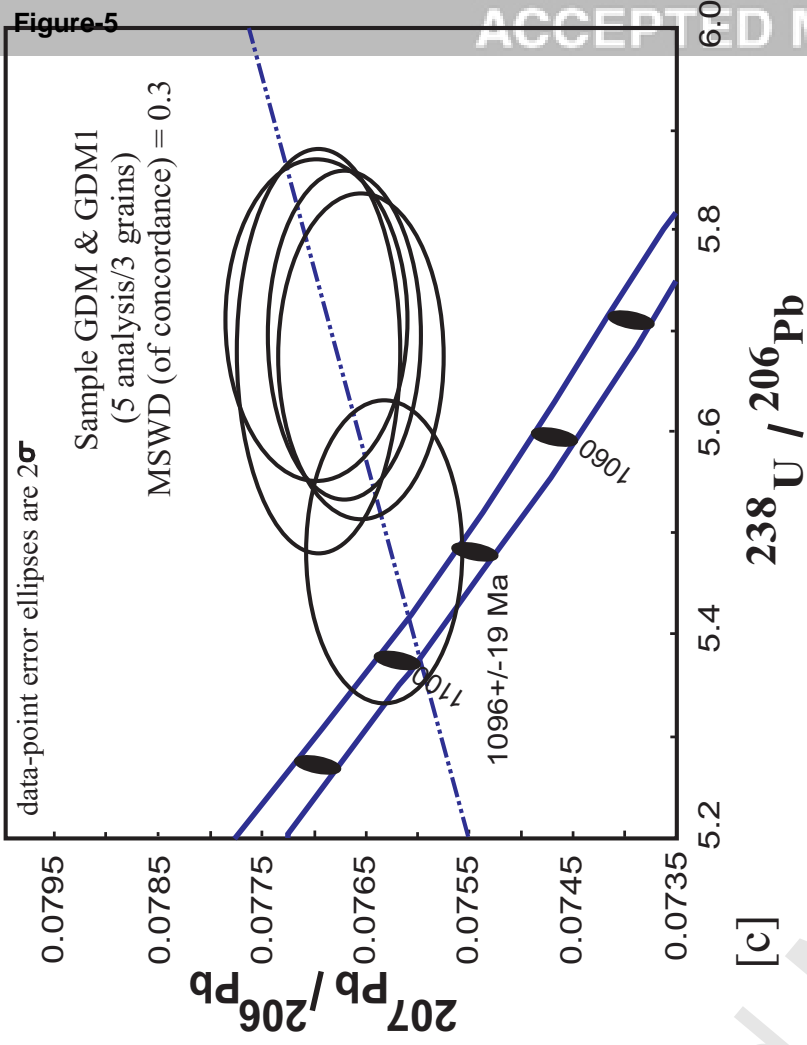
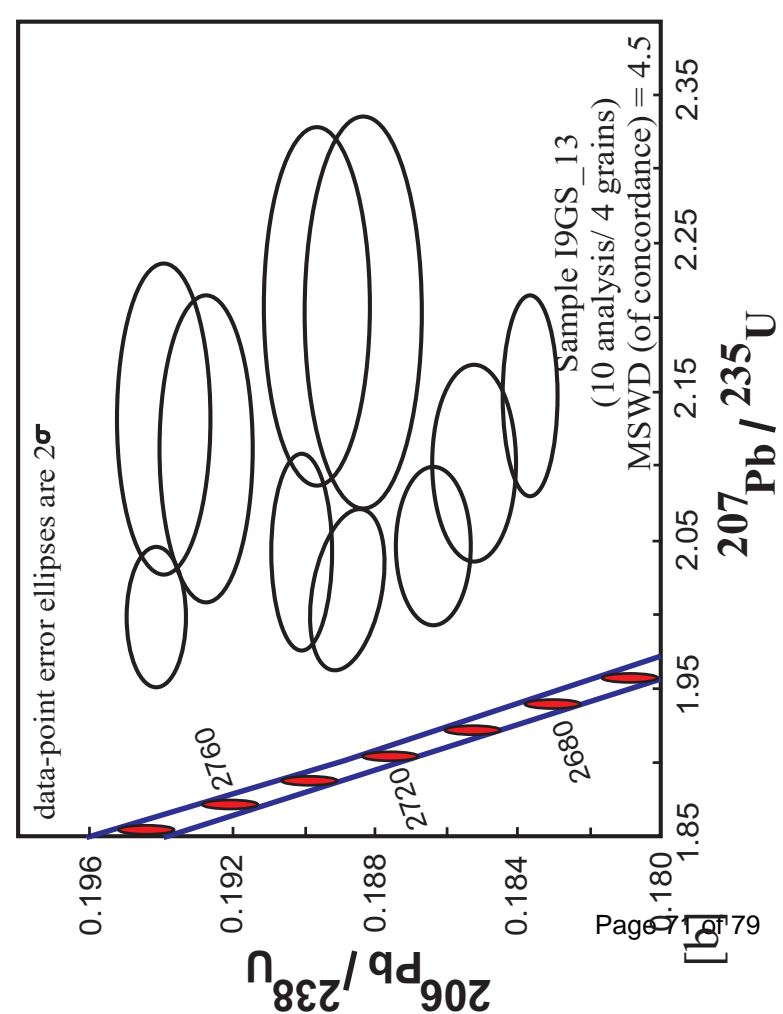
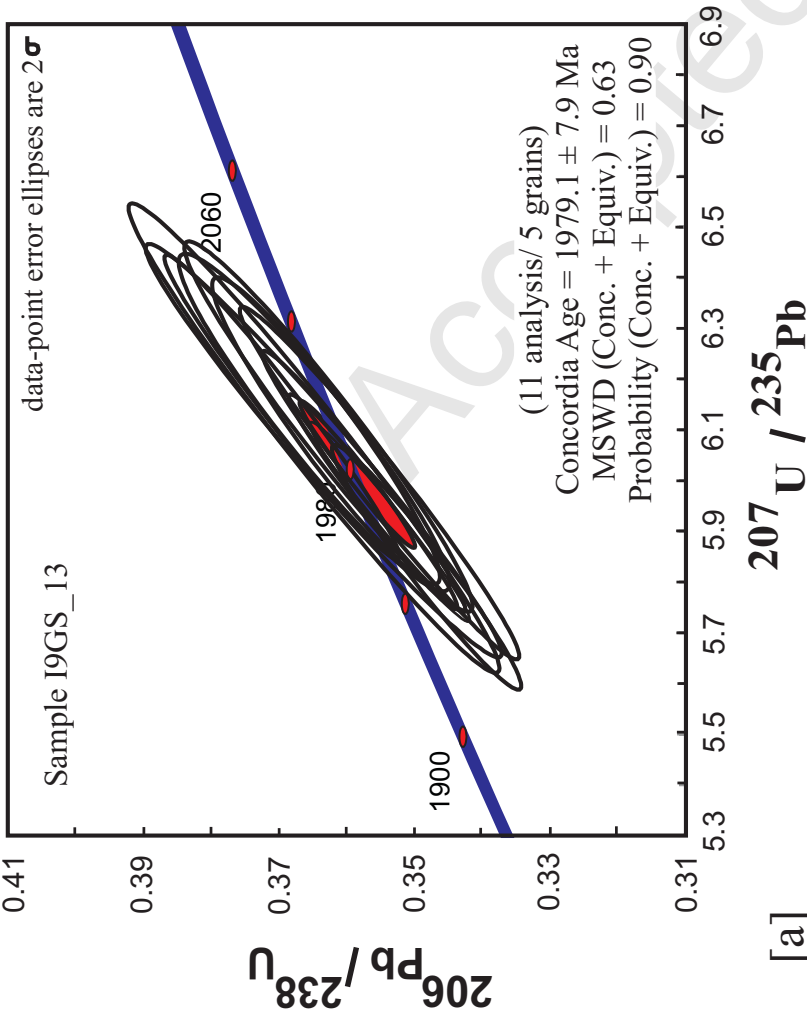
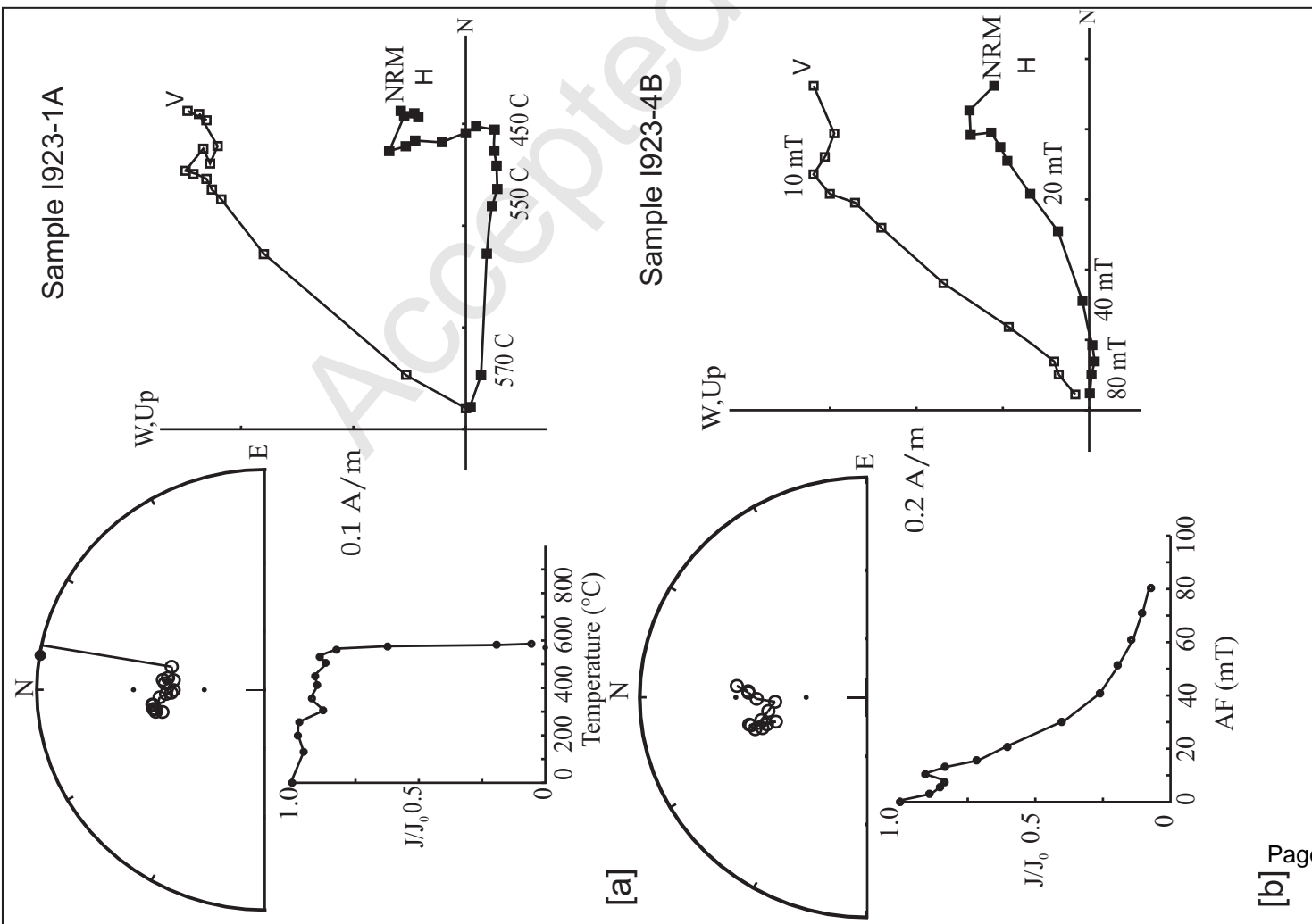
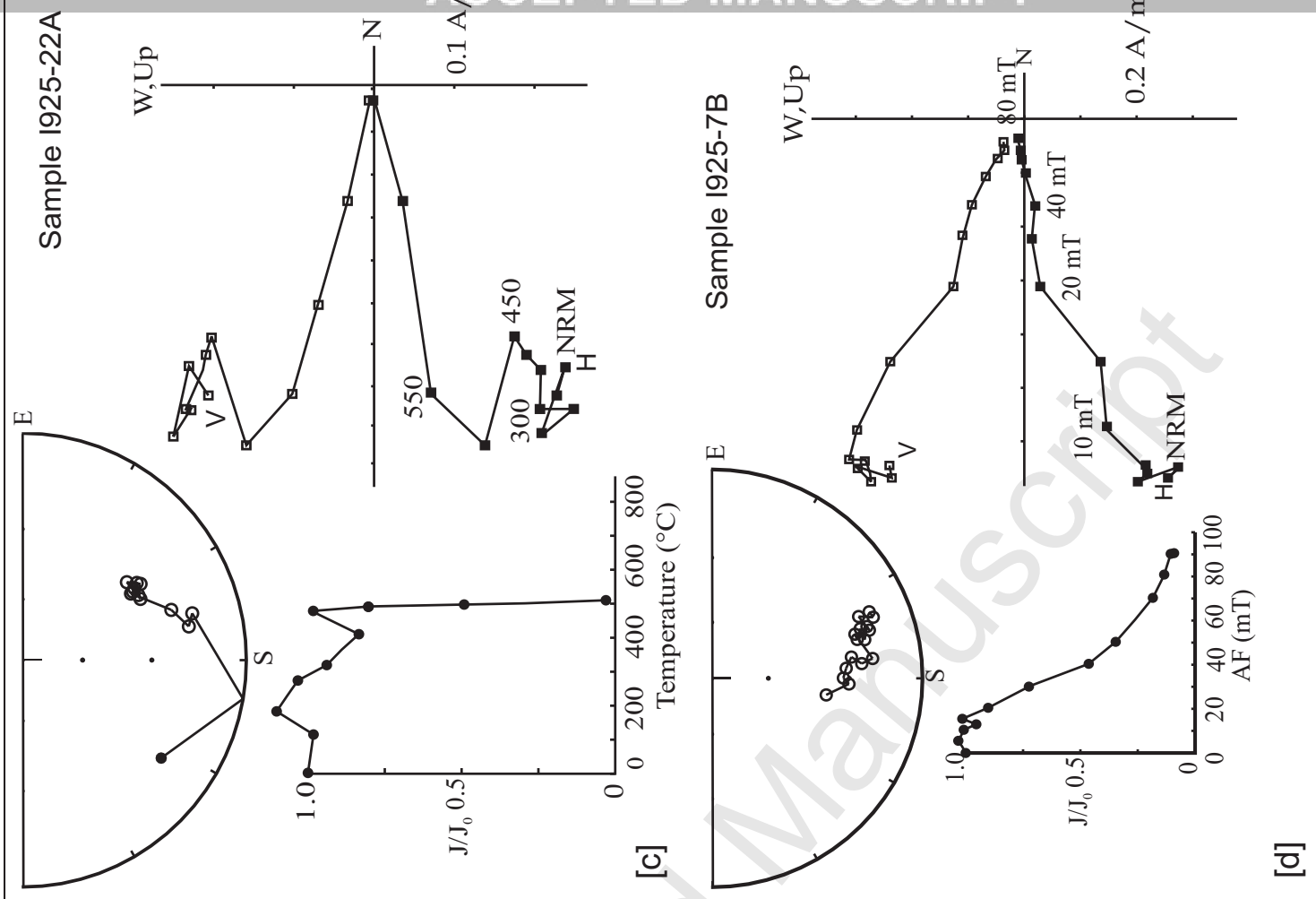


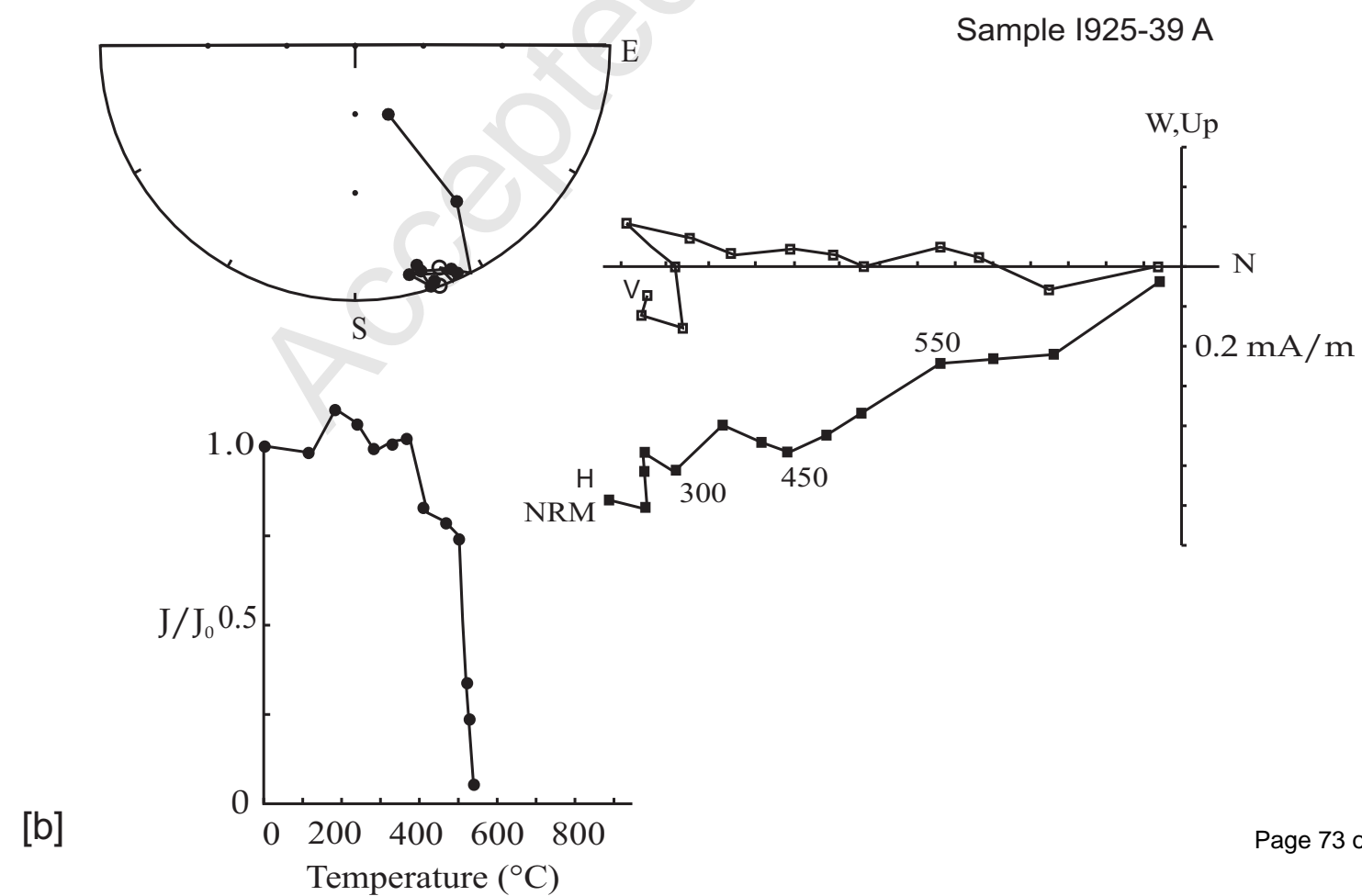
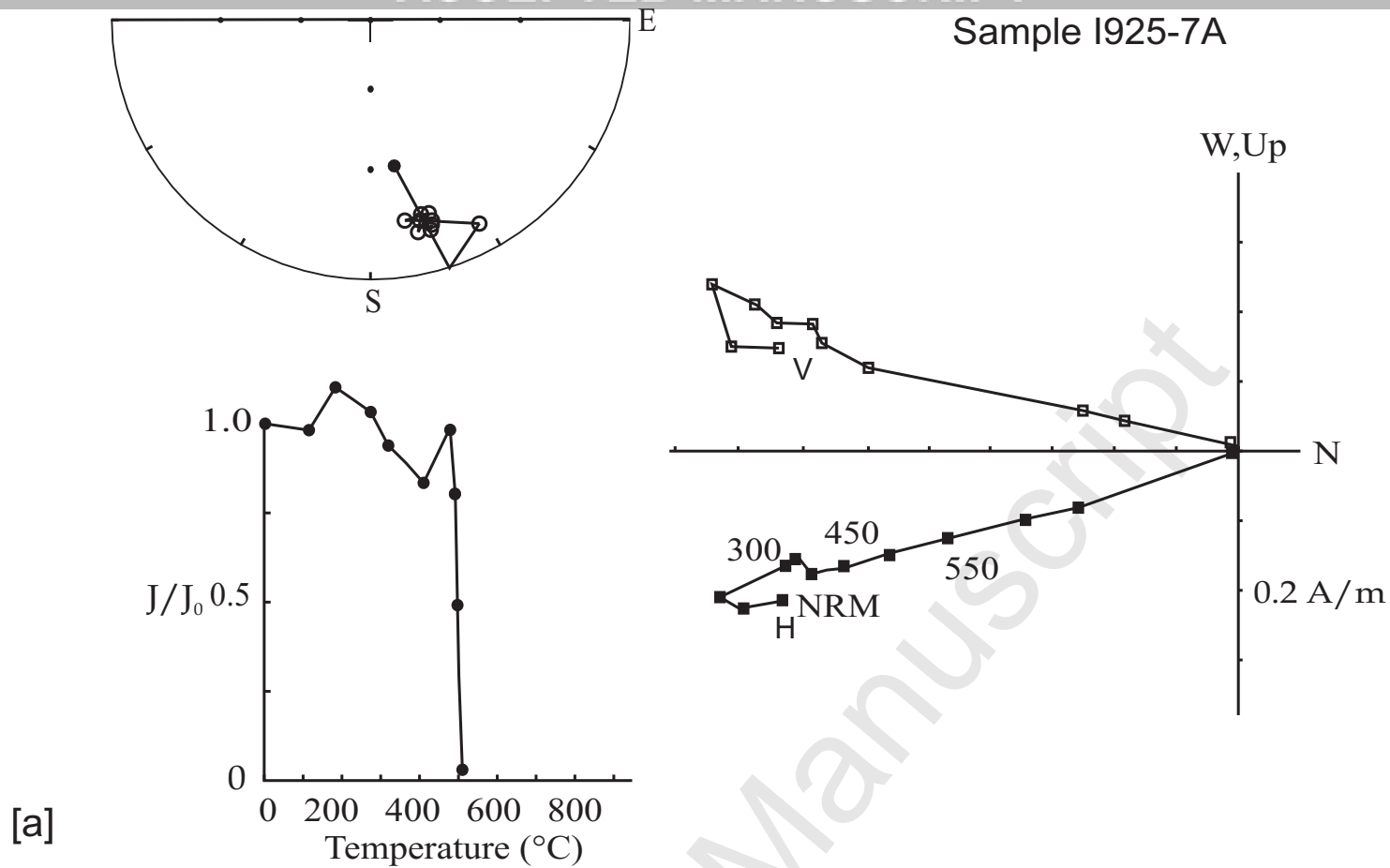
Figure-3

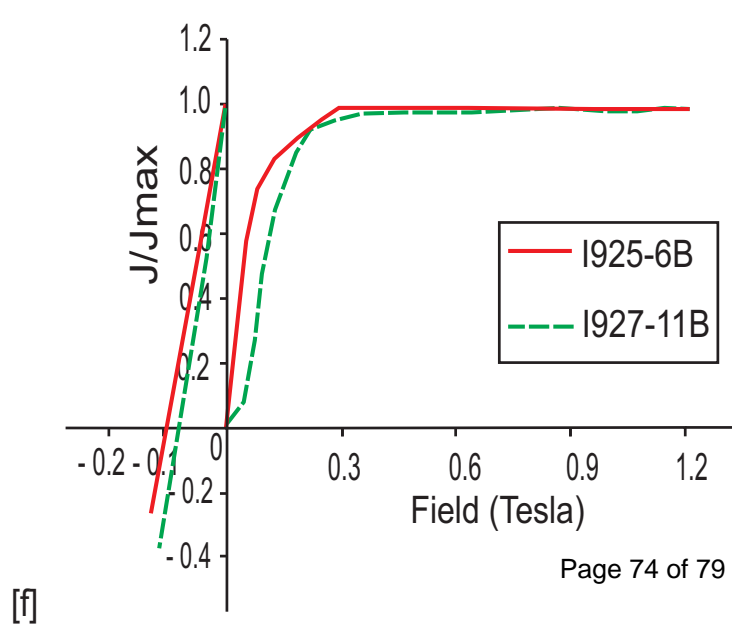
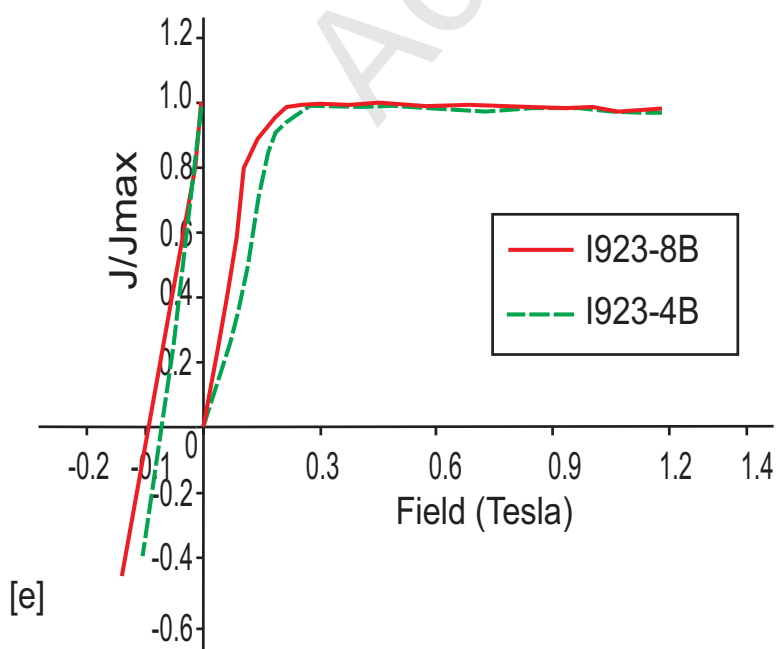
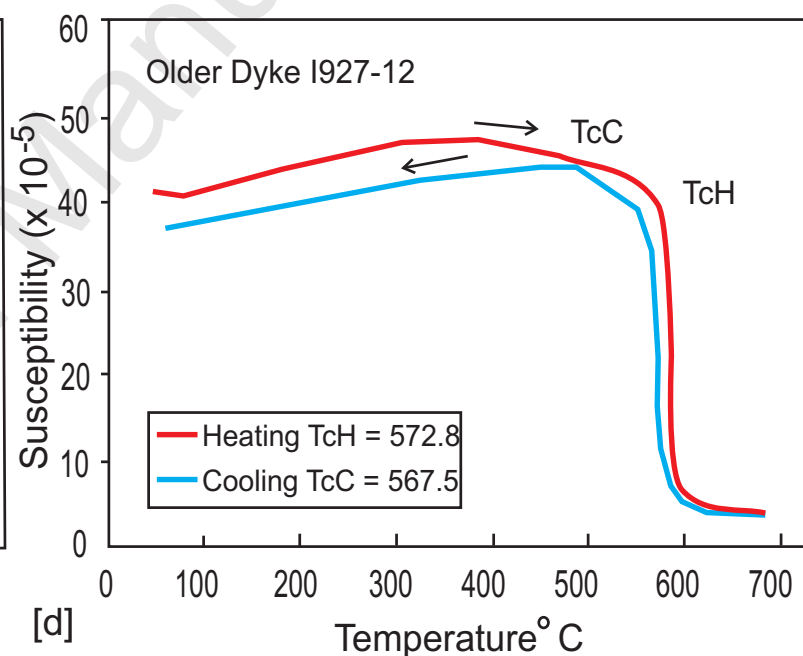
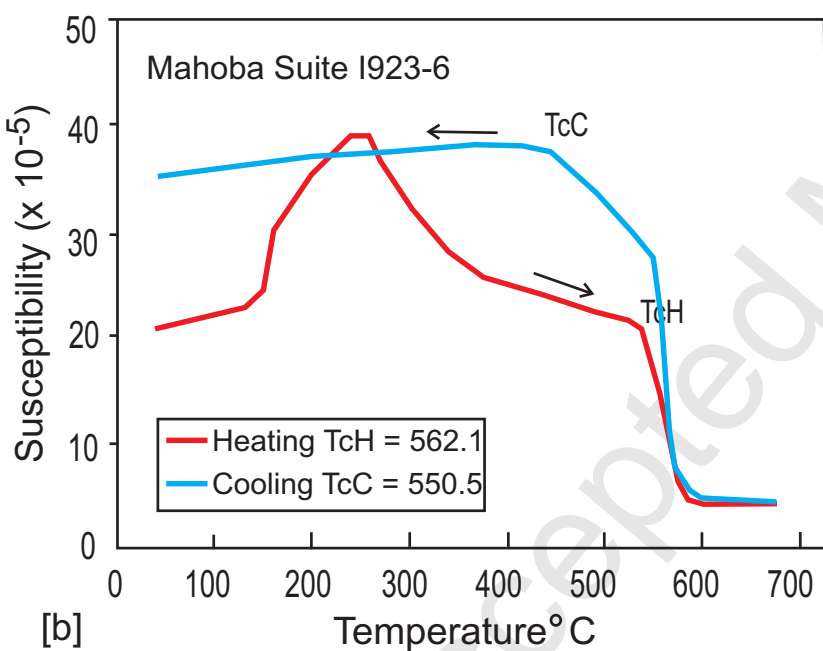
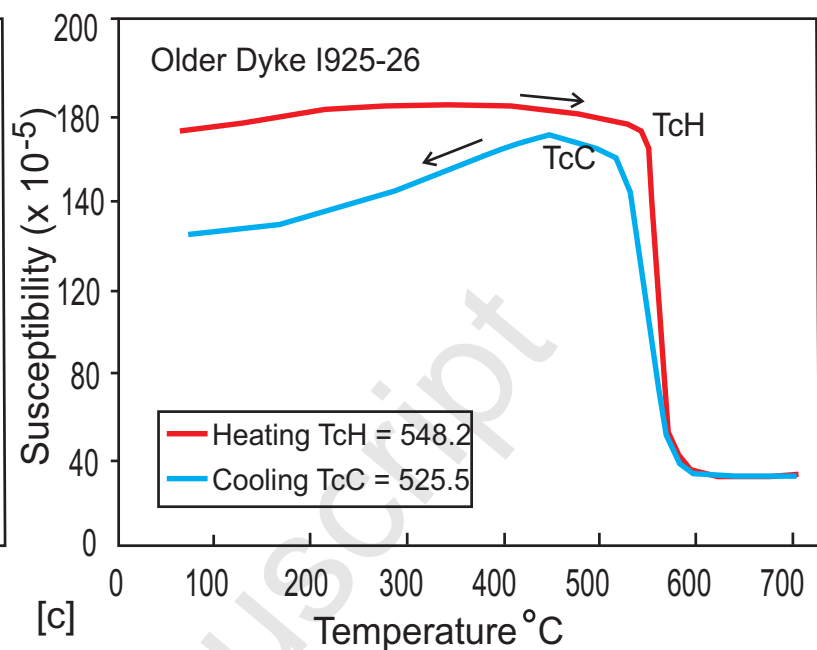
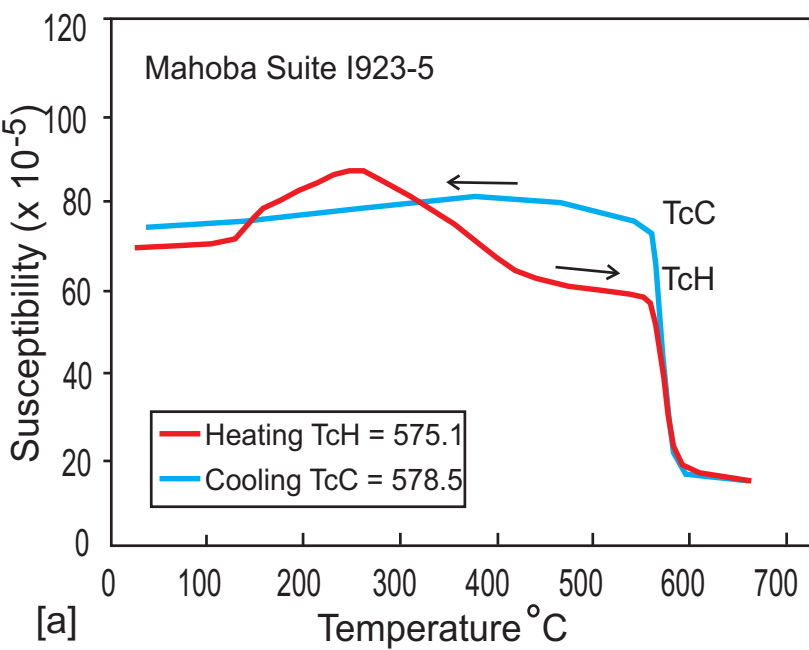
ACCEPTED MANUSCRIPT

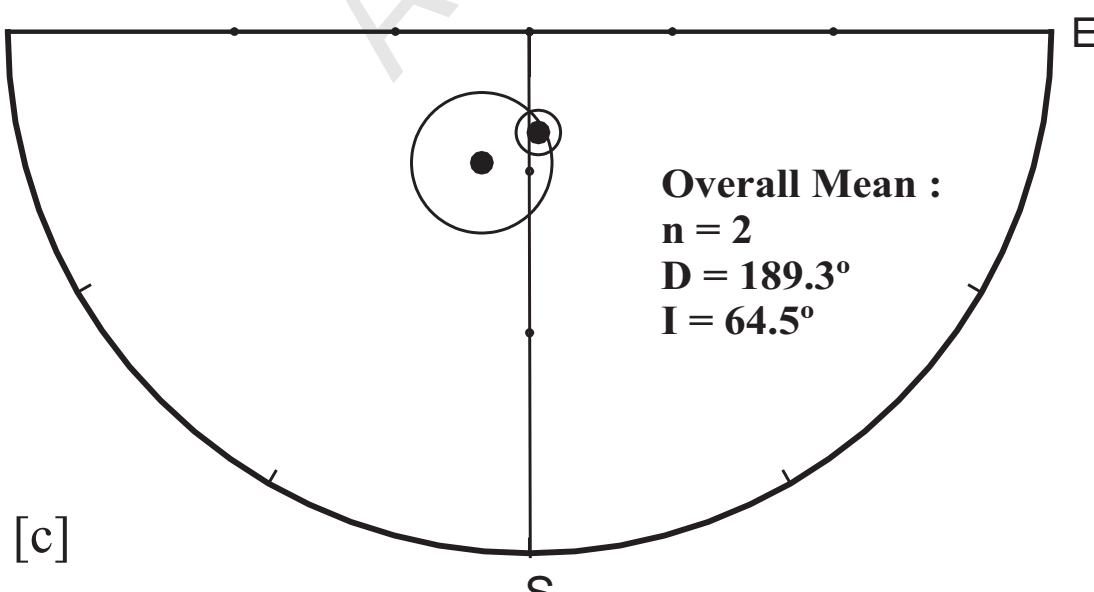
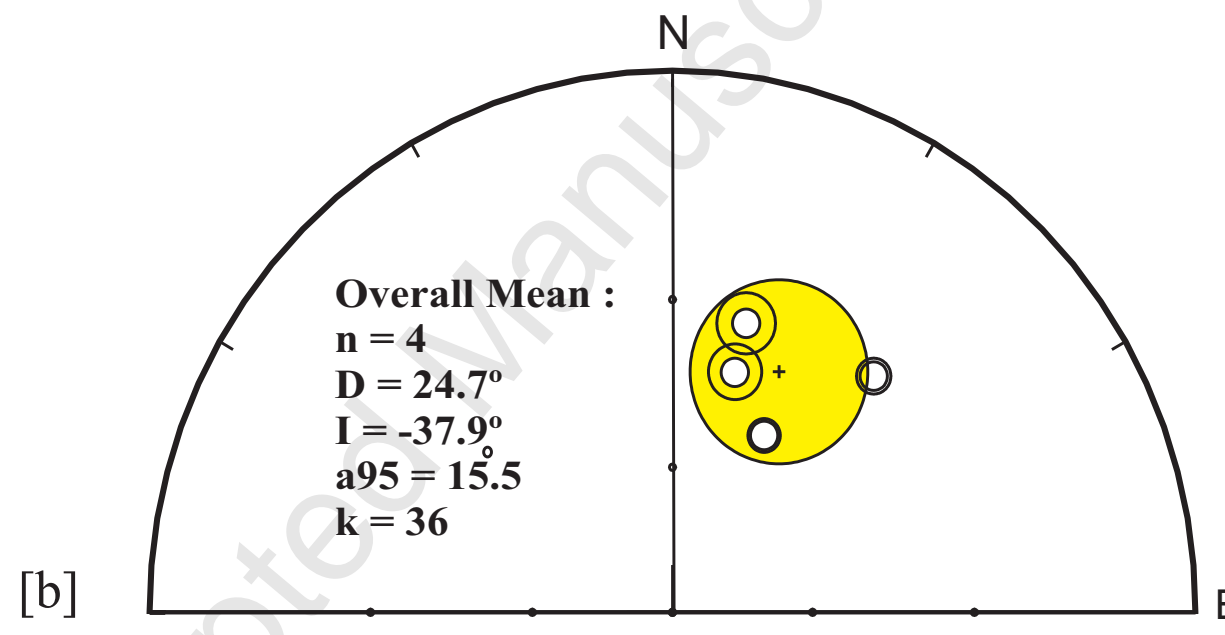
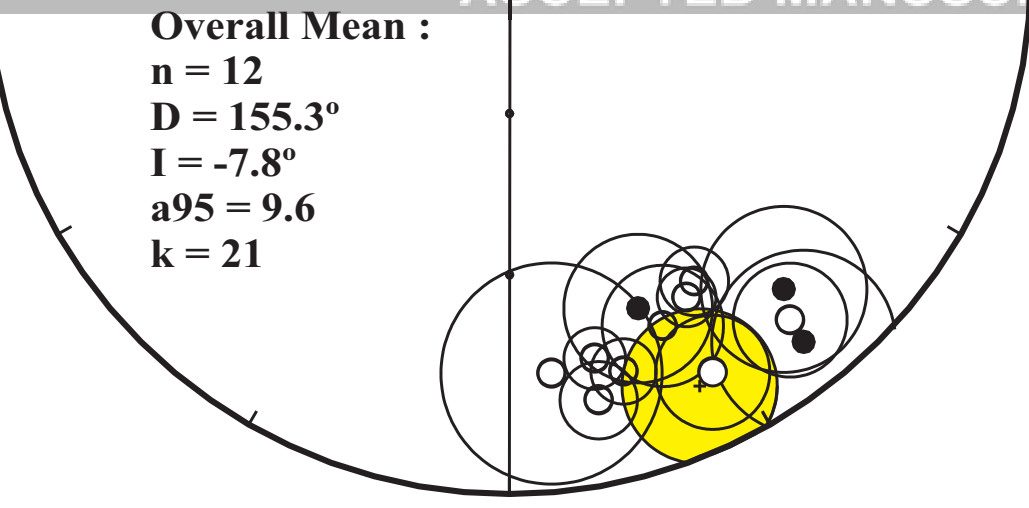


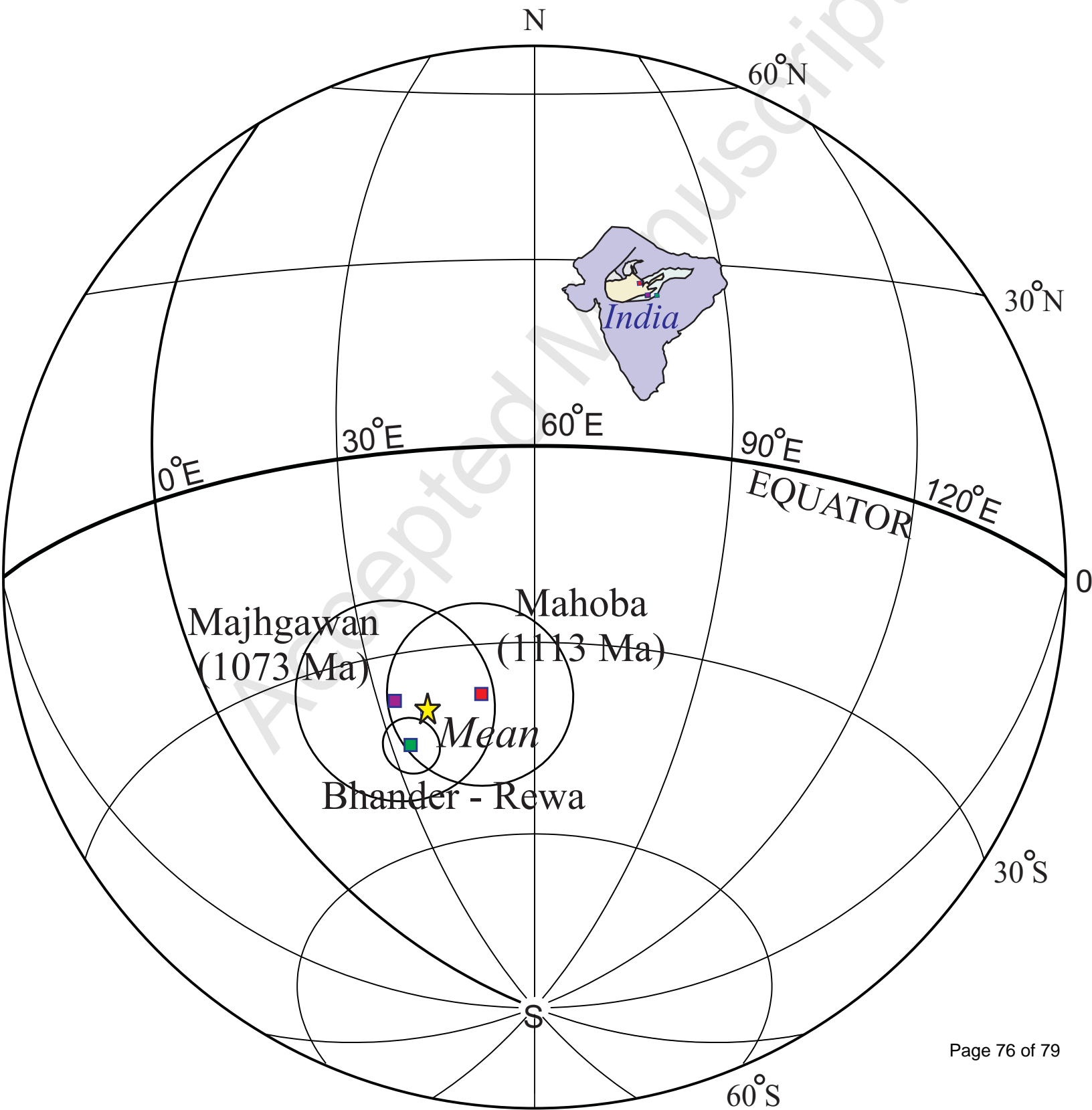




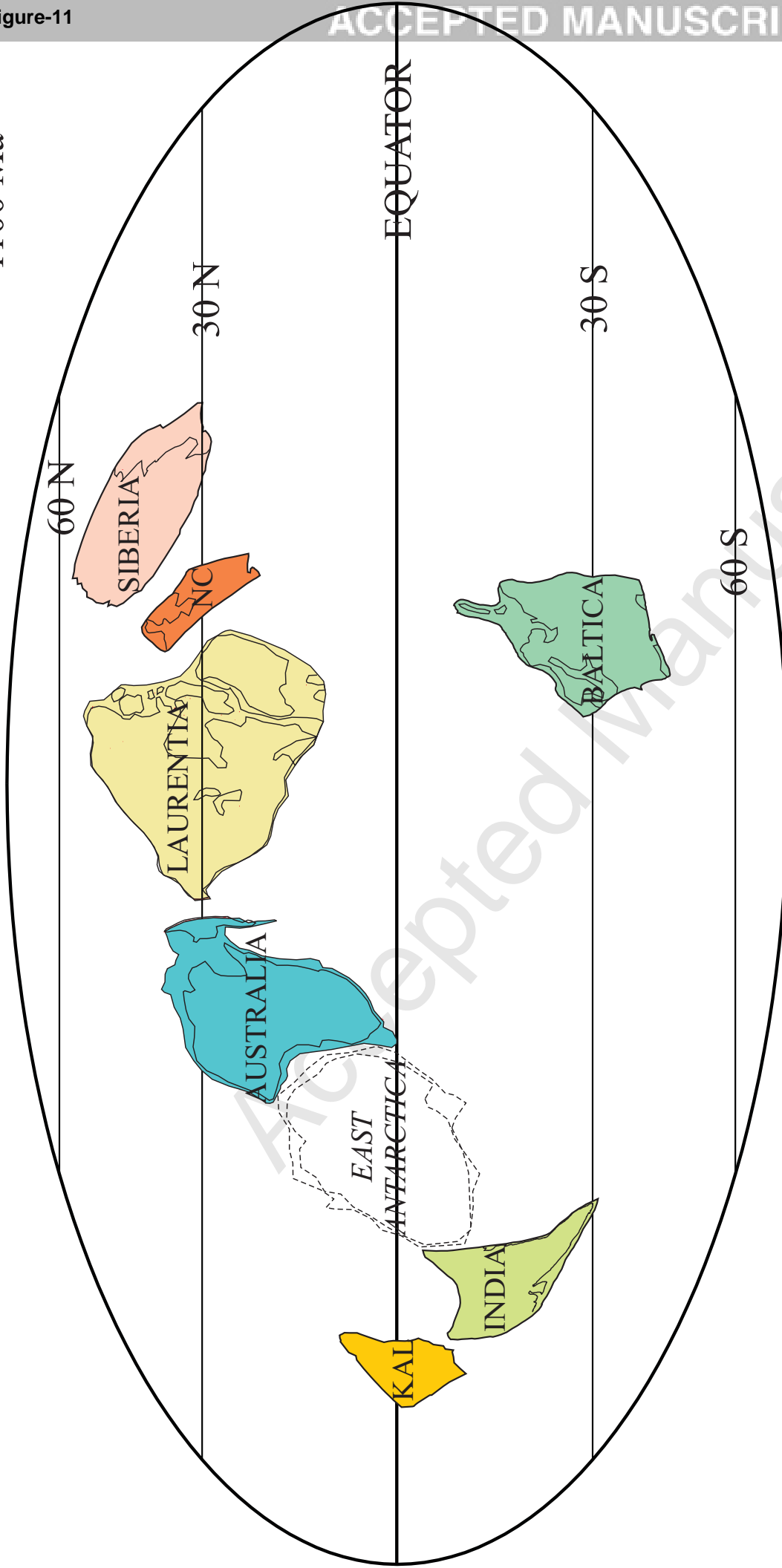


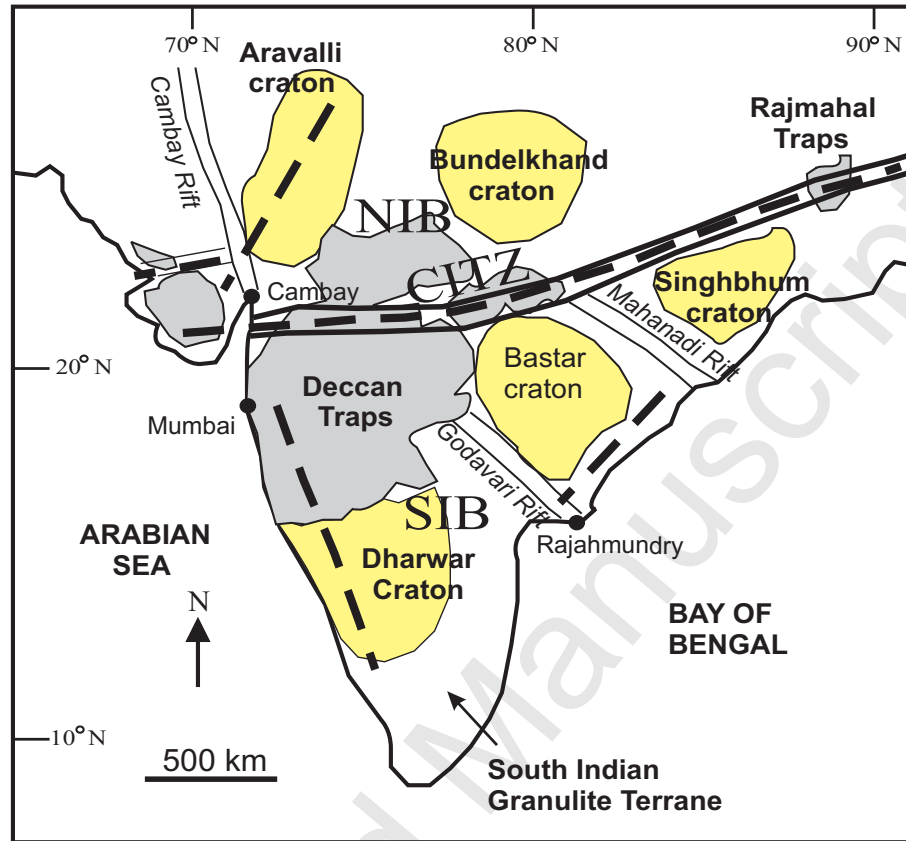




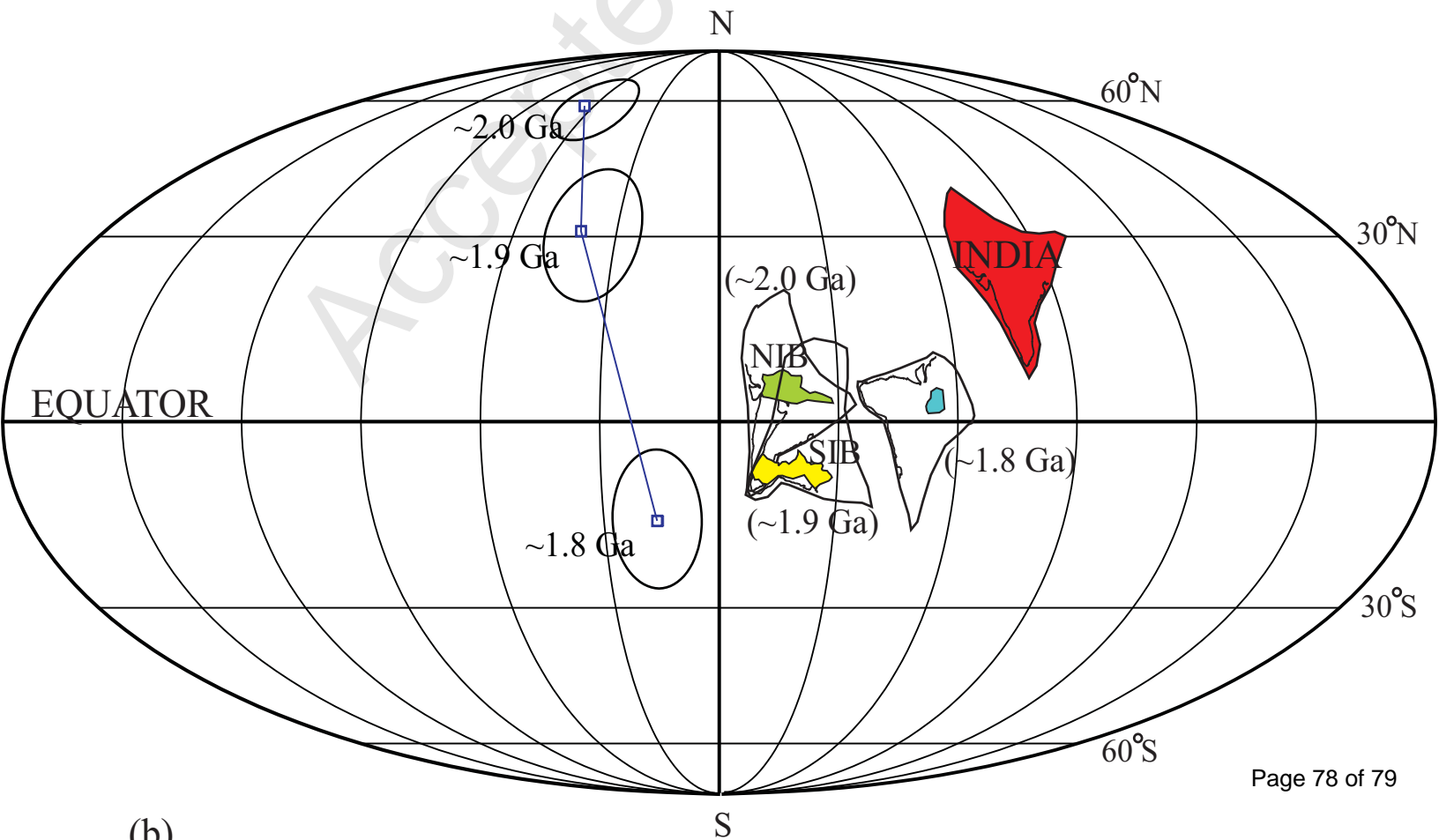


~1100 Ma



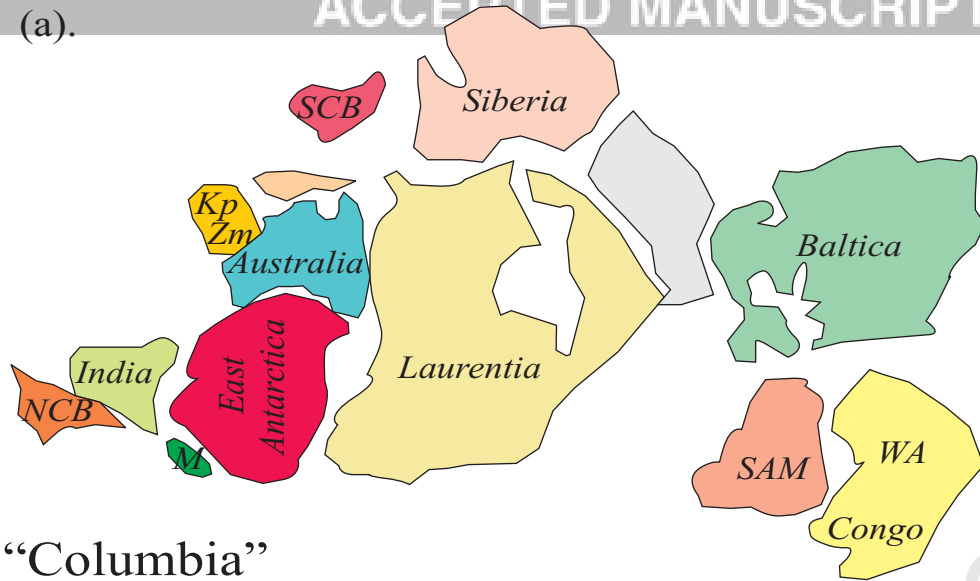


(a)

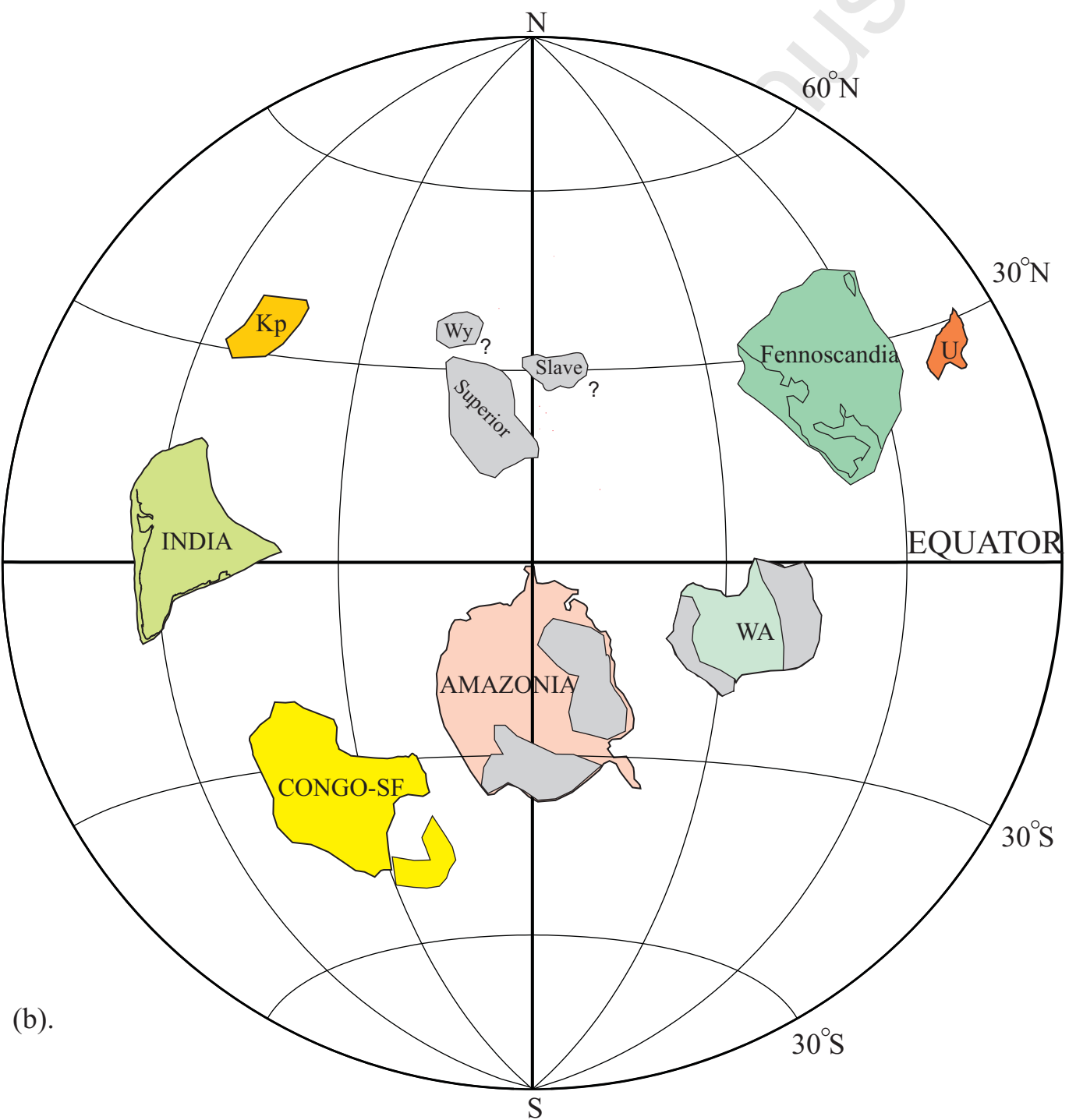


(b)

(a).



“Columbia”
Zhao et al. (2004)



(b).